



QUANTUM INNOVATION 2022

The International Symposium on Quantum Science,
Technology and Innovation

T
O
K
Y
O



Proceedings

Date 28-30 November 2022
Virtual Conference

Table of contents

Program

02	Welcome to Quantum Innovation 2022
03	Organizing Committee
04-06	Symposium Outline

Program

07-09	Program at a Glance
10	Plenary Sessions
11-12	Quantum Computing Track
13	Quantum Cryptography & Communication Track
14	Quantum Sensing Track
15-17	Quantum Sensing Track Short Presentations by Young Researchers

Abstract

18-40	Plenary Sessions
41-68	Quantum Computing Track
69-88	Quantum Cryptography & Communication Track
89-108	Quantum Sensing Track
109-152	Quantum Sensing Track Short Presentations by Young Researchers SE-03A
153-180	Quantum Sensing Track Short Presentations by Young Researchers SE-03B



QUANTUM INNOVATION 2022

The International Symposium on Quantum Science,
Technology and Innovation

Welcome to Quantum Innovation 2022

It is our pleasure to invite all of you including scientists, engineers, business delegates, young researchers and students to Quantum Innovation 2022, the International Symposium on Quantum Science, Technology and Innovation, to be held on 28-30 November 2022 as Virtual Conference.

Quantum Innovation 2022 is the second international symposium hosted by Japanese government and research institutes, that aims to bring together multi-disciplined researchers to present and exchange breaking-through ideas in quantum science and technology.

The topics of Quantum Innovation 2022 cover the latest achievements, trends and needs in quantum science and technology including quantum computing, quantum sensing, quantum cryptography and quantum communication.

We look forward to seeing you in Quantum Innovation 2022 and hope you enjoy excellent presentations from distinguished guests, share exciting discoveries and promote fruitful collaborations.

Organizing Committee

Chairs



General Chair
Kohei Itoh
 Keio University



Track Chair
 Quantum Computing
Hiroshi Imai
 The University of Tokyo



Track Chair
 Quantum Sensing
Akinari Yokoya
 National Institutes for Quantum
 Science and Technology (QST)



Track Chair
 Quantum Cryptography & Communication
Masahide Sasaki
 National Institute of Information
 and Communications Technology (NICT)

Committee members

Keisuke Fujii
 Osaka University

Takahiro Mori
 National Institute of
 Advanced Industrial Science
 and Technology (AIST)

Tadashi Sakai
 Tokyo Institute of
 Technology

Seiichiro Tani
 Nippon Telegraph and
 Telephone Corporation (NTT)

Takuya Hirano
 Gakushuin University

Takashi Mukaiyama
 Osaka University

Yutaka Shikano
 Gunma University

Yoshimichi Tanizawa
 Toshiba Corporation

Tetsuya Ido
 National Institute of
 Information and
 Communications
 Technology (NICT)

Mio Murao
 The University of Tokyo

Yutaka Tabuchi
 RIKEN

Tokuyuki Teraji
 National Institute for
 Materials Science (NIMS)

Takayuki Iwasaki
 Tokyo Institute of
 Technology

Kae Nemoto
 Okinawa Institute of
 Science and Technology
 Graduate University (OIST)

Shuntaro Takeda
 The University of Tokyo

Akihisa Tomita
 Hokkaido University

Kaoru Kenyoshi
 National Institute of
 Information and
 Communications
 Technology (NICT)

Atsushi Noguchi
 The University of Tokyo

Masahiro Takeoka
 Keio University

Hiroshi Yukawa
 National Institutes for
 Quantum Science and
 Technology (QST)

Masahiro Kitagawa
 Osaka University

Shinobu Onoda
 National Institutes for
 Quantum Science and
 Technology (QST)

Shu Tanaka
 Keio University

Symposium Outline

Aims

Addressing the state-of-the-art
quantum technology

Exploring cooperation on research,
application, education and social awareness
on quantum technology

We will bring together researchers working on quantum technology and offer a platform for discussions among them. Inviting prominent speakers from abroad and Japan, Quantum Innovation 2022 covers latest development of quantum computing, quantum sensing, quantum cryptography and quantum communication.

We also aim to give young researchers, future quantum working force candidates and aware citizens an overview of fast evolving quantum technology by listening to inspiring talks.

Scope of the Symposium

Highlights of the development of quantum
technology

Quantum Computing

Quantum Sensing

Quantum Cryptography & Communication

Development of Infrastructure for the progress
of quantum technology

Promotion of practical applications of quantum technology

Development of human resources for quantum technology

Promotion of international collaborations

Date

28-30 November 2022

Venue

Online

Schedule

28 November 2022 Plenary Sessions held in Tokyo

29-30 November 2022 Quantum Computing Track
Quantum Sensing Track
Quantum Cryptography & Communication Track

Speakers

All the speakers are to be invited.

Participants

The expected participants include researchers, engineers, business delegates, policy makers, administrators, students, and the media people, who share interests in quantum technology and innovation.

Symposium Sponsors

Cabinet Office
Ministry of Internal Affairs and Communications (MIC)
Ministry of Education, Culture, Sports, Science and Technology (MEXT)
Ministry of Economy, Trade and Industry (METI)
RIKEN
Japan Science and Technology Agency (JST)
National Institutes for Quantum Science and Technology (QST)
National Institute of Advanced Industrial Science and Technology (AIST)
National Institute of Information and Communications Technology (NICT)
Okinawa Institute of Science and Technology Graduate University (OIST)
Osaka University
The University of Tokyo
Tohoku University
Tokyo Institute of Technology
Quantum Strategic Industry Alliance for Revolution (Q-STAR)

Symposium Supporters

National Institute for Material Science (NIMS)

About QIH

Quantum technology is bringing a great impact on a wide range of industry. In order to accelerate the progress and make best use of quantum technology, industry, academia and government are expected to collaborate on promoting basic research, technology demonstration, industrialization, intellectual property management and human resource development. For promoting these activities, Japan established Quantum Technology Innovation Hubs in February 2021.



- Quantum computer development hub in RIKEN
- Global quantum industrial support hub (provisional name) in National Institute of Advanced Industrial Science and Technology (AIST)
- Quantum computer application hub represented by the University of Tokyo
- Quantum software innovation hub in Osaka University
- Quantum security network hub in National Institute of Information and Communications Technology (NICT)
- Quantum life science and function hub (provisional name) in National Institutes for Quantum Science and Technology (QST)
- Quantum materials research project in National Institute for Materials Science (NIMS)
- Quantum sensors hub represented by Tokyo Institute of Technology
- Quantum solution hub (provisional name) in Tohoku University
- International quantum education and research hub (provisional name) in Okinawa Institute of Science and Technology Graduate University (OIST)

RIKEN serves as Headquarters of the Hubs to incorporate efforts to advance quantum technology research in Japan.

Program at a Glance

Tracks

PL

Plenary Sessions

Contents / Topics

Welcome from Organizing Committee and Hosts,
Plenary Talks, Keynote

Tracks

CP

Quantum Computing Track

Contents / Topics

Quantum Computing architecture, Quantum computers with Atoms and Ions, Photonic Quantum Computers, Fault Tolerant Quantum Computing, Quantum Algorithms for Chemistry, NISQ Algorithms, Young PIs Session, Superconducting Quantum Computing, Quantum Annealing, Verifiable Quantum Computing, Semiconductor Quantum Computers, Quantum Simulations

Tracks

CC

Quantum Cryptography & Communication Track

Contents / Topics

Quantum Internet, Young Researcher Panel Session,
Quantum Cryptography

Tracks

SE

Quantum Sensing Track

Contents / Topics

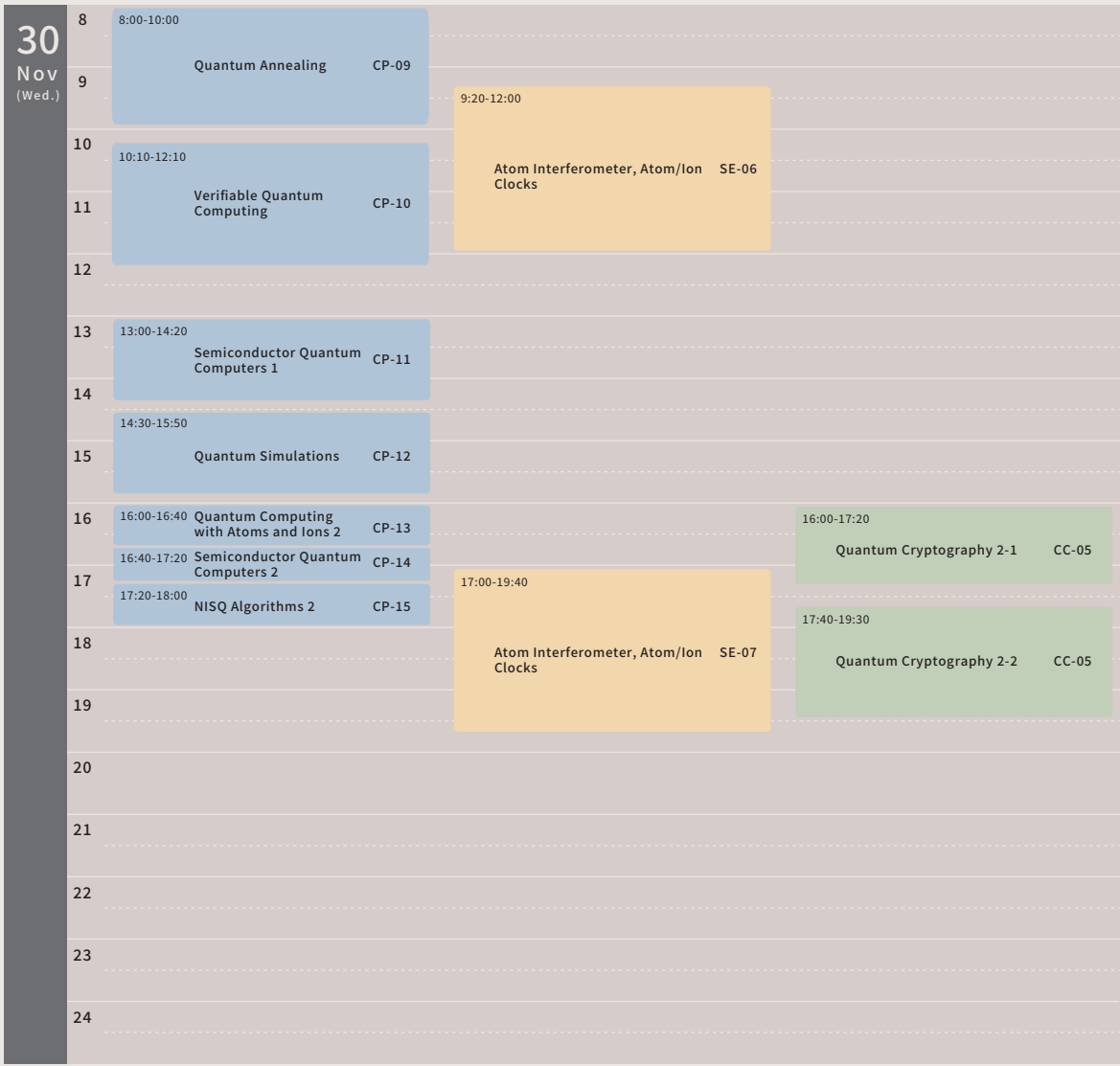
Q-sensors for Life Science, NV Center and Applications for Life Sciences, Solid-State Quantum Sensors, 5th IFQMS Short Presentation Session for Young Scientists, Solid-State Quantum Sensors, Q-sensors for Life Science, NV Center and Applications for Life Sciences, Atom Interferometer, Atom/Ion Clocks *29th Nov Sessions are a joint-program with The 5th IFQMS (The 5th International Forum on Quantum Metrology and Sensing).

All the times in the program are **Japan Standard Time (GMT+9)**

28 Nov (Mon.)	9		
	10	10:00-10:15	Opening PL-01
	11	10:30-12:30	Vision of Quantum Technology PL-02
	12		
	13	13:00-15:00	Keynote PL-03
	14		
	15		
	16	16:10-18:50	Keynote PL-03
	17		
	18		
19			

* 5th IFQMS (International Forum on Quantum Metrology and Sensing)

29 Nov (Tue.)	8	8:00-8:40	Quantum Computing Architecture CP-01	8:00-10:10			
	9	8:40-9:20	Quantum Computers with Atoms and Ions 1 CP-02	Q-Sensors for Life Science, NV Center and Applications for Life Sciences SE-01*		9:00-12:00	
	10	9:30-10:50	Photonic Quantum Computers CP-03			Quantum Internet 1 CC-01	
	11	11:00-11:40	Fault Tolerant Quantum Computing CP-04	10:30-12:00	Solid-State Quantum Sensors SE-02*		
	12						
	13	12:40-14:00	Quantum Algorithms for Chemistry CP-05	13:10-16:10	13:10-16:10	13:00-16:00	Young Researcher Session CC-02
	14	14:10-14:50	NISQ Algorithms 1 CP-06	Short Presentation Session for Young Scientists on SE-02, 04, 06, 07 Topics [5th IFQMS]	Short Presentation Session for Young Scientists on SE-01, 05 Topics [5th IFQMS]		
	15	15:00-16:40	Young Pls Session CP-07		SE-03A*	SE-03B*	
	16					16:00-18:00	Quantum Cryptography 1-1 CC-03
	17	16:50-18:50	Superconducting Quantum Computing CP-08	17:00-19:00	Solid-State Quantum Sensors SE-04*		17:00-20:00
18					18:20-20:20	Quantum Internet 2 CC-04	
19					19:20-21:10	Quantum Cryptography 1-2 CC-03	
20				19:20-21:10	Q-Sensors for Life Science, NV Center and Applications for Life Sciences SE-05*		
21							
22							
23							
24							



Plenary Sessions

All the times in the program are **Japan Standard Time(GMT+9)**

28 ^{Nov} (Mon.)	Session / Presentation	Chairperson / Presenter	Affiliation	Abstract PDF
10:00-10:15	PL-01. Opening			
	Chairperson	Shigeo Koyasu	RIKEN	
	Welcome	Hideyuki Nakano	Parliamentary Vice-Minister of Cabinet Office	
	Congratulatory Speech	Keitaro Ohno	Parliamentary Association for Quantum Technology Promotion	
10:30-12:30	PL-02. Vision of Quantum Technology			
	Chairperson	Shigeo Koyasu	RIKEN	
	10:30 Vision of quantum future society / Future society to be realized through quantum technology and strategies for its realization	Kohei Itoh	Chairperson, Strategy Review Working Group on Quantum Technology and Innovation Strategy, Government of Japan	PL-02-01
	10:45 The national quantum initiative	Gretchen Campbell	Deputy director, the National Quantum Coordination Office, OSTP	PL-02-02
11:00 European policy	Gustav Kalbe	Acting Director, Digital Excellence and Science Infrastructure, DG CONNECT, European Commission	PL-02-03	
11:15 Enabling & growing the quantum industry	Celia Merzbacher	Executive Director, Quantum Economic Development Consortium (QED-C)	PL-02-04	
11:30 Strengthening Europe's quantum industry on the global stage	Thierry Botter	Executive Director, Quantum Industry Consortium (QuIC)	PL-02-05	
11:45 Introduction of Q-STAR -Create industries & businesses with quantum technology-	Taro Shimada	Chair of the Board, Quantum STRategic industry Alliance for Revolution	PL-02-06	
12:00 Promoting Quantum Innovation through the triangle collaboration	Akihisa Tomita	Chair of Quantum ICT Forum / Hokkaido University	PL-02-07	
12:15 Moonshot Goal 6: Realization of a fault-tolerant universal quantum computer that will revolutionize economy, industry, and security by 2050	Masahiro Kitagawa	Program Director of Moonshot#6 / Osaka University	PL-02-08	
13:00-18:50	PL-03. Keynote			
	Chairperson	Yasunobu Nakamura	RIKEN	
13:00 The next wave of computing: quantum-centric supercomputing	Jerry Chow	IBM	PL-03-01	
13:40 From synchronization to chemical reaction superpositions	Gregory Scholes	Princeton University	PL-03-02	
14:20 Quantum diamond sensors — Best of both worlds	Ronald Walsworth	The University of Maryland	PL-03-03	
Break (15:00 - 16:10)				
16:10 Optical quantum computers with quantum teleportation	Akira Furusawa	The University of Tokyo	PL-03-05	
16:50 Quantum computer architecture: from NISQ processors to fault-tolerant quantum computers	Kae Nemoto	Okinawa Institute of Science and Technology Graduate University	PL-03-06	
17:30 How science is becoming and industry	Rupert Ursin	Quantum Technology Laboratories	PL-03-07	
18:10 Quantum network technology - the second life of rare-earth crystals	Wolfgang Tittel	The University of Geneva	PL-03-08	

Quantum Computing Track

All the times in the program are **Japan Standard Time**(GMT+9)

29 Nov (Tue.)	Session / Presentation	Chairperson / Presenter	Affiliation	Abstract PDF
8:00-8:40	CP-01. Quantum Computing Architecture			
	Chairperson	Teruo Tanimoto	Kyushu U	
	Greater quantum efficiency through physics-aware system software	Fred Chong	U Chicago	CP-01-01
8:40-9:20	CP-02. Quantum Computers with Atoms and Ions 1			
	Chairperson	Atsushi Noguchi	UTokyo	
	Recent advances toward a more capable trapped ion quantum computer	Patty Lee	Quantinuum	CP-02-01
9:30-10:50	CP-03. Photonic Quantum Computers			
	Chairperson	Shuntaro Takeda	UTokyo	
9:30	Blueprint for a scalable photonic fault-tolerant quantum computer	Eli Bourassa and Ilan Tzitrin	Xanadu	CP-03-01
10:10	The PhANTM algorithm: measurement-based generation and preservation of cat and grid states	Olivier Pfister	U Virginia	CP-03-02
11:00-11:40	CP-04. Fault Tolerant Quantum Computing			
	Chairperson	Keisuke Fujii	Osaka U	
	Suppressing quantum errors by scaling a surface code logical qubit	Zijun Chen	Google	CP-04-01
12:40-13:20	CP-05. Quantum Algorithms for Chemistry			
	Chairperson	Keisuke Fujii	Osaka U	
12:40	Current status of variational quantum algorithms for chemistry and beyond	Wataru Mizukami	Osaka U	CP-05-02
14:10-14:50	CP-06. NISQ Algorithms 1			
	Chairperson	Hiroshi Imai	UTokyo	
	Statistical method for quantum estimation algorithms	Naoki Yamamoto	Keio U	CP-06-01
15:00-16:40	CP-07. Young Pls Session			
	Chairperson	Mio Murao	UTokyo	
15:00	Programmable continuous-variable photonic quantum computing in the time domain	Shuntaro Takeda	UTokyo	CP-07-01
15:25	Design and optimization of fault-tolerant quantum computing	Yasunari Suzuki	NTT	CP-07-02
15:50	Quantum error correction by low-depth random clifford circuits	Yoshifumi Nakata	Kyoto U	CP-07-03
16:15	Faster emulation of noisy VQE	Tyson Jones	U Oxford	CP-07-04
16:50-18:50	CP-08. Superconducting Quantum Computing			
	Chairperson	Yutaka Tabuchi	RIKEN	
16:50	One hundred second bit-flip time in a two-photon dissipative oscillator	Zaki Leghtas	ENS	CP-08-01
17:30	Real-time decoding with a distributed control-stack architecture for fault-tolerant quantum computing	Francesco Battistel	Qblox	CP-08-02
18:10	Tileable low-crosstalk 3D-integrated superconducting circuits	Peter Leek	U Oxford	CP-08-03

Quantum Computing Track

All the times in the program are **Japan Standard Time**(GMT+9)

30 Nov (Wed.)	Session / Presentation	Chairperson / Presenter	Affiliation	Abstract PDF
8:00-10:00	CP-09. Quantum Annealing			
	Chairperson	Shu Tanaka	Keio U	
8:00	Practical quantum computing	Mark Johnson	D-Wave	CP-09-01
8:40	Search for quantum applications and taking POCs to production	Helmut Katzgraber	Amazon	CP-09-02
9:20	Quantum annealer based on kerr parametric oscillators	Tsuyoshi Yamamoto	NEC	CP-09-03
10:10-12:10	CP-10. Verifiable Quantum Computing			
	Chairperson	Seiichiro Tani	NTT	
10:10	Bob's sidekick (or how tripartite quantum correlations satisfy a type of rigidity and how this is useful for cryptography)	Anne Broadbent	U Ottawa	CP-10-01
10:50	Abstracting quantum computation	Joe Fitzsimons	Horizon Quantum Computing	CP-10-02
11:30	Quantum cryptography without one-way functions	Tomoyuki Morimae	Kyoto U	CP-10-03
13:00-14:20	CP-11. Semiconductor Quantum Computers 1			
	Chairperson	Takahiro Mori	AIST	
13:00	From a grain of sand to a $ \text{quantum}\rangle$ bit of information	James Clarke	Intel	CP-11-01
13:40	Integration of silicon spin qubits with buried nanomagnet: a trial to design integration structure with quantum device simulator	Shota Iizuka	AIST	CP-11-02
14:30-15:50	CP-12. Quantum Simulations			
	Chairperson	Yutaka Shikano	Gunma U	
14:30	Quantum simulations using phonons in trapped ions	Kenji Toyoda	Osaka U	CP-12-01
15:10	Quantum simulation for quantum many-body systems: variational quantum algorithms and beyond	Seiji Yunoki	RIKEN	CP-12-02
16:00-16:40	CP-13. Quantum Computing with Atoms and Ions 2			
	Chairperson	Atsushi Noguchi	UTokyo	
	Quantum information processing with trapped ions	Jonathan Home	ETH	CP-13-01
16:40-17:20	CP-14. Semiconductor Quantum Computers 2			
	Chairperson	Takahiro Mori	AIST	
	Building small, fast and hot hole spin qubits in Si and Ge	Dominik Zumbuhl	U Basel	CP-14-01
17:20-18:00	CP-15. NISQ Algorithms 2			
	Chairperson	Hiroshi Imai	UTokyo	
	Algorithms and architectures for the 'Late NISQ' and 'Early Fault-Tolerant' Eras	Simon Benjamin	U Oxford	CP-15-01

Quantum Cryptography & Communication Track

All the times in the program are **Japan Standard Time**(GMT+9)

29 Nov (Tue.)	Session / Presentation	Chairperson / Presenter	Affiliation	Abstract PDF
9:00-12:00	CC-01. Quantum Internet 1			
	Chairperson	TBD	TBD	
9:00	Solid-state quantum emitters for quantum networking	Elizabeth Goldschmidt	U Illinois	CC-01-01
9:30	Generation and manipulation of photonic quantum states for quantum network	Takashi Yamamoto	Osaka U	CC-01-02
10:00	Quantum communication in network channels and multipartite entanglement distribution	Masahiro Takeoka	Keio U	CC-01-03
10:30	Quantum repeater for continuous-variable entanglement distribution	Josephine Dias	OIST	CC-01-04
11:00	Entanglement distribution for QKD over telecom fiber	Christian Kurtsiefer	NUS	CC-01-05
13:00-16:00	CC-02. Young Researcher Panel Session			
	Chairperson	Simon Devitt	UTS	
		Shota Nagayama	Keio U	
		Toshihiko Sasaki	UTokyo	
		David Elkouss	OIST	
		Alexander Ling	NUS	
		Rikizo Ikuta	Osaka U	
16:00-18:00	CC-03. Quantum Cryptography 1-1			
	Chairperson	Akihisa Tomita	Hokkaido U	
16:00	Quantum key distribution: current applications and future improvements	Gregoire Ribordy	ID Quantique	CC-03-08
16:35	Quantum business rising: A new era of investment and wealth creation building the quantum economy	Corey McClelland	Qubitekk	CC-03-01
17:00	Quantum communication at Airbus	Matthieu Dollon	Airbus Defence & Space	CC-03-02
17:25	Information theoretically secure data utilization using "Quantum Secure Cloud"	Mikio Fujiwara	NICT	CC-03-03
18:00-18:20	Break			
18:20-20:20	CC-03. Quantum Cryptography 1-2			
	Chairperson	Takuya Hirano	Gakushuin U	
18:20	Field trials and recent activities of QKD research in Toshiba Corporation	Mamiko Kujiraoka	Toshiba	CC-03-04
18:45	Advancements in space quantum communications	Paolo Villoresi	U Padova	CC-03-05
19:10	Entanglement distribution and next challenges	Alexander Ling	NUS	CC-03-06
19:35	Satellite-based QKD for global quantum cryptographic network construction	Saori Yokote	SKY Perfect JSAT	CC-03-07
17:00-20:00	CC-04. Quantum Internet 2			
	Chairperson	TBD	TBD	
17:00	Resource efficient fault-tolerant one-way quantum repeater with code concatenation	Johannes Borregaard	TU Delft	CC-04-01
17:30	Entanglement of trapped-Ion Qubits separated by 230 m	Tracy Northup	U Innsbruck	CC-04-02
18:00	From quantum repeater networks to the quantum internet	Hideo Kosaka	YNU	CC-04-03
18:30	Quantum repeaters: Analytical models and optimized protocols	Peter van Loock	U Mainz	CC-04-04
30 Nov (Wed.)	Session / Presentation	Chairperson / Presenter	Affiliation	Abstract PDF
16:00-17:20	CC-05. Quantum Cryptography 2-1			
	Chairperson	Masahide Sasaki	NICT	
		Martin Ward	Toshiba	
	Panelist 1	Dirk Fischer	BSI	
	Panelist 2	Yoshimichi Tanizawa	Toshiba	
	Panelist 3	Masato Koashi	UTokyo	
	Panelist 4	Macros Curty	U Vigo	
17:20-17:40	Break			
	CC-05. Quantum Cryptography 2-2			
	Chairperson	Masahiro Takeoka	Keio U	
17:40	Telco's experience and perspective on quantum cryptography	Hyungsoo Kim	KT	CC-05-05
18:05	The UK quantum communications hub	Tim Spiller	U York	CC-05-06
18:30	Quantum communication and cryptography in France	Eleni Diamanti	CNRS	CC-05-07
18:55	DemoQuandT: The quantum communication testbed for Germany	Oleg Nikiforov	DT	CC-05-08

Quantum Sensing Track

All the times in the program are **Japan Standard Time(GMT+9)**

29th Nov Sessions are a joint-program with The 5th IFQMS (The 5th International Forum on Quantum Metrology and Sensing).

29 Nov (Tue.)	Session / Presentation	Chairperson / Presenter	Affiliation	Abstract PDF
8:00-10:10	SE-01. Q-Sensors for Life Science, NV Center and Applications for Life Sciences Chairperson	Hitoshi Ishiwata	QST	
8:00	Dynamics and mechanism of dimer dissociation of UVR8 photoreceptor	Dongping Zhong	Ohio State U	SE-01-01
8:30	Photoactivation of rhodopsins	Hideki Kandori	NITech	SE-01-02
9:10	How can we measure the quality of consciousness?	Makiko Yamada	QST	SE-01-03
9:40	Theoretical study on quantum dynamics in condensed phase molecular systems	Akihito Ishizaki	IMS	SE-01-04
10:30-12:00	SE-02. Solid-State Quantum Sensors Chairperson	Hiroimitsu Kato	AIST	
10:30	Quantum sensing and imaging with diamond spins	Ania Jayich	UCSB	SE-02-01
11:00	Hybrid diamond-doped optical fibres for remote magnetometry applications	Brant Gibson	RMIT U	SE-02-02
11:30	Quantum sensing by NV centers in diamond semiconductor	Norikazu Mizuochi	Kyoto U	SE-02-03
13:10-16:10	SE-03A. Short Presentation Session for Young Scientists on SE-02,04,06,07 Topics [5th IFQMS]			
13:10-16:10	SE-03B. Short Presentation Session for Young Scientists on SE-01,05 Topics [5th IFQMS]			
17:00-19:00	SE-04. Solid-State Quantum Sensors Chairperson	Shinobu Onoda	QST	
17:00	Controlling and exploiting defects in diamond for quantum technologies	Mark Newton	U Warwick	SE-04-01
17:30	Methods for deterministic production of colour centres in diamond	Jan Meijer	U Leipzig	SE-04-02
18:00	Synthesis of single crystal diamond with colour centres for quantum applications	Alexandre Tallaire	CNRS	SE-04-03
18:30	Introduction to quantum brilliance and its R&D programs	Marcus Doherty	ANU / Quantum Brilliance	SE-04-04
19:20-21:10	SE-05. Q-Sensors for Life Science, NV Center and Applications for Life Sciences Chairperson	Makoto Negoro	Osaka U	
19:20	Hyperpolarized solution-state NMR spectroscopy via quantum resources	Ilai Schwartz	NVision	SE-05-01
19:55	Dissolution dynamic nuclear polarization	Jan Ardenkjar-Larsen	DTU	SE-05-02
20:35	Free radical detection in living cells	Romana Schirhagl	U Groningen	SE-05-03

30 Nov (Wed.)	Session / Presentation	Chairperson / Presenter	Affiliation	Abstract PDF
9:20-12:00	SE-06. Atom Interferometer, Atom/Ion Clocks Chairperson	Tomoya Sato	Tokyo Tech	
9:20	Keeping the quantum state alive: minute-scale coherence in an atom interferometer	Holger Muller	Stanford U	SE-06-01
10:00	Toward rotation sensing using a trapped single ion	Takashi Mukaiyama	Osaka U	SE-06-02
10:40	Enhanced quantum control for the next generation of optical lattice clocks	Andrew Ludlow	NIST	SE-06-03
11:20	Quantum metrology and computing using microscopically-controlled arrays of alkaline-earth	Adam Kaufman	JILA	SE-06-04
17:00-19:40	SE-07. Atom Interferometer, Atom/Ion Clocks Chairperson	Hidekazu Hachisu	NICT	
17:00	Quantum sensors with matter waves	Philippe Bouyer	U Amsterdam	SE-07-01
17:40	Exploring quantum gases for terrestrial and space-borne interferometry	Ernst Rasel	LUH	SE-07-02
18:20	A highly charged ion based optical atomic clock	Lukas Spies	PTB	SE-07-03
19:00	Robust Yb optical lattice clock for contributing to international atomic time	Masami Yasuda	AIST	SE-07-04

Quantum Sensing Track : Short Presentation Session for Young Scientists SE-03A. Short Presentation Session for Young Scientists on SE-02,04,06,07 Topics [5th IFQMS]

*Note: Presentation order may change within the same group.
All the times in the program are **Japan Standard Time**(GMT+9)

29 Nov (Tue.)	Session / Presentation	Mentor / Presenter	Affiliation	Abstract PDF
13:10-16:10	SE-03A. Short Presentations by Young Researchers on SE-02, 04, 06, 07 Topics [5th IFQMS]			
13:10-14:30	SE-03A- α 1			
	Chair	Ryota Katsumi	TUT	
	Co-chair	Naota Sekiguchi	Tokyo Tech	
	Lock-In detected ramsey magnetometry with a bulk ensemble of diamond NV centers for high-sensitivity DC-field measurement	Sena Tsuchiya	Tokyo Tech	SE-03A- α 1-01
	Towards measurement of magnetic field generated by the brain of a living rat using N-V centers in diamond	Naota Sekiguchi	Tokyo Tech	SE-03A- α 1-02
	Identification of current multipole sources from magnetoencephalography data	Motofumi Fushimi	UTokyo	SE-03A- α 1-03
	Optimization of simultaneous measurement of magnetic field and temperature measurement by silicon vacancy quantum sensor using simultaneous resonance	Tomoaki Tanaka	QST	SE-03A- α 1-04
	Spin-dependent photocarrier generation dynamics in electrically detected NV-based quantum sensor	Hiroki Morishita	Kyoto U	SE-03A- α 1-05
	Towards nanoscale zero- to ultralow-field NMR	Till Lenz	JGU	SE-03A- α 1-06
	Dipole-dipole interaction between NV- centers	Chikara Shinei	NIMS	SE-03A- α 1-07
13:10-14:30	SE-03A- β 1			
	Chair	Yuta Kainuma	Tokyo Tech	
	Co-chair	Naoya Morioka	Kyoto U	
	Extension of dephasing time of ensemble NV centers with a continuous-excitation protocol	Ikuya Fujisaki	Tokyo Tech	SE-03A- β 1-01
	Wide temperature operation of diamond quantum sensor for electric vehicle battery monitoring	Keisuke Kubota	Tokyo Tech	SE-03A- β 1-02
	A development of wearable magnetic shield for MEG	Soichiro Shido	UTokyo	SE-03A- β 1-03
	Attempts to generate entanglement state between dipolar coupled NV centers created by molecular implantation	Kosuke Kimura	QST	SE-03A- β 1-04
	Charge stability of shallow single NV centers in p-type diamond	Taisuke Kageura	AIST	SE-03A- β 1-05
	Room-temperature electrical detection of nuclear spins in silicon carbide	Naoya Morioka	Kyoto U	SE-03A- β 1-06
	(Near) zero-field cross-relaxation features for ensembles of NV centers in diamond	Muhib Omkar	JGU	SE-03A- β 1-07
13:10-14:30	SE-03A- γ 1			
	Chair	Tomoya Sato	Tokyo Tech	
	Co-chair	Fumihiko China	NICT	
	Evaluation of a superconducting nanowire single photon detector for mid-infrared wavelengths	Satoru Mima	NICT	SE-03A- γ 1-01*
	Efficient superconducting nanostrip single-photon detectors for 2 μ m wavelength	Fumihiko China	NICT	SE-03A- γ 1-02
	Effect of pump laser linewidth on nonlinear quantum interferometric fringes	Jasleen Kaur	Kyoto U	SE-03A- γ 1-03
	Highly efficient and ultra-broadband photon pair source using chirped quasiphase matching slab waveguide matching slab waveguide	Bo Cao	Kyoto U	SE-03A- γ 1-04
	Optical trapping and movement control of gold nanoparticles on an optical nanofiber	Rui Sun	Tohoku U	SE-03A- γ 1-05
	Electromagnetic-field analysis of the plasmon-enhanced single photon emitters on an optical nanofiber	Yining Xuan	Tohoku U	SE-03A- γ 1-06
	Ultrafast measurement of biphoton wave packets using optical Kerr gating	Takahisa Kuwana	UEC	SE-03A- γ 1-07
14:50-16:10	SE-03A- α 2			
	Chair	Naota Sekiguchi	Tokyo Tech	
	Co-chair	Ryota Katsumi	TUT	
	Growth of thick CVD diamond films containing aligned nitrogen-vacancy centers for high-sensitivity quantum sensors	Takeyuki Tsuji	Tokyo Tech	SE-03A- α 2-01
	Enhancement of fluorescence collection efficiency using angle-shaped diamonds for compact magnetic sensor	Yuta Shigenobu	Tokyo Tech	SE-03A- α 2-02

Note: This program was created for fostering young scientists. Presentations with asterisks (*) are excluded from awarding.

29 Nov (Tue.)	Session / Presentation	Mentor / Presenter	Affiliation	Abstract PDF
	Transfer-printing-based integration of SiN grating structure on diamond toward highly sensitive quantum sensor	Ryota Katsumi	TUT	SE-03A- α 2-03
	NVC-SPM system to inspect electric devices	Teruo Kohashi	Hitachi	SE-03A- α 2-04*
	Enhancing sensitivity with entanglement in coupled nitrogen vacancy centres	Ernst David Herbschleb	Kyoto U	SE-03A- α 2-05
	Frequency-bin generation of entangled photons via quantum optical synthesis	Takeru Naito	UEC	SE-03A- α 2-06
	Development of highly sensitive gravimeter based on atom interferometry using hybrid system for field applications	Takeshi Hojo	UEC	SE-03A- α 2-07
14:50-16:10	SE-03A- β 2			
	Chair	Naoya Morioka	Kyoto U	
	Co-chair	Yuta Kainuma	Tokyo Tech	
	Implementation of double quantum magnetometry to continuously excited ramsey method	Yuta Araki	Tokyo Tech	SE-03A- β 2-01
	Development of highly sensitive compact quantum sensor with NV center in ^{12}C -enriched CVD diamond for bio-medical and industrial application	Yuta Kainuma	Tokyo Tech	SE-03A- β 2-02
	Development of a nonmagnetic helical sensor drive multipoint measuring mechanism for magnetocardiography in animals	Wenyu Shang	UTokyo	SE-03A- β 2-03
	Ensemble NV- center in diamond for quantum sensing created by high fluence electron beam irradiation	Shuya Ishii	QST	SE-03A- β 2-04
	Synthesis of n-type diamond using tert-butyl phosphine for high sensitivity of the NV sensor	Riku Kawase	Kyoto U	SE-03A- β 2-05
	Decoherence phenomena in nitrogen-vacancy diamond	Aulden Jones	Georgia Tech	SE-03A- β 2-06
14:50-16:10	SE-03A- γ 2			
	Chair	Fumihiro China	NICT	
	Co-chair	Tomoya Sato	Tokyo Tech	
	Improvement in the long-term stability of the interferometer gyroscope using slow and continuous atomic beams	Naoki Nishimura	Tokyo Tech	SE-03A- γ 2-01
	Bragg interferometer using slow and continuous atomic beam with sub-recoil transverse momentum width	Tomoya Sato	Tokyo Tech	SE-03A- γ 2-02*
	Development of a cryogenic suspension system for Torsion-Bar Antennae (TOBA)	Ching Pin Ooi	UTokyo	SE-03A- γ 2-03
	Torsion-bar antenna for early earthquake alert	Yuka Oshima	UTokyo	SE-03A- γ 2-04
	Optimized Design of Quasi-phase-matched crystal for Spectrally-Pure-State Generation at MIR Wavelengths Using Metaheuristic Algorithm	Wu-Hao Cai	Tohoku U	SE-03A- γ 2-05
	Experimental generalized measurement of qubits using a quantum computer	Tingrui Dong	Tohoku U	SE-03A- γ 2-06

Note: This program was created for fostering young scientists. Presentations with asterisks (*) are excluded from awarding.

Quantum Sensing Track : Short Presentations by Young Researchers SE-03B. Short Presentation Session for Young Scientists on SE-01,05 Topics [5th IFQMS]

All the times in the program are **Japan Standard Time (GMT+9)**

29 Nov (Tue.)	Session / Presentation	Mentor / Presenter	Affiliation	Abstract PDF
13:10-16:10	SE-03B. Short Presentation Session for Young Scientists on SE-01,05 Topics [5th IFQMS]			
13:10-14:30	SE-03B- α 1.			
	Chair	Noriaki Yahata	QST	
	Co-chair	Hidetoshi Kono	QST	
	Structural dynamics of the Mn4CaO5 cluster during the S2-S3 transition in photosystem II	Hongjie Li	Okayama U	SE-03B- α 1-01
	Visualization of hydrogen in Photosystem II by high-resolution Cryo-EM analysis	Fusamichi Akita	Okayama U	SE-03B- α 1-02
	Pulsed-EPR study for radical reactions with biological antioxidants utilizing quantum effect of electron spin	Hiroki Hirano	Kanagawa U	SE-03B- α 1-03
	Coherent control of radical pair by local optimization theory	Akihiro Tateno	Saitama U	SE-03B- α 1-04
	Probing the coherent spin dynamics of radical pairs in weak magnetic field using nanoseconds field switching technique	Ryusei Nozawa	Saitama U	SE-03B- α 1-05
	Role of tyrosine radical in the photoreaction of the magnetoreceptor candidate molecule cytochrome4	Hiroaki Otsuka	Waseda U	SE-03B- α 1-06
	Cavity ring-down measurements by continuous pulse trains for magnetic field effects on transient radical species.	Tsubasa Kimura	Saitama U	SE-03B- α 1-07
	Germanium vacancy defects in detonation nanodiamonds for temperature sensing	Fu Haining	Kyoto U	SE-03B- α 1-08
	Evaluation of the surface-modified nanodiamond probes by in vivo fluorescence imaging	Koki Okamoto	Tokyo Tech	SE-03B- α 1-09
	Detection of heat generation from biological system using double quantum thermometry	Hitoshi Ishiwata	QST	SE-03B- α 1-10
	The Anomalous Formation of Irradiation Induced Nitrogen-Vacancy Centers in 5-Nanometer-Sized Detonation Nanodiamonds	Frederick Tze Kit SO	Kyoto U	SE-03B- α 1-11
	Microwave antenna architecture for quantitative prediction of ODMR signals	Keisuke Oshimi	Okayama U	SE-03B- α 1-12
14:50-16:10	SE-03B- α 2.			
	Chair	Yoichi Takakusagi	QST	
	Co-chair	Ryoko Araki	QST	
	An Artificial Intelligence Nanopore Platform Detects Mutant SARS-CoV-2 including Omicron Variant by Recognizing Spike Proteins	Kaoru Murakami	Hokkaido U	SE-03B- α 2-01
	Non-equilibrium ϕ_4 theory in a Hierarchy: Towards Manipulating Holograms in Quantum Brain Dynamics	Akihiro Nishiyama	Kobe U	SE-03B- α 2-02
	Construction of dipeptide-based DNP-NMR molecular probe library focusing on kidney injury mouse model	Yuki Aketa	U Tokyo	SE-03B- α 2-03
	Nuclear hyperpolarization of liquid water by using photoexcited triplet electrons in organic nanocrystals	Naoto Matsumoto	Kyushu U	SE-03B- α 2-04
	Molecular development for highly efficient Triplet-DNP	Keita Sakamoto	Kyushu U	SE-03B- α 2-05
	DNP-NMR molecular probe for the detection of Dipeptidyl peptidase-4 activity in vivo	Akihito Goto	U Tokyo	SE-03B- α 2-06
	Generation of polarized triplet electron spins at solid-liquid interfaces	Reiya Yabuki	Kyushu U	SE-03B- α 2-07
	Photoreaction study of a primate blue-light sensitive photoreceptor using vibrational spectroscopy	Yosuke Mizuno	NITech	SE-03B- α 2-08
	Novel photoisomerization reaction in near-infrared light absorbing enzymehodopsins	Masahiro Sugiura	NITech	SE-03B- α 2-09
	Development of single-shot 3D temperature imaging system for real-time observation of thermal diffusion in vivo	Haruka Maeoka	Hiroshima U	SE-03B- α 2-10
	Bidirectional neural network and its application to image denoising, super-resolution, and image completion	Kei Majima	QST	SE-03B- α 2-11
	Understanding of protein functional expression using hybrid QM/MM molecular simulation	Masahiko Taguchi	QST	SE-03B- α 2-12

Abstract

Tracks

PL

Plenary Sessions

Contents / Topics

Welcome from Organizing Committee and Hosts,
Plenary Talks, Keynote

Tracks

CP

Quantum Computing Track

Contents / Topics

Quantum Computing architecture, Quantum computers with Atoms and Ions, Photonic Quantum Computers, Fault Tolerant Quantum Computing, Quantum Algorithms for Chemistry, NISQ Algorithms, Young Pls Session, Superconducting Quantum Computing, Quantum Annealing, Verifiable Quantum Computing, Semiconductor Quantum Computers, Quantum Simulations

Tracks

CC

Quantum Cryptography & Communication Track

Contents / Topics

Quantum Internet, Young Researcher Panel Session,
Quantum Cryptography

Tracks

SE

Quantum Sensing Track

Contents / Topics

Q-sensors for Life Science, NV Center and Applications for Life Sciences, Solid-State Quantum Sensors, 5th IFQMS Short Presentation Session for Young Scientists, Solid-State Quantum Sensors, Q-sensors for Life Science, NV Center and Applications for Life Sciences, Atom Interferometer, Atom/Ion Clocks *29th Nov Sessions are a joint-program with The 5th IFQMS (The 5th International Forum on Quantum Metrology and Sensing).

PL-02-01

Quantum technology policy in Japan

Kohei Itoh*Keio University*

Biography

President Kohei Itoh graduated from Keio University and received his M. S. and Ph. D. in Engineering from University of California, Berkeley. He joined Keio University as a faculty member in 1995 and became a full professor in 2007. He served as Dean of Faculty and Graduate School of Science and Technology of Keio University between 2017 and 2019, and as the Chair of Keio AI and Advanced Programming Consortium between 2018 and 2021. His main focus of research has been quantum computing, quantum sensing, and quantum physics, which led to more than 330 journal publications. He is one of 210 Council Members of Science Council of Japan representing ~870,000 scholars of the country to propose and advice academic and scientific policies in Japan, and has served on numerous executive boards including the Physical Society of Japan and the Japan Society of Applied Physics. He leads the Program Director of Quantum Information Technology in the MEXT Quantum Leap Flagship Program for researchers representing the field. He is a recipient of the Japan IBM Prize (2006) and the JSPS (Japan Society for the Promotion of Science) Prize (2009). He is also a founder of the IBM Quantum Computer Network Hub at Keio University.

Abstract

In January 2020, Japanese Government compiled the “Quantum Technology and Innovation Strategy,” which formed the basis of policies to enhance research and development of quantum technology in Japan. Thanks to this initiative, Japan has been able to invest significant



amounts of financial and human resources to stay as one of the main players of quantum innovation in the world. In order to accelerate such effort even further, in March 2022, Japanese government has announced the “Vision of Quantum Future Society,” that aims to enable a social reform through quantum technology. This presentation overviews an overall policy of Japan on quantum technology research and development.

The national quantum initiative

Gretchen Campbell

National Quantum Coordination Office, OSTP

Biography

Gretchen Campbell is the Deputy Director for the National Quantum Coordination Office at the White House Office of Science and Technology Policy, where she helps coordinate QIS programs across the Federal Government. Campbell is on detail from the National Institute of Standards and Technology (NIST), where she is the co-director of the Joint Quantum Institute, a joint institute between the University of Maryland and NIST, and the Group Leader for the Laser Cooling and Trapping group in the Quantum Measurement Division at NIST. She is also an Adjunct Professor in the Department of Physics at the University of Maryland. Dr. Campbell received a B.A. in Physics from Wellesley College in 2001 and received her Ph.D. from MIT in 2007. From 2007-2009, she was a NRC postdoctoral fellow at JILA and NIST in Boulder, Colorado. Dr. Campbell's research has included a wide range of experimental work in the field of ultracold atomic gases. She is a fellow of the American Physical Society. Her awards include the Arthur Flemming Award (2012); the Presidential Early Career Award in Science and Engineering (2012); the Sigma Xi Katherine Blodgett Gebbie Young Scientist Award (2013); the APS Maria Goeppert Mayer Award (2015), and the IUPAP C15 Young Scientist Prize (2015). She was also a Finalist for the Samuel J. Heyman Service to America Medals, Call to Service category (2015).

Abstract

In 2018, the United States launched the National Quantum Initiative (NQI) to accelerate research and development (R&D) in quantum information

science (QIS) within the United States. Since then, the U.S. has been advancing QIS by getting the science right, enhancing competitiveness, and enabling people. For science, the NQI Act authorized U.S. Federal departments and agencies to establish centers to address the most pressing scientific frontiers in QIS. To enhance competitiveness, the U.S. has engaged industry and international partners to drive QIS technology development toward useful applications, while also protecting national security. To enable people, the U.S. is building the QIS workforce and conducting outreach to create new opportunities.

European policy

Gustav KALBE

European Commission

Biography

Dr. Gustav Kalbe is German, born in Belgium. From 1986 to 1990 he studied Applied Physics at the Université Catholique de Louvain, Belgium. In 1991 he studied Applied Optics at the Imperial College of Science in London. In 1995 he completed his studies and earned a PhD in Physics, Molecular Spectroscopy, at the Université Catholique de Louvain, Belgium.

He started his professional career as a project manager in photonic networks at the incumbent telecom operator in Belgium. He was R&D manager when he left the company.

In 1998 he joined the Directorate General Information Society & Media of the European Commission where he started working as Project Officer managing research projects of the European Framework Programs for Research. Over the years he had several assignments in quantum technologies, photonics, and cybersecurity.

In 2014 Gustav Kalbe became Head of Unit for Administration & Finance in the European Commission, in Directorate General Communications Networks, Content and Technology.

In 2016 he was appointed Head of Unit of the newly created High Performance Computing and Quantum Technology unit in Directorate General Communications Networks, Content and Technology.

In 2018 he became responsible for the establishment and operation of the European High Performance Computing Joint Undertaking. He occupied the post of Interim Executive Director of the Joint Undertaking until its autonomy by the end of 2020.

In January 2021, he was appointed Deputy to the Director of DG Connect C “Digital Excellence and Science Infrastructure”.

Since May 2022 Gustav is the Acting Director of DG Connect C “Digital

Excellence and Science Infrastructure”.

Abstract

I will introduce the European activities and policy approach in Quantum Technologies, starting with the Quantum Technologies Flagship and some of its successes during its ramp-up phase (2018-2021). I will then present the vision and avenues for Europe’s digital transformation by 2030, as proposed in 2021 by the European Commission in the Europe’s Digital Decade, pursuing the ambition to reach a first European computer with quantum acceleration by 2025. Following this vision, the European policy approach to quantum has naturally transitioned towards higher technical maturity with the deployment of quantum-based infrastructures. In this context, first I will introduce the pilot lines (factories) for advanced quantum chip production (so-called “fabs”) as one of the new instruments of the European Chips Act, then I will present the European Quantum Communication Infrastructure (EuroQCI) Initiative aiming at building a secure quantum communication infrastructure that will span the whole EU. Finally, I will present the European High-Performance Computing Joint Undertaking (EuroHPC JU) and its roadmap to quantum computing deployment including the recent selection of six sites that will host the first European quantum computers, with a view on the Japan-EU Digital Partnership established in Spring 2022.

PL-02-04

Enabling & growing the quantum industry

Celia Merzbacher

Executive Director, Quantum Economic Development Consortium (QED-C)

Biography

Dr. Celia Merzbacher, QED-C Executive Director

Abstract

The Quantum Economic Development Consortium (QED-C) is a consortium of stakeholders that aims to enable and grow the U.S. quantum industry.

PL-02-05

Strengthening Europe's quantum industry on the global stage

Thierry Botter

Executive Director, Quantum Industry Consortium (QuIC)

Biography

Dr. Thierry Botter, Executive Director, European Quantum Industry Consortium (QuIC)

Abstract

Overview presentation of the European Quantum Industry Consortium (QuIC), Europe's largest and most influential quantum industry group.

Introduction of Q-STAR -Create industries & businesses with quantum technology-

Taro Shimada

Quantum Strategic Industry Alliance for Revolution (Q-STAR)

Biography

Taro Shimada joined Toshiba in October 2018 as Corporate Digital Business Chief Strategy Officer. He has served as Chief Digital Officer, responsible for supporting Toshiba's digital transformation and spearheading strategic business creation and promotion, since April 2019. He was appointed CEO & Representative Director of Toshiba Data Corporation in February 2020, and President and CEO of Toshiba Digital Solutions Corporation in April 2020. In March 2022, Mr. Shimada was appointed to take the reins at Toshiba, as President & CEO.

Mr. Shimada has a diverse background in hardware development, including commercial aircraft; in process consultation, ranging from automobiles to precision machinery design and heavy industry; and in product life cycle management software. As an expert in Factory Automation, he advised many of Japan's leading global manufacturers on digitization, and he remains an advisor to the Robot Revolution & Industrial IoT Initiative, and to the IoT Acceleration Lab. He has also contributed to the activities of Industrie 4.0 in Germany and Connected Industries in Japan.

Mr. Shimada began his career in 1990 at ShinMaywa Industries Kobe, where he worked on aircraft for Boeing and McDonnell Douglas. In 1999 he joined Structural Dynamics Research Corporation, a part of Siemens, and took on a series of progressively senior post at Siemens KK, and at Siemens HQ in Germany. Immediately prior to joining Toshiba, Mr. Shimada was Executive Operating Officer at Siemens K.K. He has been a guest professor at Otomon Gakuin University in Osaka, Japan, since April 2020. In May 2022, he was appointed Chairman of Q-STAR (Quantum

Strategic industry Alliance for Revolution), a consortium that promotes business creation with quantum technologies.

Away from the office Mr. Shimada relaxes by playing the drums, and enjoys all genres of music.

Abstract

As quantum technologies start the shift from R&D to commercialization, there are several areas where advances are required.

These are discussed in an overview of recent trends in quantum technology.

The latter half of the presentation introduces Q-STAR.

Now a general incorporated association, Q-STAR is accelerating its efforts to create new quantum businesses.

The presentation discusses how these activities support Q-STAR's goal of contributing to a future society where quantum technology is taken for granted.

Promoting Quantum Innovation through the triangle collaboration

Akihisa Tomita

Quantum ICT Forum / Hokkaido University

Biography

Akihisa Tomita received the B.S. and M.S. degrees in physics and the Ph.D. degree in electronics from the University of Tokyo in 1982, 1984 and 1998, respectively. He engaged in the research on photonics from 1984 to 2000 and conducted research on quantum information technology from 1998 to 2010 both in NEC Corporation. He also led the group for quantum information experiments in Quantum Computation and Information Project, ERATO and SORST, JST, from 2000 to 2010. He is a professor at Faculty of Information Science and Technology, Hokkaido University since 2010. His current research covers photonics for quantum information processing and quantum communication.

Abstract

To create a sophisticated society, it is required to establish efficient processing and analysis of large quantities of data collected from various places, decision of the optimum actions, and accomplishment of the order sent from the artificial intelligence. Highly sensitive and highly accurate sensors, high-speed computers, and communications with low latency and guaranteed security are thus necessary. Quantum information and communication technology (ICT) is a radical solution to these challenges. Though the potential of quantum ICT was already known from the mid 1980s to 2000s, its realization has long been in question. However, Quantum ICT has come to be recognized worldwide as an emerging technology in the foreseeable future, rather than a

technology that may or may not be realized. Quantum ICT Forum (QICTF) was established to bring innovation in the quantum technology and to contribute to the realization of a creative society by working on the development and diffusion of quantum ICT. In this talk, I will review the scientific and industrial activities on quantum ICT in Japan shortly. Then, I will present efforts to encourage the triangle collaboration between the industry, government, and academia.

PL-02-08

Moonshot Goal 6: Realization of a fault-tolerant universal quantum computer that will revolutionize economy, industry, and security by 2050

Masahiro Kitagawa

Japan Science and Technology Agency / Osaka University

Biography

Dr. Masahiro Kitagawa is a Professor of Graduate School of Engineering Science <https://www.es.osaka-u.ac.jp/en/> and the director of Center for Quantum Information and Quantum Biology <https://qiqb.osaka-u.ac.jp/en/>, Osaka University. He received BEng in '81, MEng in '83, and Ph.D. in quantum physics in '94 from Osaka University. He was a research scientist at NTT Basic Research Laboratories from '83 to '93. He has been working on quantum optics and quantum information since '85. He has been a faculty member of Osaka University since '93 and a Professor since '03. He has served as Research Director of JST/CREST Projects; Nuclear Spin Network Quantum Computers ('99-05), Molecular Spin Quantum Computers ('05-11), and, Hypersensitive MRI/NMR by means of Room Temperature Hyperpolarization and Quantum Coding ('16-22). His research interest covers quantum measurement and sensing, quantum communications, quantum computing, and, quantum biology. He serves as the program director of the Moonshot Goal 6 toward fault-tolerant universal quantum computer <https://www.jst.go.jp/moonshot/en/program/goal6/>, the project leader of the Quantum Software Research Hub <http://qsrh.jp/> and a member of the quantum innovation committee of the cabinet office since '20. He is a co-founder of QunaSys Inc. <https://en.qunasys.com>, a quantum software startup, and QuEL Inc. <https://quel-inc.com>, a quantum middleware startup. His paper on "Squeezed Spin States" is selected as Physical Review A 50th Anniversary Milestones <https://journals.aps.org/pr/50th>. He is a life member of American

Physical Society and a member of Physical Society of Japan.

Abstract

Moonshot goal 6 is an ambitious and challenging program towards fault-tolerant universal quantum computer. The strategy and the portfolio of the program, and, the project managers and their projects will be introduced. The moonshot international symposium to be held next July in Tokyo will be announced.

PL-03-01

The next wave of computing: quantum-centric supercomputing

Jerry Chow

IBM Quantum

Biography

Dr. Jerry M. Chow is an IBM Fellow and the Director of Quantum Infrastructure at IBM leading the effort to envision and implement IBM's quantum hardware roadmap encompassing technology, characterization, and system integration. His technical expertise is in the area of superconducting qubits quantum computing. Chow graduated magna cum laude with a BA in physics and MS in applied mathematics from Harvard University (2005) and subsequently a PhD in physics from Yale University (2010). He joined IBM as a Research Staff Member in 2010. In 2016 he co-lead the IBM Quantum Experience project, placing a real quantum processor accessible to anyone on the Cloud. In 2021, he was named an APS Fellow in the Division of Quantum Information and received the Yale Science and Engineering Association Award for Advancement of Basic and Applied Science.

Abstract

The last few years have witnessed a strong evolution in quantum computing technologies, moving from research labs to an unprecedented access by the general public via the cloud. Recent progress in quantum processor size, speed, and quality, have cleared the picture towards a long-term vision in computing, where quantum processors will play a key role in extending the computational reach of supercomputers. In this talk I will describe how modularity will enable scaling, and how quantum communication will increase computational capacity. All this orchestrated by a hybrid cloud middleware for quantum for seamless integration of classical and quantum workflows in an architectural construct that we call quantum-centric supercomputer.

From synchronization to chemical reaction superpositions

Gregory D Scholes

Princeton University

Biography

Greg Scholes is the William S. Tod Professor of Chemistry and Chair of Department at Princeton University. This year he was selected as an inaugural Ivy+ Provost Leadership Fellow with the goal of helping to advance diversity and inclusion in the American professoriate. Originally from Melbourne, Australia, he later undertook postdoctoral training at Imperial College London and University of California Berkeley. He started his independent career at the University of Toronto (2000-2014) where he was the D.J. LeRoy Distinguished Professor. He was appointed Editor-in-Chief of the Journal of Physical Chemistry Letters in 2019. Dr. Scholes was elected a Fellow of the Royal Society (London) in 2019 and a Fellow of the Royal Society of Canada in 2009.

Abstract

Synchronization abounds in nature—why is it so hard to synchronize quantum systems? I will discuss this general question and its relationship to quantum coherence and exciton delocalization. I will then report new experiments that show how a molecular exciton state can launch two a superposition of two chemical reactions. Specifically, we study femtosecond proton transfer in a symmetric molecule with two identical reactant sites that are spatially apart. With the reaction launched from a superposition of two local basis states, we hypothesize that the motions of the electrons and nuclei will ensue in lock-step as a superposition of probability amplitudes until decoherence collapses the system to a product. We see evidence for this, and conclude that this chemical system is a good test-bed to study the transition from quantum to classical.

PL-03-03

Quantum diamond sensors – Best of both worlds

Ronald Walsworth

University of Maryland

Biography

Ronald Walsworth is a Minta Martin Professor in the Department of Physics and in the Department of Electrical and Computer Engineering at the University of Maryland (UMD). He is also the Founding Director of the Quantum Technology Center (QTC) at UMD, which focuses on the development and translational applications of quantum science, as well as education of the quantum technology workforce.

Abstract

The nitrogen–vacancy (NV) quantum defect in diamond is a leading modality for magnetic, electrical, temperature, and force sensing with high spatial resolution and wide field-of-view under ambient conditions. This quantum sensing technology has diverse applications across the physical and life sciences — from probing magnetic materials to imaging integrated circuit activity to biomedical diagnostics. I will provide an overview of quantum diamond sensors and their many applications; and outline paths toward improved performance and utility.

PL-03-05

Optical quantum computers with quantum teleportation

Akira Furusawa*The University of Tokyo / RIKEN*

Biography

Akira Furusawa received his MS degree in applied physics and Ph.D. degree in physical chemistry from The University of Tokyo, Japan, in 1986 and 1991, respectively. His research interests cover the area of nonlinear optics, quantum optics, and quantum information science. He is currently Professor of Applied Physics, School of Engineering, The University of Tokyo and the Deputy Director of RIKEN Center for Quantum Computing. Professor Furusawa has authored more than 100 papers in leading technical journals and conferences, which include the first realization of unconditional quantum teleportation, which was achieved in 1998 at California Institute of Technology as a visiting scientist at Professor Jeff Kimble's lab. He received the Ryogo Kubo Memorial Award in 2006, the JSPS prize in 2007, the Japan Academy Medal in 2007, the International Quantum Communication Award in 2008, the Toray Science and Technology prize in 2015, and the Medal with purple ribbon in 2016. He is a member of the Physical Society of Japan, the Japanese Society of Applied Physics, and OPTICA.

Abstract

We did the first experiment of unconditional quantum teleportation at Caltech in 1998 [1]. Then we did various related experiments like quantum teleportation network [2], teleportation of Schrödinger's cat state [3], and deterministic quantum teleportation of photonic qubits [4]. We invented the scheme of teleportation-based quantum computing in

2013 [5]. In this scheme, we can multiplex quantum information in the time domain and we can build a large-scale optical quantum computer only with four squeezers, five beam splitters, and two optical delay lines [6]. Our present goal is to build a super quantum computer with 100GHz clock frequency and hundred cores. Toward this goal we started to combine our optical quantum computer with 5G technologies [7].

1. A. Furusawa et al., *Science* 282, 706 (1998).
2. H. Yonezawa et al., *Nature* 431, 430 (2004).
3. N. Lee et al., *Science* 332, 330 (2011).
4. S. Takeda et al., *Nature* 500, 315 (2013).
5. S. Yokoyama et al., *Nature Photonics* 7, 982 (2013).
6. W. Asavanant et al., *Science* 366, 375 (2019).
7. A. Inoue et al., arXiv:2205.14061 [quant-ph]

How science is becoming and industry

Rupert Ursin

qtlabs GmbH

Biography

Dr. Rupert Ursin is co-founder of qtlabs GmbH. He has 20+ years research experience in quantum communication at the Austrian Academy of Science. His scientific publications describe groundbreaking experiments at the time and are among the highest cited in the field – still today. His research focus is the development of quantum communication and quantum information processing technologies, especially for free space transmission up to satellites, but also for fiber-based systems. Aims of his work range from short-term engineering solutions for secure key partitioning (quantum cryptography) to speculative research (quantum teleportation and entanglement swapping). He is now CEO at the company he founded with his former postDoc Thomas Scheidl who is now CTO and CEO of qtlabs GmbH. qtlabs is doing R&D and prototyping of quantum technologies aimed at performing full scale QKD from satellites and through optical fibers; first products include, besides the tasks as a quantum engineering firm for architecture, design and simulation of quantum networks, optical ground receivers for quantum states.

Abstract

Quantum Physics originated from very deep questions about the nature of reality and locality. Only in the 80's it turned out, that might become the basis of a new kind of technology – today called quantum technology. In my presentation I will show my personal journey from experiments about basic interest in academia up to a research group leader and deputy

director at the Austrian Academy of Sciences here in Vienna. Just recently I quit my permanent position to become a full-time entrepreneur, now developing products for the so-called quantum technology revolution. I'll present the ecosystem, including a Chinese satellite mission MICIUS, we've been part of, to the European quantum Programs, the demand from the finance- and critical-infrastructure industry and the products we are developing, both for space and terrestrial applications.

Quantum network technology - the second life of rare-earth crystals

Tittel Wolfgang

University of Geneva, Delft Technical University, Schaffhausen Institute of Technology

Abstract

Starting with the demonstration of lasing more than 50 years ago, the special properties of rare-earth crystals and glasses have enabled the development of numerous solid-state lasers and amplifiers, which are crucial for the functioning of today's Internet. As a fascinating generalization of their use in optical communication infrastructure, it became clear during the past decade that, when cooled to a few Kelvin, rare-earth crystals also promise the creation of technology for quantum communication networks.

I will discuss recent advances towards the development of key ingredients of such networks: the creation of single photons using individual rare-earth ions coupled to nano-photonic cavities, as well as the reversible storage of quantum states of light in large ensembles of rare-earth ions. This work is not only interesting from a fundamental point of view, but furthermore paves the path towards a quantum repeater, which will ultimately enable quantum communications over arbitrary distances.

Abstract

Tracks

PL

Plenary Sessions

Contents / Topics

Welcome from Organizing Committee and Hosts,
Plenary Talks, Keynote

Tracks

CP

Quantum Computing Track

Contents / Topics

Quantum Computing architecture, Quantum computers with Atoms and Ions, Photonic Quantum Computers, Fault Tolerant Quantum Computing, Quantum Algorithms for Chemistry, NISQ Algorithms, Young Pls Session, Superconducting Quantum Computing, Quantum Annealing, Verifiable Quantum Computing, Semiconductor Quantum Computers, Quantum Simulations

Tracks

CC

Quantum Cryptography & Communication Track

Contents / Topics

Quantum Internet, Young Researcher Panel Session,
Quantum Cryptography

Tracks

SE

Quantum Sensing Track

Contents / Topics

Q-sensors for Life Science, NV Center and Applications for Life Sciences, Solid-State Quantum Sensors, 5th IFQMS Short Presentation Session for Young Scientists, Solid-State Quantum Sensors, Q-sensors for Life Science, NV Center and Applications for Life Sciences, Atom Interferometer, Atom/Ion Clocks *29th Nov Sessions are a joint-program with The 5th IFQMS (The 5th International Forum on Quantum Metrology and Sensing).

CP-01-01

Greater quantum efficiency through physics-aware system software

Chong Fred*University of Chicago / ColdQuanta*

Abstract

Quantum computing is at an inflection point, where 127-qubit machines are deployed, and 1000-qubit machines are perhaps only a few years away. These machines have the potential to fundamentally change our concept of what is computable and demonstrate practical applications in areas such as quantum chemistry, optimization, and quantum simulation.

Yet a significant resource gap remains between practical quantum algorithms and real machines. A promising approach to closing this gap is to design software that is aware of the key physical properties of emerging quantum technologies. I will illustrate this approach with some of our recent work that focuses on techniques that break traditional abstractions and inform hardware design, including compiling programs directly to analog control pulses, computing with ternary quantum bits, 2.5D architectures for surface codes, and exploiting long-distance communication and tolerating atom loss in neutral-atom machines.

CP-02-01

Recent advances toward a more capable trapped ion quantum computer

Patty Lee

Quantinuum

Abstract

Critical applications of quantum computation require higher performance than today's quantum computers can provide. Towards that end, Quantinuum has continued to improve the performance of H-Series quantum computers in the past year, by increasing the fidelity of quantum operations and the number of qubits in H1 systems, to achieve a Quantum Volume of 8192. With the updated hybrid computing feature, we embarked on fault-tolerant quantum computing by entangling two logical qubits on H1. Additional breakthroughs including junction transport, state preparation and measurement fidelity improvements, and a qubit re-use compiler pave the way to scaling up to larger and more capable quantum computers.

CP-03-01

Blueprint for a scalable photonic fault-tolerant quantum computer

J. Eli Bourassa

Xanadu

Abstract

This talk will present Xanadu's proposal for a scalable and fault-tolerant photonic quantum computer. Central to the architecture are Gottesman-Kitaev-Preskill bosonic qubits and squeezed states of light, stitched together into a qubit cluster state with one time and two spatial dimensions. This proposal for generating and manipulating a 3D resource state for fault-tolerant, measurement-based quantum computation combines state-of-the-art proposals for the preparation of bosonic qubits with the strengths of continuous-variable quantum computation performed using easy-to-generate squeezed states. Moreover, the architecture is based on modular, easy-to-network integrated photonic chips, opening the door to scalable fabrication and operation.

The PhANTM algorithm: measurement-based generation and preservation of cat and grid states

Olivier Pfister

University of Virginia

Abstract

We present an algorithm to reliably generate various quantum states critical to quantum error correction and universal continuous-variable (CV) quantum computing, such as Schrödinger cat states and Gottesman-Kitaev-Preskill (GKP) grid states, out of Gaussian CV cluster states. Our algorithm is based on the Photon-counting-Assisted Node-Teleportation Method (PhANTM), which uses standard Gaussian information processing on the cluster state with only the addition of local photon-number-resolving measurements. We show that PhANTM can apply polynomial gates and embed cat states within the cluster. This method also stabilizes cat states against Gaussian noise and perpetuates non-Gaussianity within the cluster. Finally, we show that existing protocols for breeding cat states can be embedded into cluster state processing using PhANTM.

CP-04-01

Suppressing quantum errors by scaling a surface code logical qubit

Zijun Chen*Google Quantum AI*

Abstract

Practical quantum computing will require error rates that are well below what is achievable with physical qubits. Quantum error correction offers a path to algorithmically-relevant error rates by encoding logical qubits within many physical qubits, where increasing the number of physical qubits enhances protection against physical errors. However, introducing more qubits also increases the number of error sources, so the density of errors must be sufficiently low in order for logical performance to improve with increasing code size. In this talk, I will discuss recent work measuring logical qubit performance scaling across multiple code sizes, and demonstrate that our system of superconducting qubits has sufficient performance to overcome the additional errors from increasing qubit number. We find our distance-5 surface code logical qubit modestly outperforms an ensemble of distance-3 logical qubits on average, both in terms of logical error probability over 25 cycles and logical error per cycle. We are able to accurately model our experiment, and from this model we can extract error budgets that highlight the biggest challenges for future systems. These results mark the first experimental demonstration where quantum error correction begins to improve performance with increasing qubit number, illuminating the path to reaching the logical error rates required for computation.

Current status of variational quantum algorithms for chemistry and beyond

Wataru Mizukami

Center for Quantum Information and Quantum Biology, Osaka Univ., Japan

Abstract

Quantum chemistry has been seen as a promising application for quantum computers so far. Driven by this expectation, the development of algorithms for quantum chemistry using quantum computers has been active over the past five years. As a result, variational quantum algorithms (VQAs) can now be used to perform a wide range of chemical calculations with quantum circuit emulators. Such state-of-the-art VQAs have been implemented in various open-source software and cloud services and are readily available to anyone. On the other hand, the challenges for the practical application of quantum chemical calculations using real quantum computers are becoming increasingly clearer. In this talk, I will first introduce our progress in quantum chemical calculations using VQA. Next, I will introduce 1) our recently-proposed perturbation theory using quantum signal processing [arXiv:2210.00718] and 2) resource estimation for phase estimation for model Hamiltonians [arXiv:2210.14109], respectively, and discuss challenges that lie ahead.

CP-06-01

Statistical method for quantum estimation algorithms

Naoki Yamamoto*Keio University*

Abstract

In this talk I will present some quantum algorithms that incorporate statistical methods for lowering the required number of entangling gates as well as the number of qubits, while maintaining quantum advantage to estimate target quantities. As a particular example, I will present the quantum-enhanced mean-value estimation algorithm; namely, the quantum algorithm for estimating the mean value of physical observables with less number of queries compared to the conventional approach.

CP-07-01

Programmable continuous-variable photonic quantum computing in the time domain

Shuntaro Takeda*The University of Tokyo*

Abstract

Photonic quantum computing has recently been dramatically scaled up, demonstrating quantum supremacy and large-scale entangled state generation. Such progress has been made by an approach combining continuous-variable and multiplexing schemes. The continuous-variable scheme offers more efficient quantum light sources and detectors than the traditional qubit-based scheme. On the other hand, the multiplexing schemes in time, frequency, and spatial modes enable us to scale up quantum computation in compact photonic circuits. The combination of these schemes is a promising route to large-scale quantum computers.

We are pursuing programmable and scalable photonic quantum computers based on the continuous-variable and time-multiplexing schemes. In particular, we proposed a loop-based photonic quantum computing architecture where a single quantum processor sequentially performs gates on time-multiplexed optical pulses arranged in a loop (Physical Review Letters 119, 120504 (2017)). In this talk, we introduce our recent development in this direction, including the demonstration of a programmable multi-step quantum processor (Science Advances 7, eabj6624 (2021)), the development of a programmable time-multiplexed quantum light source (arXiv:2209.09458), and the implementation of a quantum algorithm using a programmable photonic circuit (arXiv:2206.07214).

CP-07-02

Design and optimization of fault-tolerant quantum computing

Yasunari Suzuki*Nippon Telegraph and Telephone Corporation*

Abstract

While fault-tolerant quantum computing (FTQC) is considered the most promising way to achieve reliable quantum computing, it demands the integration of high-fidelity physical qubits and the complicated design of logic units. To steadily reduce the difficulties, we need a concrete baseline evaluation and optimization methods based on it. In this talk, I present a framework for evaluating critical components of FTQC. Then, I will explain recent our results to optimize the performance of FTQC.

CP-07-03

Quantum error correction by low-depth random Clifford circuits

Yoshifumi Nakata*Yukawa Institute for Theoretical Physics, Kyoto University*

Abstract

Quantum random encoding is a method of generating quantum error correcting codes (QECCs) by random quantum circuits and is known to have high performance of correcting various noises. While it was originally proposed as a theoretical technique, recent developments, both from theoretical and experimental approaches, have opened the possibility of realizing it by near-term quantum devices. In this work, we show that QECCs generated by one-dimensional log-depth random Clifford circuits can be efficiently decoded and have high performance against stochastic Pauli noise. More specifically, we construct a maximally-likelihood decoder based on the tensor-network method, which works efficiently if the encoding circuit is at most log-depth. Using the decoder, we numerically show that the performance of the code almost matches that of fully random ones if the circuit is at least log-depth. The combination of efficient decoding and high performance against stochastic Pauli noise show that such codes are good candidates for near-term quantum memories.

Faster emulation of noisy VQE

Tyson Ray Jones

University of Oxford

Abstract

Variational quantum eigensolving (VQE) is a much touted application of near-future quantum computers. It involves the minimisation of a high-dimensional (but polynomially growing) cost function which is classically intractable to evaluate, but quantumly efficient to explore. Many minimisation strategies have emerged in the literature, from simple quantum gradient descent which involves evaluating cost gradients, to quantum natural gradient which involves the quantum geometric tensor. Classical emulation of VQE is tantamount in its study, but the time to classically compute the aforementioned variational quantities becomes an unignorable bottleneck. Recent works have devised bespoke simulation algorithms to overcome this hurdle in noise-free settings, though they cannot capture realistic noisy behaviours of present day devices. We here present novel algorithms for asymptotically faster classical simulation of quantum gradient descent and the quantum natural gradient, where the latter is generalised for channels and replaces the geometric tensor with an approximate Fisher information matrix. Our work permits the exact numerical investigation of significantly larger variational problems in noisy settings described by arbitrary Kraus channels, which can themselves be parameterised. These schemes have been integrated into QuESTlink, a Mathematica simulator of quantum computers.

One hundred second bit-flip time in a two-photon dissipative oscillator

Zaki Leghtas

Mines ParisTech / Ecole Normale Supérieure

Abstract

Current implementations of quantum bits (qubits) continue to undergo too many errors to be scaled into useful quantum machines. An emerging strategy is to encode quantum information in the two meta-stable pointer states of an oscillator exchanging pairs of photons with its environment, a mechanism shown to provide stability without inducing decoherence. Adding photons in these states increases their separation, and macroscopic bit-flip times are expected even for a handful of photons, a range suitable to implement a qubit. However, previous experimental realizations have saturated in the millisecond range. In this work, we aim to maximize the bit-flip time in a two-photon dissipative oscillator. To this end, we design a Josephson circuit in a regime that circumvents all suspected dynamical instabilities, and employ a minimally invasive fluorescence detection tool, at the cost of a two-photon exchange rate dominated by single-photon loss. We attain bit-flip times exceeding 100 seconds in between states containing about 40 photons. This experiment demonstrates that macroscopic bit-flip times are attainable with mesoscopic photon numbers in a two-photon dissipative oscillator. This lays a solid foundation from which the two-photon exchange rate can be gradually increased, thus gaining access to the preparation and measurement of quantum superposition states, and pursuing the route towards a logical qubit with built-in bit-flip protection.

Real-Time decoding with a distributed control-stack architecture for fault-tolerant quantum computing

Francesco Battistel

Qblox

Abstract

Quantum error correction (QEC) will be fundamental to ensure fault tolerance and achieve a quantum advantage. An essential element of QEC is the decoder, which protects the logical information by using the syndrome information to infer the most likely error pattern. The decoder must be accurate but also real-time to keep the quick pace of the QEC cycle ($<1\mu\text{s}$ for superconducting qubits). However, there are two major problems to achieve such a speed: the decoding speed per se and the communication latency with the rest of the control stack. To address the communication-latency issue, we propose and implement a distributed control-stack architecture where measurement outcomes and Pauli-frame updates are shared within a few hundreds of nanoseconds. This architecture includes and interfaces to a specialized module for running user-defined decoding algorithms. We review the most advanced proposals for decoding algorithms aimed at achieving real-time execution, with a focus on the classical computational resources (FPGA, ASIC) that are employed. This talk is aimed at researchers and experts from the quantum error correction, computer science, classical architectures and digital design communities.

Tileable low-crosstalk 3D-integrated superconducting circuits

Peter Leek

University of Oxford

Abstract

Superconducting circuits are a leading candidate for the realization of practically useful quantum computers, in particular for near-term applications which may already be reached with circuits consisting of a few hundred qubits operated at high fidelity. Until recently, the topology of superconducting circuits has typically been constrained to two dimensions, which becomes difficult to scale as the number of qubits increases and signal wiring is needed for qubits in the middle of large arrays. In this talk I will present our progress [1] on scaling up a novel circuit architecture that builds on a tileable superconducting circuit unit cell with coaxial symmetry and 3D-integrated off-chip wiring [2], which provides a viable route to operating such large qubit arrays while maintaining a clean microwave environment [3].

[1] Spring et al., *Science Advances* 8 (2022)

[2] Rahamim et al., *Applied Physics Letters* 110, 222602 (2017)

[3] Spring et al., *Physical Review Applied* 14, 024061 (2020)

CP-09-01

Practical quantum computing

Mark W Johnson*D-Wave Systems Inc.*

Abstract

Quantum annealing continues to show great promise for solving hard optimization problems that occur across a wide range of business applications, though there is much still to learn about its ultimate potential. D-Wave has developed and delivered five generations of successively more powerful, commercial annealing quantum computers. With the significant technological progress that has accompanied the development of these systems, it is now possible to perform the quantum annealing algorithm far more quickly than the system decoherence time. This has opened the door to harnessing large scale coherent dynamics in the study of quantum phase transitions, as well as solving optimization problems. Here I'll review a recent example in the study of quantum critical dynamics in a programmable spin glass comprising 5000+ qubits. Insights from this work, as well as from years of experience working with customers on their important business problems, are driving development of D-Wave's next generation annealing quantum computer: Advantage2. I will review these insights, as well as plans for our next generation quantum annealing and gate model quantum computers.

CP-09-02

Search for quantum applications and taking POCs to production

Helmut Katzgraber

Quantum Solutions Lab, Amazon Web Services

Abstract

The Amazon Quantum Solutions Lab works closely with enterprise customers to identify use cases where quantum technologies might have impact in the fault-tolerant future, but also to develop creative ways to solve complex business challenges at scale today. In this presentation, I will showcase selected customer use cases and discuss where and when quantum machines can have an impact.

CP-09-03

Quantum annealer based on Kerr parametric oscillators

Tsuyoshi Yamamoto*NEC Corporation*

Abstract

Josephson parametric oscillator is a superconducting driven oscillator, in which the resonance frequency is modulated at twice of it with a modulation amplitude larger than a threshold. The oscillation states of a JPO composed of two different states with the same amplitude but opposite phase (0π or 1π) can be used as two basis states of a qubit. In this talk, I will show our study on the basic physical properties of a JPO toward the realization of a quantum annealing machine. I will also introduce our three-dimensional packaging technologies, which are necessary for the large-scale integration in the future.

Bob's sidekick (or how tripartite quantum correlations satisfy a type of rigidity and how this is useful for cryptography)

Anne Broadbent

University of Ottawa

Abstract

We present a variant of the two-prover interactive proof model, where the interaction pattern is limited to a 3-messages: setup-broadcast-response. By virtue of these limitations, classically, the model has the same power as the single-prover model where 3 messages are exchanged. In stark contrast, the quantum version of this model (which we call the ‘Bob’s sidekick’ model) gives rise to monogamy-of-entanglement’ (MoE) games, wherein the limitation on tri-partite entanglement hampers the provers, as compared to the single-prover case. We show how this limitation can be exploited for cryptographic purposes, for instance in “unclonable encryption” where the capacity of an adversary to copy a ciphertext is limited; this is achieved using an MoE game based on conjugate coding. What is more, we show the first rigidity theorem for this MoE game, which means that producing optimal winning statistics strongly constrains the quantum strategy of the provers. From this rigidity result, we derive a weak string erasure protocol, which implies bit commitment — in a model where classical bit commitment is impossible.

Based on joint work with Eric Culf (arXiv:2111.08081) and Sébastien Lord (arXiv:1903.00130).

Abstracting quantum computation

Joe Fitzsimons

Horizon Quantum Computing

Abstract

Quantum computers have the potential to drastically outperform conventional computers for a variety of tasks, from simulating molecular interactions to machine learning. However, our understanding of how to construct non-trivial quantum algorithms is still in its infancy and human intuition is not well suited to finding ways to accomplish computational tasks through quantum interference. As a result, reaching a future where quantum computing is widely used requires not only overcoming the challenges of building scalable quantum computers, but also finding new ways to program these systems to tackle new and more complex problems.

In this talk I will introduce some of the work we have been doing at Horizon Quantum Computing to simplify the task of programming quantum processors through increasing levels of abstraction, and discuss progress towards our goal of compiling classical code to take advantage of quantum processors, through automated synthesis of quantum algorithms.

CP-10-03

Quantum cryptography without one-way functions

Tomoyuki Morimae*Kyoto University*

Abstract

One-way functions are the most fundamental primitives in classical cryptography. In this talk, I show that in quantum cryptography, one-way functions are not necessarily the most fundamental ones. We construct commitments and digital signature from pseudo-random quantum states generators. Pseudo-random quantum states generators are shown to exist even if $BQP=QMA$, which means that pseudo-random quantum states generators exist even if all post-quantum classical cryptographic primitives (including post-quantum one-way functions) are broken. Our result therefore means that several quantum cryptographic primitives can be constructed without one-way functions. This is a joint work with Takashi Yamakawa (NTT). [Morimae and Yamakawa, CRYPTO2022]

CP-11-01

From a grain of sand to a $|\text{quantum}\rangle$ bit of information

James Clarke*Intel Corporation*

Abstract

A large scale quantum computer could change the world; calculations in minutes that would take the supercomputers thousands of years. Applications such as cryptography, chemistry, finance, etc are the focus. Today's quantum processors are limited to 10's of entangled quantum bits. If you believe the hype, a commercially relevant system is just around the corner that can outperform our largest supercomputers for useful calculations. The reality, however, is that a commercially relevant system is 10-15 years away.

At Intel, our approach is to rely on the continued evolution of Moore's Law to build qubit arrays with a high degree of process control. Here, we present progress toward the realization of a 300mm Si/SiGe based spin qubit device in a production environment. A spin qubit relies on the spin of a single electron in an external magnetic field to encode the two states of the qubit, where spin up vs down represent 0 vs 1. Spin Qubits are compelling as their appearance and fabrication is similar to conventional CMOS transistors that drive the microelectronics industry. At the same time, they are roughly one million time smaller than the superconducting qubits that are being pursued by other companies.

Integration of silicon spin qubits with buried nanomagnet: a trial to design integration structure with quantum device simulator

Shota Iizuka

National Institute of Advanced Industrial Science and Technology (AIST)

Abstract

Silicon spin qubit is a promising candidate as the building block for large-scale quantum computers because of their compatibility with conventional LSI fabrication technology. In the actual device fabrication, the device characteristics vary due to process variation, causing unexpected performance degradation. For example, the qubit fidelity degrades due to the quantum dot size variation. Therefore, toward large-scale integration, it is essential to consider the integration structure realizing high variation tolerance. The device simulation technology helps the situation because we can test the variation tolerance quickly. In this talk, I will discuss a case study, taking advantage of a house-made quantum device simulator, about the co-integration of the qubits and nanomagnets, proposing a high variation tolerant integration structure. That is with buried nanomagnets, which enable qubit operation with high-speed and suppressed fidelity variation. The high-speed operation results from closely placed nanomagnets near the qubits, enabling about ten times faster operation than the conventional case. Also, the proposed structure suppresses the fidelity variation due to process variation thanks to the self-aligned fabrication process. This work demonstrates that a device simulator is a powerful tool in the integration structure design toward the practical realization of large-scale quantum computers.

Quantum simulations using phonons in trapped ions

Kenji Toyoda

Center for Quantum Information and Quantum Biology, Osaka University

Abstract

Trapped ions enable the preparation of a reliable platform that can be used to quantum computation and quantum simulations. In addition to qubits comprising of internal states in ions, the quanta of the ion crystal's vibrational motion, or phonons, which offer higher information capacity per physical degree of freedom than qubits, are considered to be alternative computational resources. Phonons in trapped ions can be used to certain applications, including the simulation of strongly interacting particles, quantum walks, and analog quantum computation using bosonic degrees of freedom. In this talk, I review the application of phonons in trapped ions to quantum simulations, and explain our recent progress regarding the system of polaritons in the Jaynes-Cummings-Hubbard model and quantum walks.

Quantum simulation for quantum many-body systems: variational quantum algorithms and beyond

Seiji Yunoki

RIKEN

Abstract

As R. Feynman was originally suggested in 1982, quantum many-body systems are the most promising application for quantum computing. Considering noisy near-term quantum devices with a relatively small number of qubits, one of the main focuses in the current quantum simulation research is to identify what one can do with such noisy quantum devices that is not too trivial but still interesting. In this talk, I would like to present some of our recent attempts to simulate quantum many-body systems based on a quantum variational approach and beyond [1-5].

- [1] “Symmetry-adapted variational quantum eigensolver”, K. Seki, T. Shirakawa, and S. Yunoki, *Phys. Rev. A* 101, 052340/1-15 (2020).
- [2] “Discretized quantum adiabatic process for free fermions and comparison with the imaginary-time evolution”, T. Shirakawa, K. Seki, and S. Yunoki, *Phys. Rev. Research* 3, 013004/1-32 (2021).
- [3] “Quantum power method by a superposition of time-evolved states”, K. Seki and S. Yunoki, *PRX Quantum* 2, 010333/1-45 (2021).
- [4] “Spatial, spin, and charge symmetry projections for a Fermi-Hubbard model on a quantum computer”, K. Seki, and S. Yunoki, *Phys. Rev. A* 105, 032419/1-34 (2022).
- [5] “Parametrized quantum circuit for weight-adjustable quantum loop gas”, R.-Y. Sun, T. Shirakawa, and S. Yunoki, arXiv:2210.14662.

CP-13-01

Quantum information processing with trapped ions

Jonathan Paul Home

ETH Zürich

Abstract

Trapped-ions are among the leading systems for quantum computing, offering the highest accuracy gate operations and long coherence times. Nevertheless, along with all candidate technologies, they face the considerable scaling challenge of transitioning from systems of tens of qubits to hundreds of thousands. I will describe the state of the field, in the context of experiments performed in our group which focus on challenges and possible solutions for scaling up. This includes new technological approaches to delivering light as well as novel methods of trapping or encoding information.

CP-14-01

Building small, fast and hot hole spin qubits in Si and Ge

Dominik Max Zumbuhl*University of Basel*

Abstract

Quantum computers hold the potential to execute complex tasks exponentially faster than classical computers. Hole spins in Ge/Si core/shell nanowires experience an exceptionally strong yet electrically tunable spin-orbit interaction, allowing unprecedented qubit control. We can tune the Rabi frequency with gate voltages, going from a fast manipulation to an idle mode, demonstrating a spin-orbit switch. We show spin-flip times as short as ~ 1 ns, approach the strong driving regime, due to a very strong spin-orbit interaction, with spin-orbit length down to a few nm. This qubit can also operate at 1.5 K, where we are also implementing an exchange based CROT 2Q gate.

One of the greatest challenges in quantum computing is achieving scalability, solved with the fin field-effect transistor (FinFET) in classical computing, integrating billions of transistors on silicon chips. Here, we show that silicon FinFETs can host hole spin qubits operating above 4 K, potentially allowing in-situ integration of qubit control electronics. We achieve fast all-electrical control and single-qubit gate fidelities at the fault-tolerance threshold. Further, we demonstrate a CROT 2Q gate with spin-orbit induced anisotropic exchange interaction, opening the door to high fidelity and fast 2Q gates.

Algorithms and Architectures for the ‘Late NISQ’ and ‘Early Fault-Tolerant’ Eras

Simon Benjamin

University of Oxford

Abstract

I will discuss the opportunities for quantum advantage in the anticipated eras of ‘late NISQ’ (meaning, many physical qubits) and the early fault-tolerant (meaning, a modest number of encoded qubits). In both these periods, we will need to closely match algorithms to architectures in order to have good prospects for quantum advantage. The specific themes I will touch on include the practicality of error mitigation and error correction (e.g. [1] and [2]), leading into architectural concepts such as multicore and looped-pipeline processors [3,4]. I will note that compilation (also known as circuit synthesis) is vital to extract maximum value, and can be done either classically or using a quantum devices [5]. Finally I will describe an approach to chemistry simulation that is compatible with the Early FT Era, with the prospect of handling classically-intractable dynamics using only hundreds of logical qubits [6].

[1] arXiv:2210.00921

[2] arXiv:2211.08468

[3] Phys. Rev. Applied 18, 044064 (2022)

[4] arXiv:2203.13123

[5] arXiv:2206.11245 and arXiv:2206.11246;

[6] arXiv:2202.05864

Abstract

Tracks

PL

Plenary Sessions

Contents / Topics

Welcome from Organizing Committee and Hosts,
Plenary Talks, Keynote

Tracks

CP

Quantum Computing Track

Contents / Topics

Quantum Computing architecture, Quantum computers with Atoms and Ions, Photonic Quantum Computers, Fault Tolerant Quantum Computing, Quantum Algorithms for Chemistry, NISQ Algorithms, Young Pls Session, Superconducting Quantum Computing, Quantum Annealing, Verifiable Quantum Computing, Semiconductor Quantum Computers, Quantum Simulations

Tracks

CC

Quantum Cryptography & Communication Track

Contents / Topics

Quantum Internet, Young Researcher Panel Session,
Quantum Cryptography

Tracks

SE

Quantum Sensing Track

Contents / Topics

Q-sensors for Life Science, NV Center and Applications for Life Sciences, Solid-State Quantum Sensors, 5th IFQMS Short Presentation Session for Young Scientists, Solid-State Quantum Sensors, Q-sensors for Life Science, NV Center and Applications for Life Sciences, Atom Interferometer, Atom/Ion Clocks *29th Nov Sessions are a joint-program with The 5th IFQMS (The 5th International Forum on Quantum Metrology and Sensing).

CC-01-01

Solid-state quantum emitters for quantum networking

Elizabeth Goldschmidt

University of Illinois Urbana-Champaign

Abstract

Optically active and highly coherent emitters in solids are a promising platform for a wide variety of quantum information applications, particularly quantum memory and other quantum networking tasks. Rare-earth atoms, in addition to having record long coherence times, have the added benefit that they can be hosted in a wide range of solid-state materials. We can thus target particular materials (and choose particular rare-earth species and isotopes) that enable certain application-specific functionalities. I will discuss several ongoing projects with rare-earth atoms in different host materials and configurations. This includes investigations of inhomogeneous broadening in rare-earth ensembles and our efforts to identify and grow new materials with rare-earth atoms at stoichiometric concentrations in order to reduce the disorder-induced inhomogeneous broadening. I will also discuss our work on photonic integration of rare-earth emitters, namely developing thulium doped thin-film lithium niobate as a platform for quantum memory.

Generation and manipulation of photonic quantum states for quantum network

Takashi Yamamoto

Graduate school of Engineering Science / Center for quantum information and quantum biology, Osaka University

Abstract

Quantum network among multiple quantum devices and/or users is one of the important issues for realizing long-distance quantum communication, large-scale quantum computer and quantum sensing. Multimode quantum states and quantum frequency conversion (QFC) play an important role for this purpose. QFC translates the frequency of photons entangled with quantum devices while retaining its quantum properties for various applications. One of the examples for useful QFC is to link the quantum devices to the telecom fiber network. On the other hand, multimode quantum states are suitable for multi-user communications and the enhancement of communication capacity. In this talk, I report an efficient and wide-range generation of the quantum frequency comb based on a quadratic nonlinear optical waveguide inside a cavity, which can be useful for generating multi-dimensional photonic quantum states and frequency multiplexed photon pairs. Using the same device, we also show an efficient QFC and a frequency manipulation method.

CC-01-03

Quantum communication in network channels and multipartite entanglement distribution

Masahiro Takeoka

Keio University

Abstract

Efficient entanglement and secret-key distribution over the network channels is necessary to build a global quantum internet. One of the key technologies for this is quantum repeater. It is important to clarify what is the fundamental performance limit without quantum repeaters and how to overcome it by quantum repeaters, hopefully with relatively simpler technologies. These are intensely investigated for a point-to-point channel with two users but still many things are missing for network channels, in particular, for multipartite entanglement distribution. Here we discuss two examples: 1) fundamental limit of bipartite entanglement and key distribution and a novel multi-party quantum key distribution protocol in a quantum broadcast channel, and 2) quantum repeater-like operations for multipartite entanglement distribution in a star-type network channel.

CC-01-04

Quantum repeater for continuous-variable entanglement distribution

Josephine Dias

Okinawa Institute of Science and Technology

Abstract

Quantum communication enables various technological possibilities that are hard or impossible with classical communication. These include secure distribution of keys, transfer of quantum information and distributed quantum computation and sensing. However, utilizing these technologies over long distances remains challenging due to fiber loss or free-space attenuation. Quantum repeaters have been proposed as a way of extending the reach of quantum communication. First-generation approaches use entanglement swapping to connect entangled links along a long-distance channel. While repeaters for discrete variable encodings of quantum information have existed for some time, several approaches for continuous variable encoding quantum repeaters have been proposed within the last five years. In this talk, I will introduce our approach to a quantum repeater for continuous variables using homodyne detection with post-selection for entanglement swapping and noiseless linear amplification for entanglement distillation. I will also present a method of using a discrete variable repeater protocol to distribute continuous variable states and utilize it to compare the rates of continuous variable entanglement distribution between first generation continuous and discrete variable quantum repeaters. Such a comparison allows us to begin to benchmark the two quite different approaches.

CC-01-05

Entanglement distribution for QKD over telecom fiber

Christian Kurtsiefer*Centre for Quantum Technologies*

Abstract

A key primitive in quantum networks is entanglement distribution, and bridging large distances usually requires photons at the transparency windows of telecom fibers. Moderate photon pair rates from conventional down conversion sources limit fiber-based entanglement distribution. A bright non-degenerate photon pair source, designed for high idler photon detection efficiency on single-photon avalanche photodiodes and low signal photon dispersion in optical fiber, enables high pair rates even after propagating through 50km standard telecommunication fiber. We present application of such a source for quantum key distribution using a BBM92 protocol.

Quantum communication at Airbus

Matthieu Dollon

Airbus

Abstract

Quantum Communication addresses Quantum Cryptography and Quantum Internet: 2 domains of high interest for Airbus, with a lot of synergies with classical optical communication systems (Airbus is a worldwide leader).

Airbus leads all the preparatory activities under the umbrella of the EuroQCI flagship of the European Commission, with the partnership of ESA:

- Qosac, large system study in 2020
- QUBITS, phase A for the space component in 2021-2022
- Oqtavo, preliminary system definition of the overall system focuses on the terrestrial network

Airbus is preparing to be the prime system integrator of the future satellite, user segment and ground segment, for both the QKD system and the Quantum Internet systems. The technical solution are already under preparation, and are based on the large heritage of Airbus on optical communication and optical observation satellites. These solutions offer high throughput systems that are necessary to build a quantum communication systems, and achievable now thanks to past heritage.

For the terrestrial network, the role of Airbus is to lead the design and implementation of the SDN and associated control and management plan, in order to offer a consistent secured system in synergy with the future USC, the European Connectivity Constellation.

CC-03-03

Information theoretically secure data utilization using “Quantum Secure Cloud”

Mikio Fujiwara

NICT

Abstract

We have been developing a system that implements a secret sharing protocol on a QKD network to enable secure transmission, storage, and secondary use of data. We have developed an XOR based high-speed secret sharing and high-speed OTP encryption/decryption system for distributed data backup. The throughputs of these systems are 700 Mbps and over 2 Gbps, respectively. We named the system Quantum Secure Cloud. We named the system “Quantum Secure Cloud” and have been conducting POC in various fields. This system not only transmits and stores genome analysis data, which require long-term confidentiality, but is also expanding its functions as a platform that enables secure utilization of data. For the secondary use of secure data, we have developed a system in the Quantum Secure Cloud that uses a secure computation system based on the assumption of a trusted server, where data is restored only during computation and encrypted during input/output. The system also has a filtering function to prevent unnecessary leakage of personal information. To our knowledge, this is the first in the world to analyze whole genome data in an information-theoretically secure manner. In this presentation, we will explain the details of the system.

Field trials and recent activities of QKD research in Toshiba corporation

Mamiko Kujiraoka

Toshiba Corporation, Corporate Research & Development Center

Abstract

Quantum key distribution (QKD) provides a means for exchanging cryptographic keys, the security of which makes no assumptions about an adversary's computing power or technological capability. Toshiba corporation is leading QKD technology in research, field trials, and standardization activities. This talk presents mainly QKD field trials in medical field: a real-time transmission of genome analysis data, a transfer of online expert panel data, and a backup of large-scale genome analysis data to multiple sites in cooperation with Tohoku University Tohoku Medical Megabank Organization (ToMMo), Tohoku University Hospital, and the National Institute of Information and Communications Technology (NICT). We also overview recent activities of QKD research in Toshiba corporation.

CC-03-05

Advancements in space quantum communications

Paolo Villorosi

University of Padova

Abstract

The development of quantum technologies is in a phase of consolidation. With regard to quantum communications and, the development of fiber demonstrations has in fact been underway for over two decades, while the results along the space channels have shown the feasibility in this domain for over five years. The analysis of chronological developments and applications will be presented together with recent experimental results.

CC-03-06

Entanglement distribution and next challenges

Alexander Ling

Centre for Quantum Technologies, National University of Singapore

Abstract

In my talk, I will give an overview of entanglement distribution work that has been performed in Singapore, and our plans for the next steps. I will discuss a recent result where we look at the overall system performance for generation and detection of entangled photons in the NIR regime, and discuss how it can enable small scale local networks using telecommunication fiber.

Satellite-based QKD for global quantum cryptographic network construction

Saori Kijima Yokote

Space & Defense Business Division Space&Satellite Business Group Space Business Unit SKY Perfect JSAT Corporation

Abstract

In recent years, the development of quantum key distribution (QKD) and cryptographic techniques have been promoted worldwide. Also in Japan, various QKD research and development projects are being conducted, including a publicly solicited R&D project by the Ministry of Internal Affairs and Communications (MIC).

SKY Perfect JSAT Corporation (SJC), Asia's largest satellite operator, has been selected as the representative company of the consortium for "Research and Development of Satellite Onboard QKD and Cryptography Technologies for the Construction of Global Quantum Cryptography Network" (MIC public offering) publicly solicited by MIC in 2021.

The consortium to execute the project which consists of National Institute of Information and Communications Technology (NICT), NEC Corporation, TOSHIBA CORPORATION, and SJC, and they have been contributing on Japanese QKD and Cryptographic Technology development.

This presentation describes the latest QKD R&D and commercialization trends in several countries around the world, the concepts and the requirements of MIC public offering, and the role of the consortium in the project and its progress so far. In addition, this presentation describes about the prospects for future business development of SJC, associated with the satellite-based QKD.

CC-04-01

Resource efficient fault-tolerant one-way quantum repeater with code concatenation

Johannes Borregaard

QuTech, Delft University of Technology

Abstract

One-way quantum repeaters where loss and operational errors are counteracted by quantum error correcting codes can ensure fast and reliable qubit transmissions in quantum networks. It is crucial that the requirements of such repeaters such as the number of spin-photon interfaces per repeater station, the gate error rates, and loss rates within a repeater node are reduced to allow for near-future implementations. In this talk, I will discuss a recent proposal of a one-way quantum repeater that targets the general asymmetry between loss- and operational error rates in a communication channel in a resource efficient manner using code concatenation. Specifically, we consider a tree-cluster code as an outer loss-tolerant code concatenated with an inner 5-qubit code for protection against Pauli errors. Adopting flag based stabilizer measurements, we show that intercontinental distances of up to 10,000 km can be bridged with a minimal resource overhead by interspersing repeater stations that operates differently at the two codes. Our work demonstrates how tailored error correcting codes can significantly lower the experimental requirements for long-distance quantum communication.

CC-04-02

Entanglement of trapped-ion qubits separated by 230 m

Tracy Northup

University of Innsbruck

Abstract

Entanglement-based quantum networks hold out the promise of new capabilities for secure communication, distributed quantum computing, and interconnected quantum sensors. However, only a handful of elementary quantum networks have been realized to date. I will present recent results from our prototype network, in which two calcium ions are entangled with one another over a distance of 230 m, via a 510(2) m optical fiber channel linking two buildings. The ion-ion entanglement is based on ion-photon entanglement mediated by coherent Raman processes in optical cavities. I will discuss the advantages of trapped ions for quantum networks and the role that cavities play as quantum interfaces between light and matter. After examining the key metrics of fidelity and success probability, we will consider how this work may be extended in the future to long-distance networks of entangled quantum processors.

CC-04-03

From quantum repeater networks to the quantum internet

Hideo Kosaka

Quantum Information Research Center at Yokohama National University

Abstract

Our challenges of developing quantum repeaters using diamonds and quantum interfaces for superconducting qubits will be presented for building quantum repeater networks and quantum computer networks for the quantum Internet.

Quantum repeaters: Analytical models and optimized protocols

Peter van Loock

University of Mainz

Abstract

We give an overview of our efforts to model fiber-based, memory-based quantum repeaters for long-range quantum key distribution or more general quantum network applications.

Under given experimental assumptions such as the possibility of probabilistic or deterministic entanglement swapping we calculate and optimize the final (secret key) rates for medium-size repeaters including the most important experimental parameters. We also briefly discuss possible variations such as memory-free approaches based on bosonic quantum error correction codes.

CC-05-05

Telco's experience and perspective on Quantum Cryptography

Hans Hyungsoo KIM

KT corp.

Abstract

KT corp. has experienced lots of field trials which were derived from self-developed Quantum Cryptography technologies. And also KT's QKD-based leased line service was commercialized. In this presentation, those experiences and relative lessons learned are introduced. Based on Quantum technologies originated from Quantum Cryptography, KT's perspective towards Quantum Era is focusing on Quantum Internet.

The UK quantum communications hub

Timothy Paul Spiller

University of York UK

Abstract

For context, I'll give a short overview of the UK National Quantum Technologies Programme (NQTP) and the position of the Quantum Communications Hub within the NQTP. I'll summarise the successful outcomes of Phase 1 (2014-19) of our Hub work and the expanded portfolio of research and development that we are pursuing during Phase 2 (2019-2024). I'll feature a few examples of this work in a little more detail.

CC-05-07

Quantum communication and cryptography in France

Eleni Diamanti*CNRS and Sorbonne University*

Abstract

We discuss recent progress and current challenges and priorities in the development of quantum communication and cryptography technologies and infrastructures in the context of the French quantum national initiative. These technologies span all development stages and corresponding applications of quantum networks, from quantum key distribution to advanced functionalities based on entanglement distribution and quantum memories, and are situated in the general landscape of European and global developments in the field.

CC-05-08

DemoQuanDT: The quantum communication testbed for Germany

Oleg Nikiforov

Deutsche Telekom Technik GmbH

Abstract

The national research project DemoQuanDT aims to demonstrate the first advanced quantum communication link in Germany. It will connect Bonn, the former capital, to Berlin, today's capital, with intermediate trusted nodes in several relevant locations. The goal is to implement a carrier-grade solution with real, hardened QKD devices, key storages and state-of-the-art symmetric encryptors and decryptors. These will be subjected to functional and security tests. Specific performance evaluations and vendor benchmarks will be conducted. DemoQuanDT is DT's most relevant QKD project and is intended to verify a future 'highly-secure transport service' for critical communication in Germany. DemoQuanDT is carried out in collaboration with ADVA Optical Networking, Rohde & Schwarz Cybersecurity, KEEQuant and universities and receives funding from the Federal Ministry for Research and Education.

Abstract

Tracks

PL

Plenary Sessions

Contents / Topics

Welcome from Organizing Committee and Hosts,
Plenary Talks, Keynote

Tracks

CP

Quantum Computing Track

Contents / Topics

Quantum Computing architecture, Quantum computers with Atoms and Ions, Photonic Quantum Computers, Fault Tolerant Quantum Computing, Quantum Algorithms for Chemistry, NISQ Algorithms, Young Pls Session, Superconducting Quantum Computing, Quantum Annealing, Verifiable Quantum Computing, Semiconductor Quantum Computers, Quantum Simulations

Tracks

CC

Quantum Cryptography & Communication Track

Contents / Topics

Quantum Internet, Young Researcher Panel Session,
Quantum Cryptography

Tracks

SE

Quantum Sensing Track

Contents / Topics

Q-sensors for Life Science, NV Center and Applications for Life Sciences, Solid-State Quantum Sensors, 5th IFQMS Short Presentation Session for Young Scientists, Solid-State Quantum Sensors, Q-sensors for Life Science, NV Center and Applications for Life Sciences, Atom Interferometer, Atom/Ion Clocks *29th Nov Sessions are a joint-program with The 5th IFQMS (The 5th International Forum on Quantum Metrology and Sensing).

SE-01-01

Dynamics and mechanism of dimer dissociation of UVR8 photoreceptor

Dongping Zhong*The Ohio State University*

Abstract

UVR8 (UV RESISTANCE LOCUS 8) proteins are a class of UV-B photoreceptors in high plants. UVR8 is a homodimer that dissociates into monomers upon UV-B irradiation (280 to 315 nm), which triggers various protective mechanisms against UV damages. Uniquely, UVR8 does not contain any external chromophores and utilizes the natural amino-acid tryptophan (Trp) to perceive UV-B light. Each UVR8 monomer has 14 tryptophan residues. However, only the two Trp residues (W285 W233) are critical to the light-induced dimer-to-monomer transformation. Here, combining time-resolved spectroscopy, extensive site-directed mutations and quantum calculations, we have revealed the entire dynamics of UV perception to lead to monomerization, including a series of critical dynamic processes of a striking energy-flow network, exciton charge separation and recombination, charge neutralization, salt-bridge unzipping, and protein solvation, providing a complete molecular picture of the initial biological function.

SE-01-02

Photoactivation of rhodopsins

Hideki Kandori*Nagoya Institute of Technology*

Abstract

Rhodopsins are photoreceptive membrane proteins that bind retinal chromophore. In animals, rhodopsins work for vision, while microbial rhodopsins work for various functions such as light-driven ion-pumps, light-gated ion-channels, light sensors and light-activated enzymes. Optogenetics, which revolutionized brain sciences, started using channelrhodopsin as a tool.

Color tuning mechanism in our vision is a key question in the field, as we can discriminate various colors using three proteins (blue, green, and red absorbing rhodopsins) with a common chromophore, 11-cis retinal. There have been little structural studies, while our vibrational spectroscopy revealed unique structural features of our color visual rhodopsins.

Light causes specific retinal isomerization; 11-cis to all-trans in animal rhodopsins, and all-trans to 13-cis in microbial rhodopsins. An important aspect of photoisomerization in rhodopsins is that the shape-changing reaction occurs even at 77 K, where protein environment cannot move by freezing. Therefore, specific isomerization mechanism attracts many researchers.

In my talk, I will introduce recent topics of animal and microbial rhodopsins, including color tuning mechanism of our color-sensitive rhodopsins, and unusual photoisomerization pathway and temperature effect found in new microbial rhodopsins.

SE-01-03

How can we measure the quality of consciousness?

Makiko Yamada*QST*

Abstract

Many of the major neuroscience studies to date on the quality of consciousness, aka qualia, have utilized visual illusions. For example, in polysemic figures such as Rubin's vase or binocular rivalry, only one of the two visual images rises to consciousness and switches at regular intervals. By exploiting such illusions, brain activity that changes in correlation with the content of consciousness has been identified, even though the external stimuli are constant. However, most previous studies have trivialized the quality of consciousness into a binary question of whether a particular visual image was seen or not, and examined the corresponding brain activity, and have not been able to capture qualia themselves (e.g., subjectively perceived redness of an apple) in terms of brain activity.

In my talk, I will present two of our new approaches to the quality of consciousness, which has been difficult to define. One is to apply the Yoneda Lemma to characterize qualia in relation to their surroundings and identify qualia structure from brain activity patterns. The other applies the idea of "quantum cognition" to test whether the experience of consciousness is determined by measurement by examining violations of Bell's inequality.

SE-02-01

Quantum sensing and imaging with diamond spins

Ania Claire Bleszynski Jayich

UC Santa Barbara

Abstract

Solid state spin qubits, in particular the nitrogen vacancy (NV) center in diamond, offer a path towards truly nanoscale imaging of condensed matter and biological systems with sensitivity to single nuclear spins. Here I discuss our NV-based magnetic imaging experiments as applied to condensed matter systems, where we have imaged current flow patterns in graphene in order to reveal the transition from ohmic to electron-collision-dominated flow regimes. A grand challenge to improving the spatial resolution and magnetic sensitivity of the NV is mitigating surface-induced quantum decoherence, which I will discuss in the second part of this talk. Decoherence at interfaces is a universal problem that affects many quantum technologies, but the microscopic origins are as yet unclear. Our studies guide the ongoing development of quantum control and materials control, pushing towards the ultimate goal of NV-based single nuclear spin imaging.

SE-02-02

Hybrid diamond-doped optical fibres for remote magnetometry applications

Brant Gibson*RMIT University*

Abstract

The ability to persistently monitor weak magnetic fields is a key objective in long-term surveillance. One approach to meeting this goal is the development of optical fibre-based magnetometers capable of remote operation. Diamond containing the negatively-charged nitrogen vacancy colour centre (NV) is emerging as an important system for the sensing of various physical parameters including magnetic field and temperature. Many existing diamond NV magnetometers require complex microscopes to monitor the fluorescence signal, which can restrict NV to laboratory settings. Here I will discuss the fabrication and characterization of an intrinsically magneto-sensitive optical fibre with potential applications as a high-efficiency remote magnetic sensing platform. The hybrid fibre allows for optical interrogation of NV-spin states via bound modes in a highly-stable waveguide structure. Our results open the possibility of robust, field-deployable fibre optical magnetometry for a broad range of quantum sensing applications.

SE-02-03

Quantum sensing by NV centers in diamond semiconductor

Norikazu Mizuochi*Kyoto University*

Abstract

The NV center in diamond has been attracting attention from the viewpoint of the application of ultrasensitive sensors and quantum information devices. In the NV center, the spin of the single NV center can be observed at room temperature despite the spin in the solid. In addition, it has the longest Hahn-echo electron spin coherence time (2.4 ms) and inhomogeneous electron spin dephasing time (1.5 ms) among room-temperature solid state systems [1]. We consider that the elongation of coherence times in n-type semiconductor diamond paves the way to the development and application of diamond-based quantum-information, sensing, and spintronics devices.

The dynamic range is also important from the viewpoint of the application. Conventional sensors have difficulty simultaneously achieving high sensitivity and a large range. On the other hand, we have demonstrated to widen the dynamic range while maintaining sensitivity, which can be applied to the NV center [2]. In addition, we will also show our recent research on low-frequency quantum sensing.

We thank supports from MEXT-QLEAP (No. JPMXS0118067395, JPMXS0120330644), JSPS KAKENHI (No. 21H04653).

[1] E. D. Herbschleb, et al., Nature Communications, 10, 3766 (2019).

[2] E. D. Herbschleb et al., Nature Communications, 12, 306 (2021).

SE-04-01

Controlling and exploiting defects in diamond for Quantum Technologies

Mark Newton*University of Warwick*

Abstract

Point defects in diamond have great potential for use in a range of quantum technologies. For example as single photon sources and quantum bits that can be exploited in quantum information processing and as the heart of sensors that will transform the way we do analytical science and medical imaging. The negatively charged nitrogen-vacancy centre is an amazing defect in diamond that possesses properties highly suited to many of these applications. However, it does have some challenging weaknesses and full exploitation of the optical and spin properties of this and other defects necessitates that we control their position, orientation and environment to optimise all of the desirable properties simultaneously, especially near the surface of the diamond. I will review our understanding of the production of intrinsic defects and present new data on the creation of defect complexes by doping, electron irradiation, short pulse laser irradiation, ion implantation and annealing. The success and failure of different combinations of processing steps to control and optimise the local defect environment will be discussed and the ongoing search for alternate colour centres with comparable spin properties and superior optical properties will be reviewed.

SE-04-02

Methods for deterministic production of colour centres in diamond

Jan Meijer*Leipzig*

Abstract

The NV centres in diamond are currently the only solid-state qubits that allow miniaturised construction and guarantee operation at room temperature. This is the only way to build processors for broad commercial use. While the methods for controlling and reading out these centres have been known and tested for years, the production of the centres has been the main unsolved technological challenge.

In order to achieve successful coupling of the NV centres, a very small spacing window has to be considered. When addressing the NVs, their defined alignment in the crystal is also necessary. Many NVs can only be read out electrically.

Here, many material-scientific but also technical boundary conditions have to be taken into account. The lecture shows new approaches to overcome this challenge. The solutions could also be of importance for other applications.

SE-04-03

Synthesis of single crystal diamond with colour centres for quantum applications

Alexandre TALLAIRE*Institut de Recherche de Chimie Paris CNRS*

Abstract

The negatively charged nitrogen-vacancy centre (NV) in diamond is a point-like defect that has focused a lot of attention in the past few years due to its potential in quantum applications, especially for sensing. It has bright single photon emission and the electronic spin state of this defect can be optically read-out and manipulated leading to exceptionally long coherence time even at room temperature. Harnessing the outstanding properties of NVs mainly relies on the progresses in the synthesis of high quality and purity diamond material using the chemical vapour deposition technique (CVD). Individual or ensembles of NV centres can be created in an environment with low nuclear spin bath using ^{12}C -enriched CVD diamond plates. In addition, NV density can be controlled over a wide range of concentration, from a few ppb to a few ppm with specific spatial localization. An additional advantage includes the ability to promote one orientation among the 4 possible axes of the NV dipole by growing on specific orientations such as (111) and (113). These requirements are however very challenging and are setting an increasing pressure to the diamond synthesis capabilities by CVD. In this talk I will describe the efforts dedicated to the growth of nitrogen-doped CVD diamond single crystals by CVD that have allowed optimizing the material for quantum sensing applications.

SE-04-04

Introduction to quantum brilliance and its R&D programs

Marcus Doherty

Quantum Brilliance Pty Ltd

Abstract

Quantum Brilliance is an Australian-German company developing room-temperature quantum computers based upon diamond. Quantum Brilliance is distinguished by its distinct and complementary vision of ‘quantum accelerators’. Being quantum computers that are the same size as today’s GPUs and CPUs, which are deeply integrated with classical computers to accelerate applications across the spectrum of edge computing (e.g. in satellites and autonomous vehicles) to centralised supercomputing (e.g. as massively parallelised clusters). Indeed, Quantum Brilliance has already constructed a prototype quantum computer and integrated it into the Pawsey Supercomputing Centre in Australia. Alongside this premier hardware product, Quantum Brilliance is working with partners (e.g. NVIDIA) to drive the development of the software frameworks, languages and libraries required to employ quantum computers as accelerators in hybrid computing.

In this talk, I will briefly introduce Quantum Brilliance before outlining its research and development programs.

SE-05-01

Hyperpolarized solution-state NMR spectroscopy via quantum resources

Ilai Schwartz*NVision Imaging Technologies GmbH*

Abstract

Nuclear spin hyperpolarization provides a promising route to overcome the challenges imposed by the limited sensitivity of NMR spectroscopy. The current leading approach for hyperpolarizing nuclear spins, dissolution DNP, requires deep cryogenic temperatures (~1K) and long polarization buildup times (~1 hour) thus limiting the applicability of hyperpolarization. In this talk I will present our alternative method for enabling nuclear hyperpolarization of a wide range of molecules at room temperature and under a minute utilizing quantum resources - optically polarizable electron spins in crystals and singlet states in gaseous hydrogen molecules.

We demonstrate that utilizing the quantum resource a molecule of choice can be sufficiently polarized to serve as a “polarization source”. Mixing a high enough concentration of the polarization source molecule into the solution enables polarization of an extremely wide range of analytes via the intermolecular nuclear Overhauser effect (NOE), and achieves enhancements up to 2600 in benchtop NMR spectrometers.

I will discuss the recent advances achieved by using various polarization sources, the ongoing development for making the system widely accessible to the NMR community and potential “killer applications” of the technology.

Dissolution dynamic nuclear polarization

Jan Ardenkjaer-Larsen

Technical University of Denmark

Abstract

Hyperpolarized Magnetic Resonance is a new medical imaging modality that offers exceptional possibilities to follow changes in metabolism. The method is enabled by a more than 10,000 fold enhancement of the nuclear magnetisation from metabolic contrast agents that probe central metabolic pathways. The contrast agent is typically enriched in ^{13}C and polarized by dissolution Dynamic Nuclear Polarization (dDNP). The contrast agent circulates via the vasculature to the tissue of interest, where it is taken up by the tissue cells and metabolized into specific products. MR is unique in several ways: 1) it already provides anatomical and morphological images with high resolution and contrast based on the tissue water protons, 2) it does not expose the patient to any ionizing radiation, and 3) it is a spectroscopic method that allows quantification of the individual metabolites. The first tracer in clinical development is ^{13}C -pyruvate. Pyruvate is at a pivotal point in glycolysis and allows us to directly probe the Warburg effect through the elevated lactate-to-pyruvate ratio. The hope is that more accurate diagnosis and staging can be made, and that the method will provide an early read-out of response to treatment. The first clinical studies have been performed with encouraging results, e.g. aggressiveness staging of prostate cancer.

SE-06-02

Toward rotation sensing using a trapped single ion

Takashi Mukaiyama

Osaka University

Abstract

Matter-wave interferometers typically exploit entanglement between the internal state and the motional state of matter. The development of a gyroscope using an ion trap is being pursued because of the high sensitivity to rotation and insensitivity to translational acceleration. Here we aim to realize a rotation measurement using a trapped single ion based on a matter-wave Sagnac interference by exciting the motion of the ions to form a two-dimensional circular orbit. Although the matter-wave interference of ions in multi-dimensional motion is essential for gyroscopes using circular orbits, only one-dimensional interference was realized before our achievement. Our experiment has succeeded in observing matter-wave interference of ions in three-dimensional motion by exciting the motion of 171Yb^+ ions using a mode-locked laser. To realize a large interferometric area, we have developed a technique to significantly increase the ion orbital area by moving the ion trap center in a short time scale. We have also constructed a whole experimental setup on a rotatable optical table, such that we can rotate the entire system with an angular velocity up to 2 degrees per second.

SE-06-03

Enhanced quantum control for the next generation of optical lattice clocks

Andrew Ludlow*National Institute of Standards and Technology*

Abstract

Atomic clocks operating in the optical domain are now capable of measuring time at up to eighteen digits of precision. With the level of clock stability that has also been demonstrated in optical clocks based on ultracold atoms in an optical lattice, a promising route to even higher performance exists. Here we explore new techniques for enhanced control of lattice-trapped atoms towards next-generation optical lattice clocks. First, we consider two novel laser cooling strategies that exploit the high atom-laser coherence possible with divalent atomic structure. The first is a pulsed cooling process that replaces two-photon Raman cooling techniques with single-photon velocity-selection on the clock transition. The second is an excited state Sisyphus cooling mechanism that offers efficient three-dimensional cooling in a lattice. We demonstrate sub-recoil cooling of ytterbium in both cases, which aid in loading very shallow lattices to reduce lattice-induced light shifts. We also demonstrate coherent delocalization of ytterbium through controlled tunneling in a Wannier-Stark lattice, aimed at reducing atomic interactions within the lattice. Finally, we discuss progress on the development of portable ytterbium lattice clocks for future measurements beyond the lab.

SE-06-04

Quantum metrology and computing using microscopically-controlled arrays of alkaline-earths

Kaufman M Adam*JILA, University of Colorado Boulder, NIST*

Abstract

Quantum science with neutral atoms has seen great advances in the past two decades. Many of these advances follow from the development of new techniques for cooling, trapping, and controlling atomic samples. As one example, the technique of optical tweezer trapping of neutral atom arrays has been a powerful tool for quantum simulation and quantum information, because it enables scalable control and detection of individual atoms with switchable interactions. In this talk, I will describe ongoing work at JILA where we have explored a new type of atom - two-electron atoms - for optical tweezer trapping and manipulation. While the increased complexity of these atoms leads to challenges, they also offer new scientific opportunities by virtue of their rich internal degrees of freedom. Accordingly, they have impacted multiple areas in quantum science, ranging from quantum information processing to quantum metrology, and intersections therein. I will report on my group's progress in these areas.

SE-07-01

Quantum sensors with matter waves

Philippe Bouyer*Univ. of Amsterdam - Technical University Eindhoven*

Abstract

The past decades has seen dramatic progress in our ability to manipulate and coherently control the motion of atoms. Although the duality between wave and particle has been well tested since de Broglie introduced the matter-wave analog of the optical wavelength in 1924, manipulating atoms at a level of coherence allowing for precision measurement has only become possible thanks with our ability to produce atomic samples of few microdegrees above absolute zero. Since the initial experiments many decades ago, the field of coherent atom optics has grown in many directions. This progress has both fundamental and applied significance. The exquisite control of matter waves offers the prospect of a new generation of force sensors of unprecedented sensitivity and accuracy, from applications in navigation and geophysics, to tests of general relativity or study of highly-entangled quantum states. The spectacular sensitivity of matter-wave interferometers can be used for very precise measurements. It is for example possible to measure the acceleration of gravity with an accuracy of 1 part per billion, the rotation of the Earth with an accuracy better than 1 millidegree per hour and detect minute changes in gravity caused by mass displacements. These devices are so precise that they are used today as reference for fundamental constants (mass, gravity), and are powerful candidates to test general relativity on ground, underground or in space. Projects are currently ongoing to verify the universality of free fall or to detect gravitational waves in a frequency range yet unreachable with current detectors.

Nevertheless the future of matter-wave inertial sensors goes far beyond lab-based inertial sensors. While these experiments are typically quite large, require a dedicated laboratory, and are designed to operate well only in environments where the temperature, humidity, acoustic noise is tightly constrained, many efforts have been put in designing compact, robust and mobile sensors. The development of this technology lead to a new generation of atomic sensors that have been operated in airplanes [10] and in rockets, that are commercially available and could be the next generation of navigation unit.

SE-07-02

Exploring quantum gases for terrestrial and space-borne interferometry

Maria Ernst*Leibniz Universität Hannover*

Abstract

Ultra-cold quantum gases promise to boost the sensitivity of inertial matter-wave interferometers, open the avenue to achieve higher accuracies and allow to conceive new devices. Exploiting quantum gases for high-precision interferometry places high demands on their control and manipulation. The talk presents latest experiments to lower the expansion energies of atomic ensembles and new possibilities arising from twin-lattice interferometry. They are fascinating tools for ground and space-borne interferometry. Our research to advance the necessary methods and achieve the targeted resolution benefits of various platforms such as the very-long-baseline atom interferometer, the Bremen drop tower, the Einstein elevator in Hannover, sounding rockets and the international space station. The DLR-mission MAIUS-1 demonstrated Bose-Einstein condensation and performed first interferometry experiments during the space travel of a sounding rocket. NASA's Cold Atom Laboratory as well as the NASA-DLR funded BECCAL facility continue this research in orbit on the ISS. These experiments explore methods needed for high-precision interferometry as proposed for Earth observation or fundamental physics experiments.

E.M.R. for the QUANTUS, MAIUS and BECCAL cooperation, dq-mat, terra-Q and quantum frontiers

SE-07-03

A highly charged ion based optical atomic clock

Lukas J. Spieß*Physikalisch-Technische Bundesanstalt*

Abstract

Optical atomic clocks are the most accurate devices ever built and are used as time standards as well as probes for fundamental physics. They are usually based on transitions in neutral or singly charged atoms. The large class of highly charged ions (HCI) remained so far unexplored. This is despite favourable properties of HCI, like a small sensitivity to external fields and a high sensitivity to physics beyond the Standard Model. Over the last decade several key hinderances were eliminated by sympathetic cooling of HCI and interrogation using quantum logic spectroscopy. Here, an optical clock based on the dipole-forbidden, optical transition in Ar^{13+} is presented. A comprehensive analysis of the systematic shifts shows a systematic uncertainty of $2 \cdot 10^{-17}$ with a clear path to below 10^{-18} . Clock comparison to the well-known octupole transition in singly charged Yb yielded an absolute frequency eight orders of magnitude more accurate than any previous value. The measured isotope shift ($^{40}\text{Ar} - ^{36}\text{Ar}$) is compared to high-precision calculations and reveals for the first time the quantum electrodynamic nuclear recoil in a many-electron atom. The applied techniques are universal and open high precision spectroscopy for a large variety of HCI.

SE-07-04

Robust Yb optical lattice clock for contributing to International Atomic Time

Masami Yasuda

National Institute of Advanced Industrial Science and Technology (AIST), National Metrology Institute of Japan (NMIJ)

Abstract

Recent rapid progress of the optical frequency standards motivates the discussion on the redefinition of the SI second, which is presently defined by fixing the cesium microwave frequency value. The Consultative Committee for Time and Frequency (CCTF) set mandatory conditions which must be fulfilled before the redefinition. One of the most difficult conditions is the regular contribution of the optical frequency standards to the International Atomic Time (TAI), whose fulfilment index is less than 20 % in 2021. We will present our research activities on a robust ytterbium (Yb) optical lattice clock aiming for the highest uptime for continuous operation. We implemented a laser frequency relocking system fully utilizing our fiber-based optical frequency combs. A remote monitoring system allows an unattained operation of the clock. Thanks to these innovations, almost continuous operation of the clock with e.g., an uptime of 94.5 % for 30 days was made possible. After the verification by CCTF Working Group on Primary and Secondary Frequency Standards, we conduct on-time calibration of TAI 11 times in 2021 and 2022. The most recent calibrations utilize an improved gravitational redshift determined by a precise leveling and local gravity measurement by Geospatial Information Authority of Japan.

Abstract

Tracks

PL

Plenary Sessions

Contents / Topics

Welcome from Organizing Committee and Hosts,
Plenary Talks, Keynote

Tracks

CP

Quantum Computing Track

Contents / Topics

Quantum Computing architecture, Quantum computers with Atoms and Ions, Photonic Quantum Computers, Fault Tolerant Quantum Computing, Quantum Algorithms for Chemistry, NISQ Algorithms, Young Pls Session, Superconducting Quantum Computing, Quantum Annealing, Verifiable Quantum Computing, Semiconductor Quantum Computers, Quantum Simulations

Tracks

CC

Quantum Cryptography & Communication Track

Contents / Topics

Quantum Internet, Young Researcher Panel Session,
Quantum Cryptography

Tracks

SE

Quantum Sensing Track Short Presentations by Young Researchers

SE-03A, SE-03B

5th IFQMS

The 5th International Forum
on Quantum Metrology and Sensing

PROCEEDINGS

Short Presentation Session for Young Scientists
Part 1: SE-03A

29 November, 2022
Online Conference (Zoom)

Joint Program Session with Quantum Innovation 2022



Quantum Sensing Track : Short Presentation Session for Young Scientists
SE-03A. Short Presentations Session for Young Scientists on SE-02, 04, 06, 07 Topics [5th IFQMS]

*Note: Presentation order may change within the same group.

All the times in the program are Japan Standard time (GMT+9)

Nov 29 (Tue.)	Session / Presentation	Mentor / Presenter	Affiliation	ID
13:10-14:30	SE-03A-α1			
	Chair	Ryota Katsumi	TUT	
	Co-chair	Naota Sekiguchi	Tokyo Tech	
	Lock-In detected ramsey magnetometry with a bulk ensemble of diamond NV centers for high-sensitivity DC-field measurement	Sena Tsuchiya	Tokyo Tech	SE-03A- α 1-01
	Towards measurement of magnetic field generated by the brain of a living rat using N-V centers in diamond	Naota Sekiguchi	Tokyo Tech	SE-03A- α 1-02
	Identification of current multipole sources from magnetoencephalography data	Motofumi Fushimi	UTokyo	SE-03A- α 1-03
	Optimization of simultaneous measurement of magnetic field and temperature measurement by silicon vacancy quantum sensor using simultaneous resonance	Tomoaki Tanaka	QST	SE-03A- α 1-04
	Spin-dependent photocarrier generation dynamics in electrically detected NV-based quantum sensor	Hiroki Morishita	Kyoto U	SE-03A- α 1-05
	Towards nanoscale zero- to ultralow-field NMR	Till Lenz	JGU	SE-03A- α 1-06
	Dipole-dipole interaction between NV- centers	Chikara Shinei	NIMS	SE-03A- α 1-07
13:10-14:30	SE-03A-β1			
	Chair	Yuta Kainuma	Tokyo Tech	
	Co-chair	Naoya Morioka	Kyoto U	
	Extension of dephasing time of ensemble NV centers with a continuous-excitation protocol	Ikuya Fujisaki	Tokyo Tech	SE-03A- β 1-01
	Wide temperature operation of diamond quantum sensor for electric vehicle battery monitoring	Keisuke Kubota	Tokyo Tech	SE-03A- β 1-02
	A development of wearable magnetic shield for MEG	Soichiro Shido	UTokyo	SE-03A- β 1-03
	Attempts to generate entanglement state between dipolar coupled NV centers created by molecular implantation	Kosuke Kimura	QST	SE-03A- β 1-04
	Charge stability of shallow single NV centers in p-type diamond	Taisuke Kageura	AIST	SE-03A- β 1-05
	Room-temperature electrical detection of nuclear spins in silicon carbide	Naoya Morioka	Kyoto U	SE-03A- β 1-06
	(Near) zero-field cross-relaxation features for ensembles of NV centers in diamond	Omkar Dhungel	JGU	SE-03A- β 1-07
13:10-14:30	SE-03A-γ1			
	Chair	Tomoya Sato	Tokyo Tech	
	Co-chair	Fumihiko China	NICT	
	Evaluation of a superconducting nanowire single photon detector for mid-infrared wavelengths	Satoru Mima	NICT	SE-03A- γ 1-01*
	Efficient superconducting nanostrip single-photon detectors for 2 μ m wavelength	Fumihiko China	NICT	SE-03A- γ 1-02
	Effect of pump laser linewidth on nonlinear quantum interferometric fringes	Jasleen Kaur	Kyoto U	SE-03A- γ 1-03
	Highly efficient and ultra-broadband photon pair source using chirped quasiphasematching slab waveguide matching slab waveguide	Bo Cao	Kyoto U	SE-03A- γ 1-04
	Optical trapping and movement control of gold nanoparticles on an optical nanofiber	Rui Sun	Tohoku U	SE-03A- γ 1-05
	Electromagnetic-field analysis of the plasmon-enhanced single photon emitters on an optical nanofiber	Yining Xuan	Tohoku U	SE-03A- γ 1-06
	Ultrafast measurement of biphoton wave packets using optical Kerr gating	Takahisa Kuwana	UEC	SE-03A- γ 1-07

Nov 29 (Tue.)	Session / Presentation	Mentor / Presenter	Affiliation	ID
14:50-16:10	SE-03A-α2			
	Chair	Naota Sekiguchi	Tokyo Tech	
	Co-chair	Ryota Katsumi	TUT	
	Growth of thick CVD diamond films containing aligned nitrogen-vacancy centers for high-sensitivity quantum sensors	Takeyuki Tsuji	Tokyo Tech	SE-03A- α 2-01
	Enhancement of fluorescence collection efficiency using angle-shaped diamonds for compact magnetic sensor	Yuta Shigenobu	Tokyo Tech	SE-03A- α 2-02
	Transfer-printing-based integration of SiN grating structure on diamond toward highly sensitive quantum sensor	Ryota Katsumi	TUT	SE-03A- α 2-03
	NVC-SPM system to inspect electric devices	Teruo Kohashi	Hitachi	SE-03A- α 2-04*
	Enhancing sensitivity with entanglement in coupled nitrogen vacancy centres	Ernst David Herbschleb	Kyoto U	SE-03A- α 2-05
	Frequency-bin generation of entangled photons via quantum optical synthesis	Takeru Naito	UEC	SE-03A- α 2-06
	Development of highly sensitive gravimeter based on atom interferometry using hybrid system for field applications	Takeshi Hojo	UEC	SE-03A- α 2-07
14:50-16:10	SE-03A-β2			
	Chair	Naoya Morioka	Kyoto U	
	Co-chair	Yuta Kainuma	Tokyo Tech	
	Implementation of double quantum magnetometry to continuously excited ramsey method	Yuta Araki	Tokyo Tech	SE-03A- β 2-01
	Development of highly sensitive compact quantum sensor with NV center in 12C-enriched CVD diamond for bio-medical and industrial application	Yuta Kainuma	Tokyo Tech	SE-03A- β 2-02
	Development of a nonmagnetic helical sensor drive multipoint measuring mechanism for magnetocardiography in animals	Wenyu Shang	UTokyo	SE-03A- β 2-03
	Ensemble NV- center in diamond for quantum sensing created by high fluence electron beam irradiation	Shuya Ishii	QST	SE-03A- β 2-04
	Synthesis of n-type diamond using tert-butyl phosphine for high sensitivity of the NV sensor	Riku Kawase	Kyoto U	SE-03A- β 2-05
	Decoherence phenomena in nitrogen-vacancy diamond	Aulden Jones	Georgia Tech	SE-03A- β 2-06
14:50-16:10	SE-03A-γ2			
	Chair	Fumihiro China	NICT	
	Co-chair	Tomoya Sato	Tokyo Tech	
	Improvement in the long-term stability of the interferometer gyroscope using slow and continuous atomic beams	Naoki Nishimura	Tokyo Tech	SE-03A- γ 2-01
	Bragg interferometer using slow and continuous atomic beam with sub-recoil transverse momentum width	Tomoya Sato	Tokyo Tech	SE-03A- γ 2-02*
	Development of a cryogenic suspension system for TOrsion-Bar Antennae (TOBA)	Ching Pin Ooi	UTokyo	SE-03A- γ 2-03
	Torsion-bar antenna for early earthquake alert	Yuka Oshima	UTokyo	SE-03A- γ 2-04
	Optimized Design of Quasi-phase-matched crystal for Spectrally-Pure-State Generation at MIR Wavelengths Using Metaheuristic Algorithm	Wu-Hao Cai	Tohoku U	SE-03A- γ 2-05
	Experimental generalized measurement of qubits using a quantum computer	Tingrui Dong	Tohoku U	SE-03A- γ 2-06

Note: This program was created for fostering young scientists. Presentations with asterisks (*) are excluded from awarding.

Lock-In Detected Ramsey Magnetometry with a Bulk Ensemble of Diamond NV Centers for High-Sensitivity DC-Field Measurement

Sena Tsuchiya¹, Daisuke Nishitani¹, Yusei Aoki¹, Takeharu Sekiguchi¹, Takayuki Shibata², Takayuki Iwasaki¹, and Mutsuko Hatano^{1,3}

¹Department of Electrical and Electronics Engineering, School of Engineering, Tokyo Institute of Technology

²DENSO CORPORATION

³National Institutes for Quantum Science and Technology

tsuchiya.s.ag@m.titech.ac.jp

Introduction

Nitrogen-vacancy (NV) centers in diamond have attracted much attention as high sensitivity quantum magnetic sensors that can be operated at room temperature. Our group has demonstrated magnetocardiography of living rats by combining continuous-wave optically detected magnetic resonance (CW-ODMR) with lock-in (LI) detection¹. However, further improvement of DC-field sensitivity is necessary to detect magnetoencephalography signals. Double-quantum (DQ) Ramsey magnetometry² based on pulsed ODMR scheme is expected to achieve much higher sensitivity by improving both spin dephasing time T_2^* and contrast². Combination with LI detection of fluorescence intensity should reduce noise, remove signal offset, and allow real-time measurement. In this study, we implemented LI detection under pulsed optical excitation and detection with DQ Ramsey sequences to demonstrate the sensitivity improvement.

Methods

The diamond sample used was grown by HPHT with ¹²C-enriched source in NIMS, and the NV centers were created by electron beam irradiation (1×10^{17} cm⁻²) and annealing in QST. The concentrations of NV and P1 (substitutional nitrogen) centers were 0.05 ppm and 1.1 ppm. Fig. 1(a) shows our experimental setup. Pulsed optical excitation at 532 nm and the DQ-4-Ramsey sequence² with resonant dual-frequency microwave (MW) were applied to a bulk ensemble of NV centers in diamond. The illumination volume was roughly $(60 \times 160 \times 470)$ μm^3 . The fluorescence signal modulated by the DQ-4-Ramsey sequence was detected and demodulated by a LI amplifier. The MW pulse width (0.22 μs) for this sequence was calibrated from the DQ-Rabi oscillation measurements.

Results and discussion

Fig. 1(b) shows the LI detected DQ-4-Ramsey fringes with microwave frequencies tuned to the central resonance of the ¹⁴N hyperfine triplet. The inset FFT spectrum shows clearly this triplet structure with the splitting doubled by the DQ sequence. Fig. 1(c) shows MW frequency dependence of the Ramsey signal at a fixed free-precession time τ using the SQ(single quantum)-2-Ramsey² and DQ-4-Ramsey sequences. The DQ-4-Ramsey signal exhibits a 15% steeper slope than the SQ-2-Ramsey signal. The magnetic field sensitivity can be estimated from repeated measurements of the Ramsey signal with a fixed $\Delta\nu$ at the steepest slope. We will discuss the sensitivity improvement factors such as lock-in detection for enhancing signal-to-noise ratio and DQ-4-Ramsey sequence for the Ramsey slope improvement.

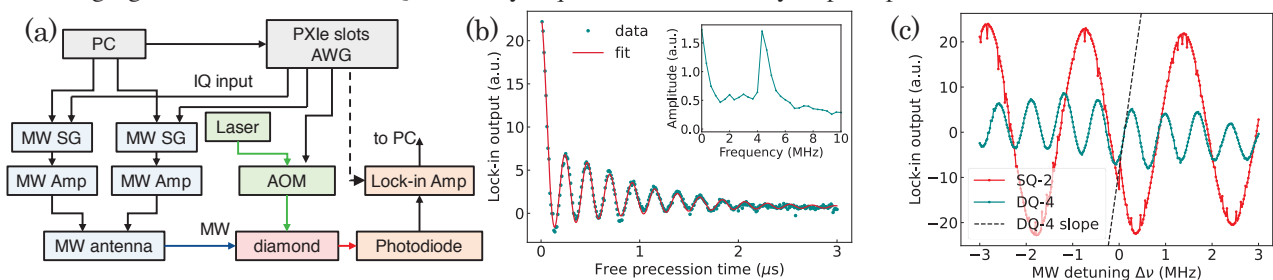


FIG. 1. (a) Experimental set up for LI detected Ramsey measurements. (b) DQ-4-Ramsey signal by LI detection at frequency detuning of $\Delta\nu = 0.0$ MHz, in the time domain and frequency domain (inset). (c) Detuning sweep of the LI detected DQ-4-Ramsey ($\tau = 0.46$ μs) and SQ-2-Ramsey ($\tau = 0.40$ μs). The dashed line represents the steepest slope of the DQ-4-Ramsey signal.

Acknowledgement

This work was supported by MEXT Q-LEAP Grant Number JPMXS0118067395. We thank Dr. M. Miyakawa, Dr. T. Taniguchi (NIMS), Dr. S. Ishii, S. Saiki, and S. Onoda (QST) for providing the diamond sample.

Reference

¹K. Arai et al., Commun. Phys. **5**, 200 (2022). ²C. A. Hart et al., Phys. Rev. Appl. **15**, 044020 (2021).

Towards measurement of magnetic field generated by the brain of a living rat using N -V centers in diamond

Naota Sekiguchi¹, Motofumi Fushimi², Ken-ichi Kajiyama¹, Ryoma Matsuki¹, Takayuki Iwasaki¹, Masaki Sekino², and Mutsuko Hatano¹

¹Department of Electrical and Electronics Engineering, Tokyo Institute of Technology, Tokyo 152-8552, Japan

²Department of Bioengineering, University of Tokyo, Tokyo 113-8656, Japan

Sekiguchi.n.ac@m.titech.ac.jp

Measurement of a biomagnetic field is of great importance to understand neuron activities in a living body. Ultrasensitive magnetometers such as superconducting quantum interference device sensors and optically-pumped atomic magnetometers have successfully measured a magnetic field generated by an internal organ including brain and been applied to clinical diagnosis. While these conventional magnetometers exhibit extreme field sensitivity of the order of $\text{fT}/\sqrt{\text{Hz}}$, spatial resolution is limited to centimeters due to intrinsic structures of those sensor heads. Recently, diamond quantum sensor based on negatively charged nitrogen-vacancy (N -V) centers has attracted much attentions because of its high spatial resolution. Good field sensitivity of $15 \text{ pT}/\sqrt{\text{Hz}}$ at low frequency has been demonstrated using an ensemble of N -V centers [1], and N -V center based magnetocardiography of a living rat [2] with millimeter-scale resolution has been reported. Magnetoencephalography (MEG) using N -V centers, however, has not been realized and requires a field sensitivity on the order of $\text{pT}/\sqrt{\text{Hz}}$. We develop a sensitive diamond magnetometer based on a N -V center ensemble for MEG of a living rat.

Figure 1 shows our experimental setup. A rat was anesthetized and laid on a warm bed. Electrocardiogram of the rat was monitored using electrodes stucked into limbs. We stimulated the somatosensory of the rat by applying current pulses with $300\text{-}\mu\text{s}$ width and repetition frequency of about 4 Hz via another electrode stucked into a hind limb. This stimulation is supposed to generate a somatosensory evoked field (SEF) from the brain of the rat, which can be detected with a quantum diamond sensor above the rat head. The single-crystalline diamond was synthesized by a temperature-gradient method under high-pressure and high-temperature. N -V centers were produced by electron beam irradiation followed by high-temperature annealing in vacuum. We used an optically-detected magnetic resonance signal of N -V center ensemble that oriented along the z axis. A linearly polarized laser light of 532 nm illuminated the diamond. A small portion of the laser beam was picked up to compensate the intensity fluctuation. Fluorescence from the diamond was collected by a lens and detected by a photodiode. A bias magnetic field of about 1 mT generated by a ring permanent magnet was applied to the diamond along the z axis to sufficiently split the $|\pm 1\rangle$ ground states. The magnetic resonance between $|0\rangle \leftrightarrow |\pm 1\rangle$ was induced by a frequency modulated microwave (MW) field: sidebands resonant to the hyperfine states were generated by mixing an RF with the MW; the carrier frequency of MW was modulated at around 10 kHz to adopt a lock-in technique. The acquired signal was accumulated in accordance with the stimulation pulses. We will discuss the present situation including the noise floor and detectable field in the short presentation.

This work was supported by MEXT Q-LEAP Grant Number JPMXS0118067395.

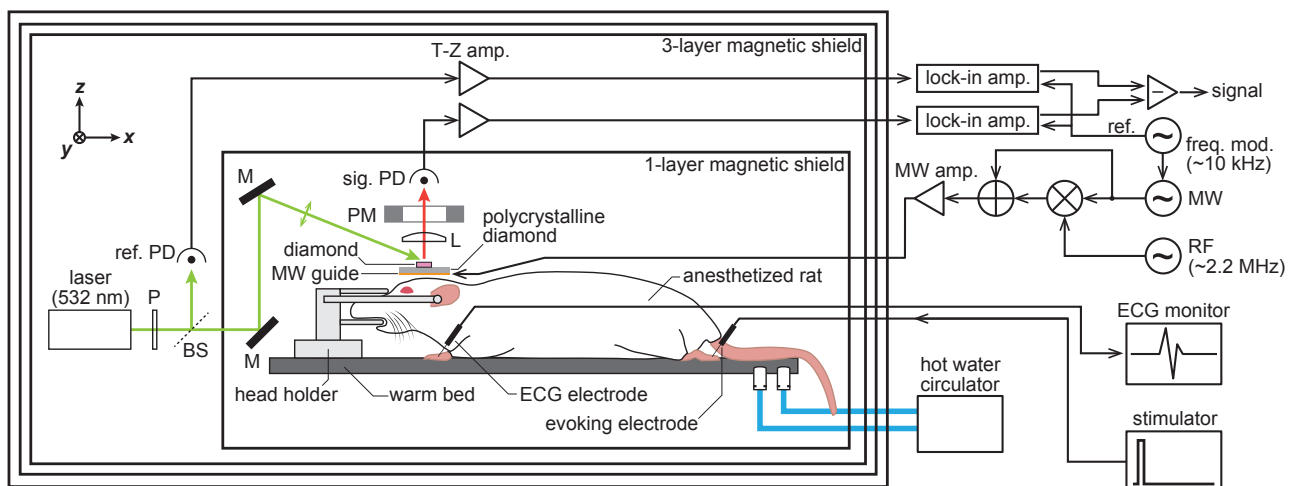


FIG 1. Experimental setup. P: polarizer; BS: beam splitter; PD: photodiode; M: mirror; L: lens; PM: permanent magnet; T-Z amp.: transimpedance amplifier.

[1] J. F. Barry *et al.*, Proc. Natl. Acad. Sci. **113**, 14133 (2016).

[2] K. Arai *et al.*, Commun. Phys. **5**, 200 (2022).

Identification of current multipole sources from magnetoencephalography data

Motofumi Fushimi¹, Mutsuko Hatano², Takaaki Nara³, and Masaki Sekino¹

¹Department of Bioengineering, Graduate School of Engineering, The University of Tokyo

²Department of Electrical and Electronics Engineering, School of Engineering, Tokyo Institute of Technology

³Department of Information Physics and Computing, Graduate School of Information Science and Technology, The University of Tokyo

motofumi-fushimi@g.ecc.u-tokyo.ac.jp

Introduction

In magnetoencephalography (MEG) source identification, current sources are typically modeled as equivalent current dipoles (ECDs). However, actual neural sources have non-negligible spatial pattern, which can be accounted for using equivalent current multipoles (ECMs). We extend the previously proposed algebraic method for the multipole source identification in the two-dimensional (2D) case [1] to the three-dimensional (3D) case to enhance applicability of the framework to the realistic MEG problem. This can also be seen as an extension of the 3D dipole and dipole-quadrupole identification method [2] to general-order multipoles.

Methods

By adopting the concentric sphere head model, the radial component of the magnetic field is represented by the current source according to the Biot-Savart law as shown in Fig. 1. The multipole expansion of the equation relates the unknown multipole source parameters (location and moment) to the MEG data [3]. We derived an algebraic equation for multipole parameters, the detail of which will be shown in the presentation. We validated the proposed method by numerical simulations with two distinct current quadrupoles and octupoles.

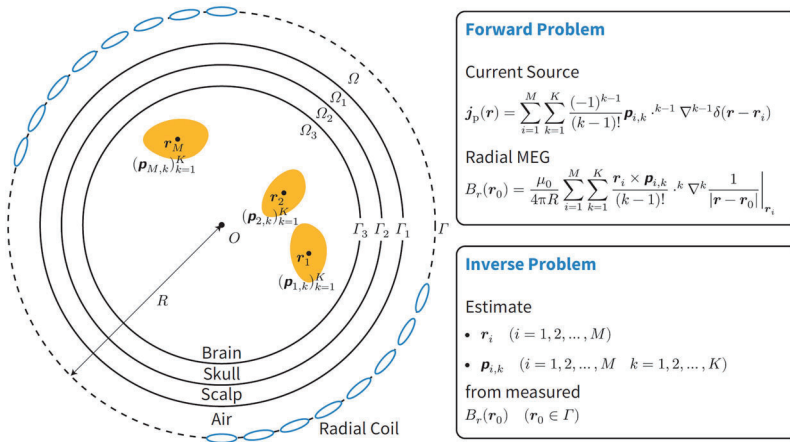


FIG. 1. Problem formulation of the MEG current source identification in the present study.

Results and Discussion

The proposed method could stably estimate both the two quadrupoles and octupoles, which has not been achieved in previous methods, validating the efficacy of the method. In contrast, the results of the ECD model had huge errors because the ECD model erroneously tries to explain MEG data resulting from multipoles by dipoles. The resulting figures will also be presented in the conference.

Acknowledgements

This work was supported by MEXT Q-LEAP Grant Number JPMXS0118067395.

Reference

- ¹T. Nara *et al.*, *Phys. Med. Biol.*, 52(13), 3859-3879 (2007).
- ²T. Nara *et al.*, *Math. Probl. Eng.*, 2013, 413980 (2014).
- ³G. Nolte *et al.*, *Biophys. J.*, 73(3), 1253-1262 (1997).

Optimization of simultaneous measurement of magnetic field and temperature measurement by silicon vacancy quantum sensor using simultaneous resonance

Tomoaki Tanaka¹, Yuichi Yamazaki¹, Kazutoshi Kojima², and Takeshi Ohshima¹

¹National Institutes for Quantum Science and Technology

²National Institute of Advanced Industrial Science and Technology

tanaka.tomoaki@qst.go.jp

Background and Purpose

Silicon vacancies (V_{Si}) in silicon carbide (SiC) have attracted great attention because we can measure magnetic field and temperature in some devices by fabricating V_{Si} in the devices^{1,2}. Simultaneous measurement of magnetic field and temperature using SiC- V_{Si} quantum sensor requires simultaneous Optically Detected Magnetic Resonance (ODMR) measurement of the ground and excited states. However, the ODMR contrast (= sensitivity) of the excited state is about one order of magnitude smaller than that of the ground state. So, the temperature measurement is time-consuming. To solve this problem, we have proposed and demonstrated a new temperature measurement method, Simultaneous Resonance (SR) ODMR, which based on the modulation of the ODMR contrast of the ground state by simultaneous resonance of the ground and excited states³. This method converts part of the contrast of the ground state into that of the excited state. It is necessary to optimize the RF power ratio which is related to the contrast ratio between the ground and excited states to minimize the measurement time in magnetic field and temperature (SR) simultaneous measurement. Therefore, the purpose of our study is to optimize the power ratio of the RF using the simultaneous measurement by SR ODMR.

Methods and Results

V_{Si} dots were fabricated on p-type 4H-SiC epitaxial thin film (5.6 μm) using a particle beam writing (ion species: He, energy: 0.5 MeV, irradiation dose: 3×10^5 /dots). The size and depth of the dots are $5 \times 5 \mu\text{m}^2$ and $\sim 1 \mu\text{m}$, respectively. Three signal generators were used for the measurements, one fixed at the resonance frequency of the ground state (70 MHz) for SR, and the others swept near those of the ground and excited states (20-170, 300-600 MHz) for the ground state and SR ODMR measurements, respectively.

Figure 1 shows the spectra of ground and SR excited states by ODMR simultaneous measurements. Signal intensities indicated by red and blue arrows are observed. The former is a resonance of the ground state, and the latter is that of the excited states. We can find that another dip indicated by green arrow around 500 MHz exists. The sweep condition indicates that this frequency corresponds to 70 MHz of the ground state measurement. This suggests that the resonance of the ground state occurs in both the ground state and SR ODMR measurements. As a result of their competition, the dip appears at around the 500 MHz on the SR ODMR side. We measured the changing of ODMR contrast of the ground and excited states when we change the RF power of signal generators. The signal intensity was almost the same at the RF power ratio of 1:9 for SR and ground state ODMR. At this condition, the contrast of SR is more than four times that of traditional excited state measurement. This suggests that we achieved faster measurement than conventional simultaneous ground and excited states measurement.

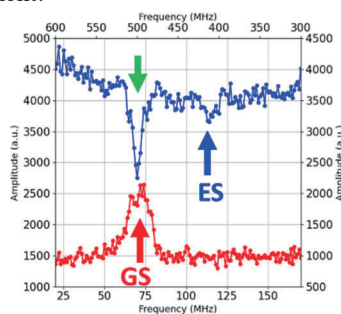


FIG. 1. Simultaneous ODMR measurement of ground and SR excited states (GS and ES) spectra.

Acknowledgement

This work was supported by MEXT Q-LEAP Grant Number JPMXS118067395, ATLA Grant number JPJ004596, and KAKENHI Grant Number 20H00355, 21H04553.

Reference

- ¹M. Niethammer *et al.*, Phys. Rev. Appl. **6**, 034001 (2016).
- ²T. M. Hoang *et al.*, Appl. Phys. Lett. **118**, 044001 (2021).
- ³Y. Yamazaki *et al.*, The 69th JSAP Spring Meeting, 25a-E301 (2022).

Spin-Dependent Photocarrier Generation Dynamics in Electrically Detected NV-Based Quantum Sensor

Hiroki Morishita,^{1,2} Naoya Morioka,^{1,2} Tetsuri Nishikawa,^{1,3} Hajime Yao,^{1,3}
Shinobu Onoda,⁴ Hiroshi Abe,⁴ Takeshi Ohshima,⁴ and Norikazu Mizuochi^{1,2}

¹ Institute for Chemical Research, Kyoto University, Gokasho, Uji, Kyoto 611-0011, Japan.

² Center for Spintronics Research Network, Institute for Chemical Research, Kyoto University, Gokasho, Uji, Kyoto 611-0011, Japan.

³ Department of Molecular Engineering, Graduate School of Engineering, Kyoto University, Nishikyo-Ku, Kyoto, Kyoto, 615-8510, Japan.

⁴ National Institutes for Quantum Science and Technology, Takasaki, Gunma, 370-1292, Japan.
h-mori@scl.kyoto-u.ac.jp

A nitrogen-vacancy (NV) center in diamond is a promising candidate for room-temperature quantum sensors thanks to its long electron spin coherence in ambient conditions [1]. In previous demonstrations, the NV electron spin was detected optically, but another method called photoelectrically detected magnetic resonance (PDMR) is attracting attention. The PDMR technique can read out NV electron spin [2-6] and coupled nuclear spins [7,8]. The electrical detection technique is advantageous for developing and integrating quantum sensors and other quantum devices [7]. However, the mechanism for the electrical detection of NV spins is not fully understood. In this study, we perform the pulsed PDMR measurements using the ensemble of NV centers (concentration of $\sim 1.4 \times 10^{17} \text{ cm}^{-3}$) created by 2 MeV electron irradiation with a fluence of $1 \times 10^{17} \text{ cm}^{-2}$ at 745 °C, followed by annealing at 1000 °C for 1 h in an argon atmosphere. We observe positive contrast in PDMR (Fig. 1(a)) even though a negative PDMR contrast is usually observed. To discuss the sign of the PDMR contrast, we numerically analyze the dynamics of photocarrier generation by NV centers using a seven-level rate model. We found that the sign of the PDMR contrast depends on the difference in the photocurrent generated from the excited states and the metastable state of NV centers.

Furthermore, we demonstrate AC magnetic field sensing using spin coherence with the PDMR technique. AC magnetic field measurement with the PDMR technique is still challenging because the noise from a fluctuating magnetic environment is greater than the measured signal. Using a phase-cycling-based noise-canceling technique to suppress the noise, we demonstrate AC magnetic field sensing with the PDMR technique (Fig. 1(b)). We observe electrically detected AC magnetic field sensing with a sensitivity of $\sim 29 \text{ nT}/\sqrt{\text{Hz}}$. In this talk, we will discuss the mechanism of the NV center's electrical detection and the sensitivity of the electrically detected AC magnetic field sensing.

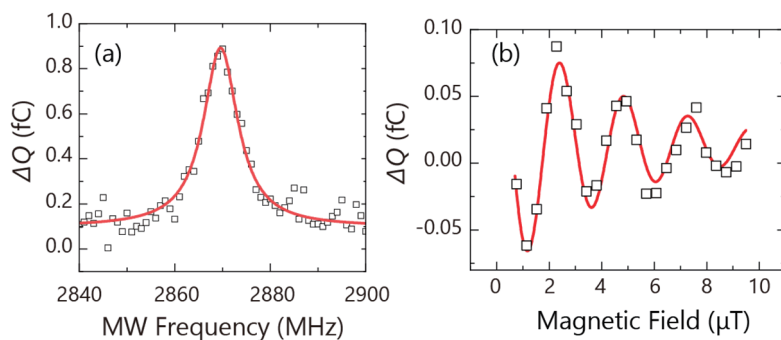


FIG.1 (a) Pulsed PDMR spectrum. (b) AC magnetic field sensing with the PDMR technique

Acknowledgments

We thank T. Ono, T. Moriyama, and Y. Shiota for their technical help. This work was supported by MEXT Q-LEAP (No. JPMXS0118067395), KAKENHI (No. 19H02546), and Kyoto University Nano Hub.

Reference

- ¹ E. D. Herbschleb et al., *Nat. Commun.* **10**, 3766 (2019). ² E. Bourgeois et al., *Nat. Commun.* **6**, 8577 (2015).
- ³ F. M. Hrubesch et al., *Phys. Rev. Lett.* **118**, 037601 (2017). ⁴ M. Gulka et al., *Phys. Rev. Applied* **7**, 044032 (2017)
- ⁵ P. Siyushev et al. *Science* **363**, 728 (2019). ⁶ T. Murooka et al., *App. Phys. Lett.* **118**, 253502 (2021).
- ⁷ H. Morishita et al., *Sci. Rep.* **10**, 792 (2020). ⁸ M. Gulka et al., *Nat. Commun.* **12**, 4421 (2021).

Towards nanoscale zero- to ultralow-field NMR

Till Lenz^{1,2*}, Omkar Dhungel^{1,2}, Arne Wickenbrock^{1,2}, Lykourgos Bougas¹, John W. Blanchard^{2,3}, Gopalakrishnan Balasubramanian⁴, Anjusha Vijayakumar Sreeja⁵, Fedor Jelezko⁵, and Dmitry Budker^{1,2,6}

¹Johannes Gutenberg-Universität Mainz, 55128 Mainz, Germany

²Helmholtz Institut Mainz, 55099 Mainz, Germany

³Quantum Technology Center, University of Maryland, College Park, Maryland 20742, USA

⁴Helmholtz-Zentrum Dresden-Rossendorf (HZDR), Bautzner Landstr. 400, 01328 Dresden

⁵Institute for Quantum Optics, Ulm University, Albert-Einstein-Allee 11, 89081 Ulm, Germany

⁶Department of Physics, University of California, Berkeley, California 94720-7300, USA

*tilllenz@uni-mainz.de, presenter

Abstract: Nuclear magnetic resonance (NMR) is a widely used tool in chemical analysis as well medical diagnostics. While medical diagnostics is the most prominent branch of the NMR subfield magnetic resonance imaging (MRI), chemical analysis is usually performed without imaging via NMR spectroscopy. While we will focus on NMR spectroscopy, both techniques require strong expensive magnets and are limited to sample sizes larger than the micron scale. To overcome these requirements and limitations we propose nanoscale zero- to ultralow-field (ZULF) NMR [1,2]. To achieve the goal of nanoscale ZULF NMR, we, together with our collaborators, demonstrated a technique for magnetometry with NV centers in the ZULF regime [3,4] (i.e. Zeeman interaction weaker than j -couplings) Moreover, we are exploring different potential samples and have identified some promising candidates.

Reference

- [1] J. W. Blanchard, D. Budker, and Andreas Trabesinger, Lower than low: Perspectives on zero-to ultralow-field nuclear magnetic resonance, *Journal of Magnetic Resonance*, **323**, 106886 (2021) 1
- [2] D. Budker, Extreme nuclear magnetic resonance: Zero field, single spins, dark matter. . . , *Journal of Magnetic Resonance*, **306**, Pages 66-68 (2019)
- [3] H. Zheng, J. Xu, G. Z. Iwata, T. Lenz, J. Michl, B. Yavkin, K. Nakamura, H. Sumiya, T. Ohshima, J. Isoya, J. Wrachtrup, A. Wickenbrock, and D. Budker, Zero-Field Magnetometry Based on Nitrogen-Vacancy Ensembles in Diamond, *Phys. Rev. Applied*, **11**, 064068 (2019)
- [4] T. Lenz, A. Wickenbrock, F. Jelezko, G. Balasubramanian, and D. Budker, Magnetic sensing at zero field with a single nitrogen-vacancy center, *Quantum Science and Technology*, **6**, 3 (2021)

Dipole-dipole interaction between NV⁻ centers

Chikara Shinei¹, Yuta Masuyama², Masashi Miyakawa¹, Hiroshi Abe², Shuya Ishii², Seiichi Saiki², Shinobu Onoda², Takashi Taniguchi¹, Takeshi Ohshima² and Tokuyuki Teraji¹

¹ National Institute for Materials Science

² National Institutes for Quantum Science and Technology

SHINEI.Chikara@nims.go.jp

Introduction

Negatively charged nitrogen vacancy center (NV⁻) ensemble with $S=1$ is a promising color center for highly sensitive magnetometers.¹ Dipole-dipole interaction (DDI) between the NV⁻ center and paramagnetic defect is one of decoherence mechanisms. In recent study, some studies showed the interaction between the NV⁻ center and neutral substitutional nitrogen (N_s^0) with $S=1/2$. The strength of DDI is usually expressed as the multiple of DDI coefficient and concentration of paramagnetic defect. DDI coefficient of N_s^0 : $D_{N_s^0}$ is reported as $11.2 \text{ ms}^{-1} \text{ ppm}^{-1}$.¹ For increasing the NV sensing sensitivity, increasing of $[NV^-]$ is needed. Strength of dipole-dipole interaction between NV⁻ centers is expected to be strong in increasing of $[NV^-]$. The effect of interaction on coherence time T_2 of NV⁻ center is expected¹ but is not still clear.

In this study, we investigated DDI coefficient of the NV⁻ center. The DDI coefficient of the NV⁻ center was evaluated using diamond single crystals with substantial amounts of NV⁻ center being comparable to that of N_s^0 .

Method

Nitrogen doped diamond single crystals used in this study were grown using either HPHT synthesis or CVD method. After the diamond growth, electron beam irradiation was applied with the total fluences of 10^{17} - 10^{18} e/cm^2 to create vacancies in the diamond. it was followed by vacuum annealing at 1000°C for 2h to form NV centers in the diamond crystals. Concentration of defects and T_2 are evaluated by EPR and Han echo method, respectively.

Result and Discussion

First, we investigated dependence of $[N_s^0]$ on T_2 of ensemble of NV⁻ center. Fig. 1(a) shows relationship between T_2 and $[N_s^0]$. Most of the data indicates good inverse proportionality between T_2 and $[N_s^0]$, with some exceptional data shown with some deviation from solid line indicating. A larger ratio of $[NV_T^-]$ to $[N_s^0]$ would be associated with a tendency to greater deviation. This result shows that the decoherence contribution of the spin bath of NV⁻ and NV⁰ centers to the NV⁻ center spin of interest cannot be ignored. Second, we observe D_{NV^-} center using the data with relatively large $[NV_T^-]/[N_s^0]$. We also obtained NV⁻ component of T_2 : $T_2\{NV^-\}$ using equation below,

$$\frac{1}{T_2\{NV^-\}} = D_{NV^-} \times [NV^-] = \frac{1}{T_2} - \{D_{N_s^0} ([N_s^0] + [NV^0])\}.$$

Fig. 1(b) portrays relationship between $T_2\{NV^-\}$ and $[NV^-]$. The solid line represents the fitting function curve ($\frac{1}{T_2\{NV^-\}} = D_{NV^-} \times [NV^-]$) with respect to plotting data. We obtained D_{NV^-} of $11.2 \text{ ms}^{-1} \text{ ppm}^{-1}$ through data fitting. This value is nearly equal to that of D_{NV^-} of $10 \text{ ms}^{-1} \text{ ppm}^{-1}$ estimated using the relation between DDI coefficient and spin multiplicity.¹ We observed DDI between NV⁻ centers with $[NV^-]$ ranging from 0.2 ppm to 2 ppm.

Summary

We observed good inverse proportionality between $T_2\{NV^-\}$ and $[NV^-]$. This observation indicates that DDI between NV⁻ centers occurs with $[NV^-]$ ranging from 0.2 ppm to 2 ppm.

Reference

¹ J. F. Barry, J. M. Schloss, E. Bauch, M. J. Turner, C. A. Hart, L. M. Pham, and R. L. Walsworth, Rev. Mod. Phys. **92**, 015004 (2020).

Acknowledgement

This work was supported by MEXT Q-LEAP (JPMXS0118068379 and JPMXS0118067395). T. Teraji acknowledges the support of JST CREST (JPMJCR1773), MIC R&D for construction of a global quantum cryptography network (JPMI00316), and JSPS KAKENHI (Nos. 20H02187, 20H05661 and 19H02617). T. Teraji and S. Onoda acknowledge the support of JST Moonshot R&D (JPMJMS2062).

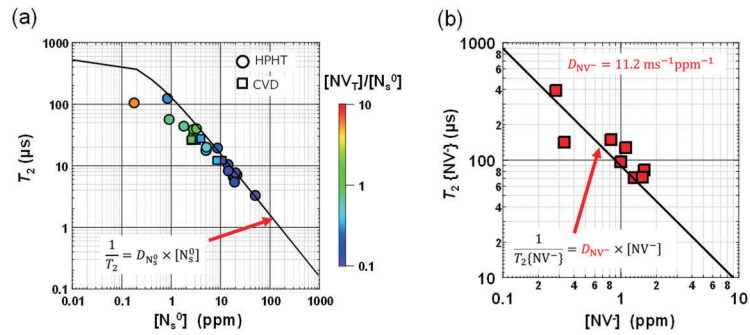


FIG. 1. (a) Relationship between T_2 and concentration of N_s^0 . (b) Relationship between $T_2\{NV^-\}$ and concentration of NV^- .

Extension of dephasing time of ensemble NV centers with a continuous-excitation protocol

Ikuya Fujisaki¹, Yuta Araki¹, Yuji Hatano¹, Takeharu Sekiguchi¹, Takayuki Shibata²,
Takayuki Iwasaki¹ and Mutsuko Hatano¹

¹Department of Electrical and Electronics Engineering, School of Engineering, Tokyo Institute of Technology

²DENSO Corporation

fujisaki.i.aa@m.titech.ac.jp

Introduction

Quantum magnetic sensors based on nitrogen-vacancy (NV) centers in diamond are expected to be applied to biological and chemical applications with its high sensitivity. However, the DC magnetic field sensitivity of NV centers is still insufficient for further applications such as magnetoencephalography (MEG). We focused on CE-Ramsey¹ (Continuous Excitation Ramsey), which is not only advantages for miniaturization thanks to its experimental simplicity, but also has high sensitivity compared to conventional Ramsey. CE-Ramsey has a technical issue of long overhead time due to low laser power limited to suppress optical broadening. Dephasing time T_2^* is a key parameter to improve sensitivity, but T_2^* of typical bulk diamond is limited due to high nitrogen density. In this work, we developed a protocol that combines CE-Ramsey with double quantum (DQ) coherence and spin bath driving (SBD)² and demonstrated that dephasing time can be extended in the CE protocol.

Methods

We built a compact sensor-head with a CPC lens. Radio frequency system and microwave system are established to manipulate spin bath and NV centers (Fig.1 (a)). We compared dephasing time between CE-SQ-Ramsey and CE-DQ-Ramsey, with and without SBD. The diamond sample ($[NV^-] \sim 0.8$ ppm, $[N_3^0] \sim 8$ ppm) was obtained by electron irradiation (5×10^{17} cm⁻²) and vacuum annealing (2 hours) after CVD growth (110 um thick) with ¹²C-enriched methane on a type-IIa substrate.

Results and discussions

We first confirmed coherent control of P1 centers in the spin bath under CE protocol by measuring their spectra and their Rabi oscillations (Fig.1 (b)) with CE-DEER (Double Electron-Electron Resonance) sequences based on the CE-Hahn-Echo. We applied SBD to CE-DQ-4-Ramsey and compared dephasing time. The results showed that the dephasing time is about 2-fold improved by applying DQ and SBD (Fig.1 (c)).

Acknowledgement

This work was supported by MEXT Q-LEAP Grant Number JPMXS0118067395.

We thank Dr. H. Kato (AIST) and Dr. S. Onoda, Dr. T. Ohshima (QST) for supplying diamond samples.

Reference

1. C. Zhang *et al.*, Phys. Rev. Appl. **15**, 1 (2021).
2. E. Bauch *et al.*, Phys. Rev. X **8**, 31025 (2018).

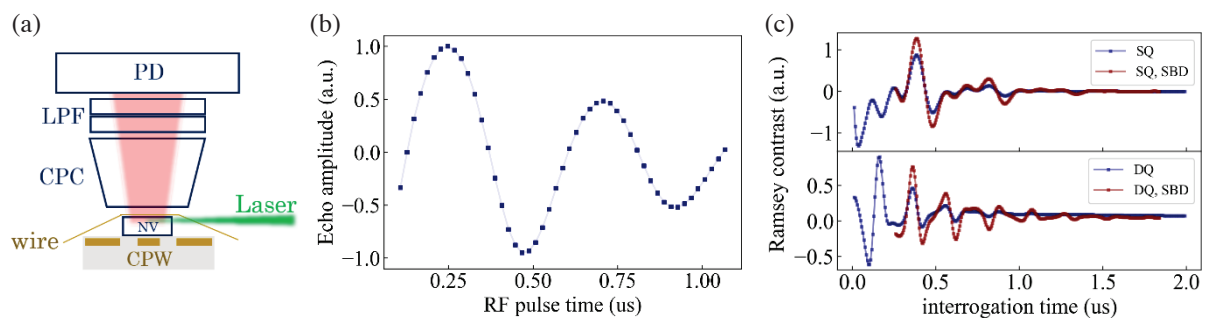


Fig.1. (a) Experimental setup. Microwave and radio frequency are applied with wire and CPW(Coplanar wave guide) respectively. (b) CE-P1 Rabi shows that coherent control of spin bath with CE protocol. Pulse time of RF (radio frequency) is swept in CE-DEER sequences. (c) 2-fold extension of dephasing time by applying DQ and SBD to CE-Ramsey.

Wide temperature operation of diamond quantum sensor for electric vehicle battery monitoring

Keisuke Kubota¹, Yuji Hatano¹, Yuta Kainuma¹, Daisuke Nishitani¹,
Takashi Taniguchi², Tokuyuki Teraji², Shinobu Onoda³, Takeshi Ohshima³, Takayuki Iwasaki¹,
and Mutsuko Hatano^{1,3}

¹Department of Electrical and Electronic Engineering, School of Engineering, Tokyo institute of technology,
2-12-1 Ookayama, Meguro, Tokyo 152-8552, Japan

²National Institute for Materials Science, 1-1 Namiki, Tsukuba, Ibaraki 305-0044, Japan

³National Institutes for Quantum Science and Technology, 1233 Watanuki-machi, Takasaki, Gunma 370-1292, Japan
kubota.k.ai@m.titech.ac.jp

Introduction

The diamond quantum sensors containing NV centers for electric vehicle(EV) battery monitoring are realized [1]. Sensors for EV batteries require a wide range of operating temperatures; however, the dependence of the sensitivity of the diamond quantum sensor system on its wide operating temperature has not been reported. Therefore, we measured the magnetic field sensitivity in the temperature range from -150° to 150°C to investigate its potential for battery monitoring.

Methods

The overall configuration of the measurement system used in the experiment, including the sensor head, is shown in Fig.1 (a). The diamond sensor was a (111) HPHT crystal with the size of approximately 3.6 mm^3 . 1×10^{18} electrons/cm² electron beam irradiation and 1000°C for 1 hour annealing after it realized 5 ppm NV density. The diamond sensor was attached to the top of the multimode fiber and the surrounding microwave antenna with copper belt was attached to realize the sensor head with a size of $1 \times 1 \times 0.5\text{ cm}^3$. The green excitation light from the fiber, with an intensity of approximately 200 mW at the end of the fiber, was irradiated to the diamond sensor. Liquid nitrogen and a heater were used to vary the temperature.

Result and discussion

Fig.1 (b) shows the temperature dependence of the measured sensitivity of the magnetic field. The sensitivity of approximately $5\text{ nT/Hz}^{1/2}$ was confirmed in the temperature range of -150 – 150°C in the measurement system at atmospheric pressure as shown in Fig.1 (a). This sensitivity means that 10 mA current can be measured almost in 500 Hz bandwidth in the temperature range between -150 and 150°C . The confirmed current sensitivity in such a wide temperature range makes it suitable for the batteries that are currently used or under development. Fig.1 (c) shows the temperature dependence of the shot noise sensitivity obtained from the contrast, line width, and photodiode (PD) current. On the high temperature side, as we had expected, the sensitivity deteriorated with increasing temperature. This deterioration is mainly due to the contrast deterioration, which can be attributed to the accelerated initialization of the spin state due to the faster singlet state transition rate [2]. On the low temperature side, we had expected that the sensitivity would be improved, but it deteriorated. Deterioration in contrast was the main cause, but it is difficult to explain the physical reasons. Considering that the line width is thinner at lower temperatures, water vapor condensation at microwave antenna may have increased antenna loss because this experimental setup was open to the atmosphere.

This work was supported by MEXT Quantum Leap Flagship Program (Q-LEAP) Grant Number JPMXS 0118067395 and JPMXS0118068379.

References

- [1] Y. Hatano et al., Sci. Rep. 12, 13991 (2022) [2] D. Toyli et al., Phys. Rev. X 2, 031001 (2012)

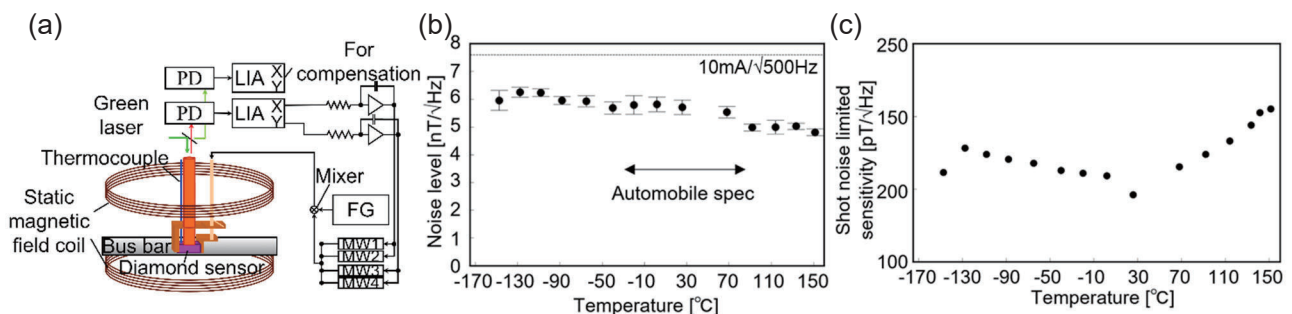


Fig.1 (a) Structure of the entire sensitivity measurement system. The dimension of the sensor head was approximately $1 \times 1 \times 0.5\text{ cm}^3$. (b) Temperature dependence of the measured sensitivity. It was confirmed that the current sensitivity requirements for EV batteries were obtained in the measured temperature range. (c) Measured temperature dependence of shot noise sensitivity obtained from contrast, line width, and PD current.

A development of wearable magnetic shield for MEG

Soichiro Shido¹, Masato Hasegawa², Motofumi Fushimi¹, Shinichi Chikaki¹, Masaki Sekino¹

¹Department of Bioengineering, School of Engineering, The University of Tokyo

²Department of Electrical Engineering and Information Systems, School of Engineering, The University of Tokyo
shido-soichiro@g.ecc.u-tokyo.ac.jp

Introduction

MEG is a technique for measuring the magnetic field generated by the electrical activity of neurons. The brain's magnetic field is about 100fT, which is very small, about 1/100 million of the geomagnetic field. MEG is currently used primarily for the diagnosis of epilepsy¹. MEG has a high potential to become brain imaging technology.

However, the current MEG is limited with superconducting quantum interference devices (SQUIDS)². Vacuum space of SQUID makes it difficult to use closer than ~2 cm to the scalp. That was one of the problems. Recently, new sensor-enabled construction of wearable MEG systems. Optically pumped magnetometers (OPM) have made it possible.

One of the great missions of operating MEG is controlling the magnetic field. MEG systems have magnetic shield rooms (MSR). Originally they have mainly two types of shields. multiple layers of high magnetic permeability metal (e.g. mu-metal) to exclude low-frequency (DC to ~10 Hz) magnetic fields, and a layer of metal with a high electrical conductivity (such as copper or aluminum) to attenuate higher-frequency (>10 Hz) magnetic fields². However, thanks to wearable sensors (OPM, NV) MEG systems are getting more wearable with the movement of participants. These MSRs often result in a 'remnant' DC magnetic field. So, OPMs are built with electromagnetic coils. (Fig.1) is the outlook of a typical system. Compared to the system, we propose a wearable shield system (Fig.2).

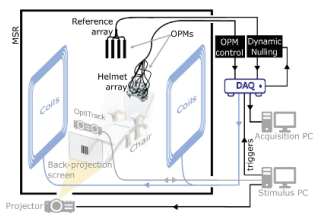


FIG. 1. Typical OPM-MEG system⁴

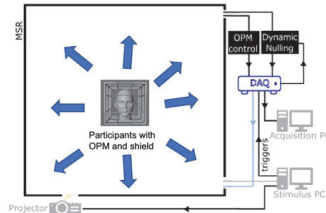


FIG. 2. Our proposal system⁴

In this system, participants can move freely inside the MSR. With this system, we can give participants a comfortable experience of MEG. For the building of the shield, the major steps were the design of the helmet (Fig.3), the optimal design of the coils with target field method (Fig.4), the design of the control system(Fig.5), and the design of the circuit.

In this control system, we applied a PI control system, and the purpose value of this system is to attenuate the Magnetic field into 2nT which is the typical ability of shields with electromagnetic coils. For the circuit, Gradient magnetic field circuit is used. With this circuit, only the ratio of voltage and resistor changes the current of the circuit. So, it is easy and simple to control. To simulate the ability of this shield, we compared designed coil and the Merritt coil which is one of the coils generate uniform magnetic shields. In particular, the magnetic field was not uniform at the bottom of the shield. This may be due to the asymmetry of the shape of the head from front to back. Therefore, it is necessary to consider various improvement plans, such as design changes that take this shape into account and control methods that do not require a uniform magnetic field for the entire helmet.



FIG. 3. The helmet designed in this research

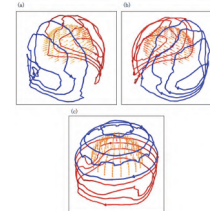


FIG. 4. Coils designed in this research

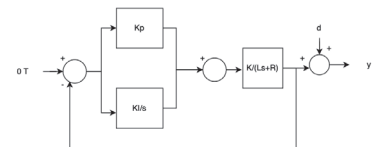


FIG. 5. Control system of this shield

Acknowledgement

This work was supported by MEXT Q-LEAP Grant Number JPMXS0118067395.

Reference

- 1 Baker, Elife,3, e01867(2014).
- 2 Cohen, Science,161,664-666(1972).
- 3 Hoburg, IEEE Transactions on Electromagnetic Compatibility,37,574-579(1995).
- 4 M Rea, NeuroImage,241,118401(2021).

Attempts to generate entanglement state between dipolar coupled NV centers created by molecular implantation

Kosuke Kimura^{1,2}, Shinobu Onoda¹, Keisuke Yamada¹, Wataru Kada², Tokuyuki Teraji³, Junichi Isoya⁴, Nozomu Kosuge^{1,2}, Tomoya Baba^{1,2}, Osamu Hanaizumi², and Takeshi Ohshima¹

¹ National Institutes for Quantum Science and Technology

² Graduate School of Science and Technology, Gunma University

³ National Institute for Materials Science

⁴ Faculty of Pure and Applied Sciences, University of Tsukuba

kimura.kosuke@qst.go.jp, t222d002@gunma-u.ac.jp.

Introduction

Generating quantum entanglement states is one of the most important steps in quantum technologies such as quantum information processing and quantum sensing, etc. The generation of entanglement states has been demonstrated on the various quantum systems. Among them, the entanglement between some solid-state spin qubits has the generation advantage at room temperature. Generation of entanglement state between Nitrogen-Vacancy (NV) centers in diamond, known as solid-state electron spin qubits, has been demonstrated by Double Electron-Electron Resonance (DEER)^{1,2}. The decoherence of NV center limits the fidelity of entanglement state. It is expected that the short free evolution time for entanglement ($2\tau_{ent}$) reduce the limitations caused by decoherence. The spin state reaches the maximum quantum entanglement state at the free evolution time $2\tau_{ent} = 1/v_{dip}$ by DEER, where v_{dip} is dipole coupling strength. By making the dipole-dipole interaction as strong as possible, high fidelity due to short free evolution time is expected. We have created the strongly coupled NV centers by molecular ion implantation^{3,4}. In this study, we report the generation of entanglement state between dipolar coupled double NV centers created by implanting $C_5N_4H_n$ ions. In addition, we report the attempts to shorten $2\tau_{ent}$ by changing DEER pulse sequence.

Experiments and Results

To create dipolar coupled NV centers, $C_5N_4H_n$ ions were accelerated at 65 keV and implanted into diamond. A $C_5N_4H_n$ ion decomposes into individual atoms by collision with diamond, and each nitrogen atom is implanted 9 ± 4 nm apart. The implanted nitrogen atom was combined with a vacancy by annealing process (1000°C, 2h) to create NV centers.

The created NV centers were observed using confocal fluorescence microscopy (CFM). The measurement of DEER was performed with a 532 nm pulsed laser and pulsed microwaves at room temperature in the static magnetic field (FIG. 1). The electron spins of two NV centers with different resonance frequencies (2.6279 GHz for NV_A , 2.6778 GHz for NV_B) able to be manipulated individually. Preparing both NV centers in state $|m_{S,A} = 0, m_{S,B} = 0\rangle$ by optical pumping, an echo measurement is carried out on NV_A . To apply $\pi/2$ pulse on NV_B before the second $\pi/2$ on NV_A , fluorescence is a periodical signal of $\cos(2\pi v_{dip}\tau)$. The result of the DEER measurement is shown in FIG. 2. The measured v_{dip} was 99.9 kHz and $2\tau_{ent} = 1/v_{dip}$ was calculated as 10 μs . In the presentation, the entanglement generation with other pulse sequences will be discussed.

Acknowledgments

This work was supported by JST Support for Pioneering Research Initiated by the Next Generation JPMJSP2146, JSPS KAKENHI No. 21H04646, 20H02187, 20H05661, JST moonshot R&D Grant Number JPMJMS2062, MIC R&D for construction of a global quantum cryptography network JPMI00316, and MEXT Quantum Leap Flagship Program (MEXT Q-LEAP) Grant Number JPMXS0118067395 and JPMXS0118068379.

References

- ¹ P. Neumann, *et al.*, Nat. Phys. **6**, 249 (2010). ² F. Dolde, *et al.*, Nat. Phys. **9**, 139 (2013).
³ M. Haruyama, *et al.*, Nat. Commun. **10**, 2664 (2019). ⁴ K. Kimura, *et al.*, Appl. Phys. Express **15**, 066501 (2022).

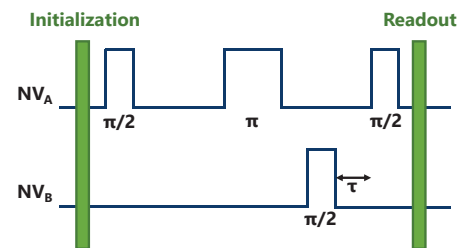


FIG. 1 DEER pulse sequence.

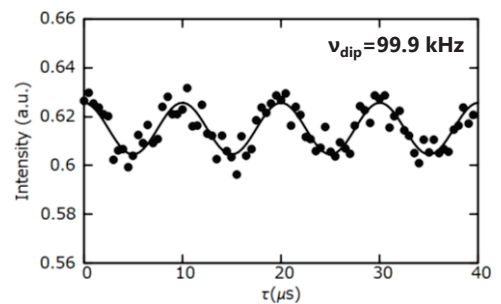


FIG. 2 Typical DEER spectrum.

Charge stability of shallow single NV centers in p-type diamond

Taisuke Kageura^{1,2}, Yosuke Sasama¹, Chikara Shinei¹, Tokuyuki Teraji¹,
Keisuke Yamada³, Shinobu Onoda³, and Yamaguchi Takahide¹

¹National Institute for Materials Science (NIMS)

²National Institute of Advanced Industrial Science and Technology (AIST)

³National Institutes for Quantum and Radiological Science and Technology (QST)

kageura.taisuke@aist.go.jp

Introduction

A stable negatively charged state of nitrogen vacancy (NV) centers in diamond is important for diamond quantum applications such as highly sensitive quantum sensing and high-performance quantum information processing. However, it has been found that the charge state of single NV centers near the surface, called shallow single NV centers, is quite unstable compared with NV centers in bulk¹. Shallow single NV centers are significant to realize high-performance quantum devices such as nanoscale NMR, so the origin of the charge instability needs to be revealed. Here we investigated how the presence of small amounts of boron acceptors in bulk and surface states affect the charge stability of shallow single NV centers².

Results and Discussion

We prepared four lightly boron-doped diamond thin films ($[B] \leq 1 \times 10^{15} \text{ cm}^{-3}$, $[N] < 6 \times 10^{11} \text{ cm}^{-3}$) synthesized by microwave plasma chemical vapor deposition method and formed single NV centers at about 3.6 nm from the diamond surface by ion implantation. We have investigated the charge-state stability of the shallow single NV centers by using photoluminescence spectra and optically detected magnetic resonance (ODMR) measurements. Surprisingly, we found that negatively charged state can be created despite the existence of boron acceptors; Among 20 NV centers for which CW-ODMR was measured, 19 NV centers showed a decrease in fluorescence intensity at a frequency corresponding to the applied magnetic field of 1-2 mT. This negatively charged state could not be explained by the conventional band-bending model, but it could be explained by photoexcitation induced by green laser irradiation. Then we evaluated the charge stability under pulse measurement in the presence of laser non-irradiation time by Rabi oscillation contrast values (Fig. 1). Clear Rabi oscillations were observed except for the sample with higher boron concentration ($[B] = 1 \times 10^{15} \text{ cm}^{-3}$) and acid boiled surface, which means that negatively charged state can be created even under pulse measurement. The variation of contrast values in Fig. 1(b) indicates the difference in charge stability of individual NV centers. This charge instability in lightly doped diamond can be explained by electron transfer between the NV center and the local environment. The charge stability is determined by whether the donor or the acceptor is closer to the NV center.

This study provides a new insight into the charge stability of a single NV center in low-doped diamond and contributes to the further development of NV quantum devices.

This work was partially supported by MEXT Q-LEAP Grant Number JPMXS0118068379 and JPMXS0118067395, JST CREST (JPMJCR1773), JST Moonshot R&D (JPMJMS2062), MIC R&D for construction of a global quantum cryptography network (JPMI00316), JSPS KAKENHI (No. 20H02187, 20H05661, 19H02617 and 21J01804).

Reference

¹D. Bluvstein et al., *Physical Review Letters*, 122, 076101 (2019)

²T, Kageura et. al, *Carbon*, 192, 473 (2022).

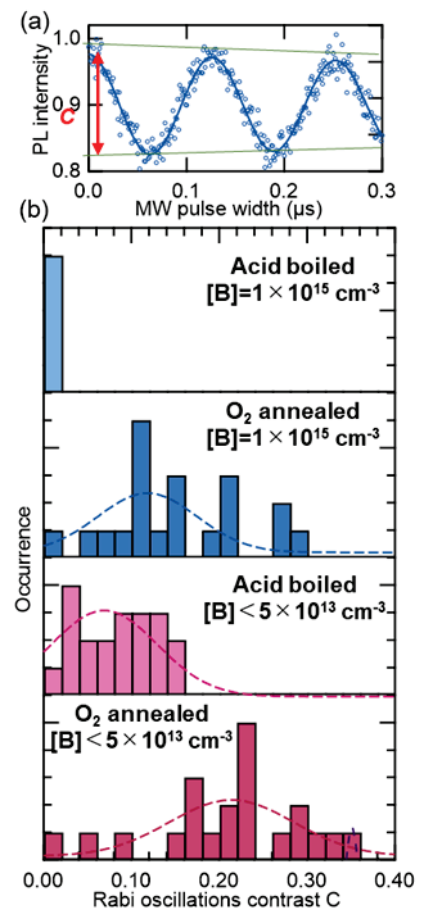


FIG. 1. (a) Typically observed Rabi oscillations and (b) the distributions of Rabi contrast

Room-temperature electrical detection of nuclear spins in silicon carbide

Naoya Morioka^{1,2}, Tetsuri Nishikawa¹, Hiroshi Abe³, Hiroki Morishita^{1,2},
Takeshi Ohshima³, and Norikazu Mizuochi^{1,2}

¹ Institute for Chemical Research, Kyoto University

² Center for Spintronics Research Network, Institute for Chemical Research, Kyoto University

³ National Institutes for Quantum Science and Technology

morioka.naoya.8j@kyoto-u.ac.jp

Spin-active color centers in silicon carbide (SiC) are promising candidates for scalable quantum sensors and quantum information devices operating at room temperature due to their excellent spin coherence properties and the maturity of SiC's wafer-scale semiconductor technology. By making use of the excellent controllability of semiconductor properties and device operation of SiC, the realization of electrical detection of spin information in SiC can benefit in developing integrated quantum devices compared with conventional optical spin detection techniques. Recently, electrical detection of electron spins of the V2 center in 4H-SiC¹ was reported by photoelectrically detected magnetic resonance² (PDMR). However, in the previous demonstration, the PDMR spectra of V2 centers were broad due to the inhomogeneous magnetic field caused by magnetized Ni electrodes, which is a typical ohmic contact material for SiC. The broad linewidth inhibited resolving the signal of nuclear spins, which are useful resources as quantum memories for quantum information processing³ and sensitivity-enhanced quantum sensing.⁴ In this study, we optimized the contact and the device structures, and we obtained the PDMR spectrum of an ensemble of V2 centers with a linewidth of 2.8 MHz, which is narrow enough to observe the hyperfine split resonance peaks coupled to the next-nearest-neighbor (NNN) ²⁹Si nuclear spins (Fig. 1). By addressing the hyperfine split peaks, nuclear-spin-state-dependent spin control and its electrical detection are possible. By applying these techniques, the nuclear magnetic resonance signal of ²⁹Si was successfully detected electrically at room temperature with PDMR-based electron-nuclear double resonance (ENDOR) (Fig. 2).⁵ This is an achievement of electron spin coherence and nuclear spin detection in an identical device. In the ENDOR spectrum in Fig. 2, three peaks were observed, probably originating from three nonequivalent NNN sites.⁶ These results suggest that room-temperature PDMR would enable selective coherent control of nuclear spins, facilitating the development of electrically-driven integrated quantum devices.

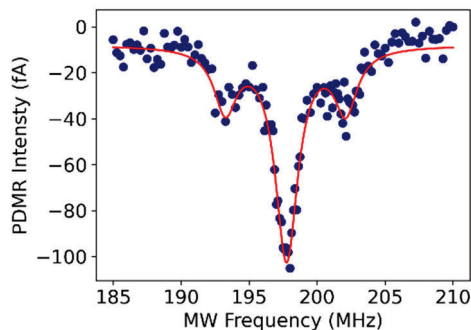


FIG. 1. PDMR spectrum of V2 centers in 4H-SiC.

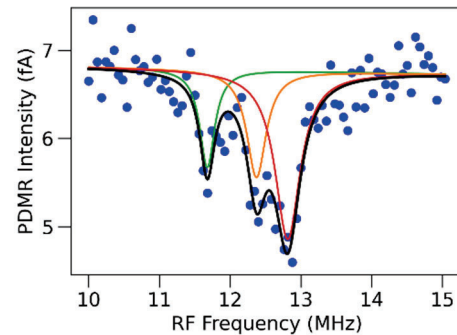


FIG. 2. PDMR-ENDOR spectrum of NNN ²⁹Si nuclear spins coupled to V2 centers in 4H-SiC.

Acknowledgments

This work was supported by MEXT Q-LEAP Grant Number JPMXS0118067395, JSPS KAKENHI Grant Numbers JP20H00355, JP21H04553, JP21K20502, and JP22H01526, JST SPRING Grant Number JPMJSP2110, and Kyoto University Nanotechnology Hub in MEXT ARIM project.

Reference

- ¹M. Niethammer et al., Nat. Commun., 10, 5569 (2019).
- ²E. Bourgeois et al., Nat. Commun., 6, 8577 (2015).
- ³C. E. Bradley et al., Phys. Rev. X, 9, 031045 (2019).
- ⁴M. Pfender et al., Nat. Commun., 10, 594 (2019).
- ⁵T. Nishikawa et al., Appl. Phys. Lett., accepted (2022).
- ⁶V. Ivády et al., Phys. Rev. B, 96, 161114 (2017).

(Near) zero-field cross-relaxation features for ensembles of NV centers in diamond

Omkar Dhungel¹, Till Lenz¹, and Dmitry Budker^{1,2}

¹*Johannes Gutenberg University Mainz, Germany*

Helmholtz Institute Mainz 55128, Germany

²*Department of Physics, University of California, Berkeley, California 94720-300, USA*

budker.uni-mainz.de

Conventional magnetometry using NV centers in diamond relies on the application of microwaves and bias magnetic field. However, there are applications, for example, the study of high-temperature superconductors, zero- to ultralow-field (ZULF) NMR, investigation of biological samples, and magnetic materials where either the microwaves or the bias magnetic field might disturb the system. To overcome such limitations, we study the zero-field cross-relaxation feature [1] for ensembles of NV centers. A study of cross-relaxation features with respect to the sample cut and, NV density will be presented. Multiple cross-relaxation features [2,3] are observed when transverse field is present and these features follow a specific pattern when the azimuthal angle of a transverse field is changed, which is useful for vector-magnetometry applications.

Reference

¹S. Anishchik, V. Vins, A. Yelissev, N. Lukzen, N. Lavrik, and V. Bagryansky, “Low-field feature in the magnetic spectra of nv- centers in diamond,” *New Journal of Physics*, vol. 17, no. 2, p. 023040, 2015.

²R. Akhmedzhanov, L. Gushchin, N. Nizov, V. Nizov, D. Sobgayda, I. Zelensky, and P. Hemmer, “Microwave-free magnetometry based on cross-relaxation resonances in diamond nitrogen-vacancy centers,” *Physical Review A*, vol. 96, no. 1, p. 013806, 2017.

³R. Akhmedzhanov, L. Gushchin, N. Nizov, V. Nizov, D. Sobgayda, I. Zelensky, and H. Philip, “Magnetometry by cross-relaxation-resonance detection in ensembles of nitrogen-vacancy centers,” *Phys. Rev. A*, vol. 100, p. 043844, Oct 2019.

Evaluation of a superconducting nanowire single photon detector for mid-infrared wavelengths

Satoru Mima¹, Fumihiro China¹, Masahiro Yabuno¹, Shigeyuki Miyajima¹, Shigehito Miki^{1,2}, Yuki Gama³, Toshiyuki Tashima³, Masaya Arahata³, Yu Mukai³, Ryo Okamoto³, Shigeki Takeuchi³, Hirotaka Terai¹

¹Advanced ICT Research Institute, National Institute of Information and Communications Technology

²Graduate School of Engineering, Kobe University

³Graduate School of Engineering, Kyoto University

mima@nict.go.jp

Introduction

Superconducting nanowire single photon detectors (SNSPDs) have attractive features such as high efficiency, low jitter, low dark counts, and high counts rates, and are expected to be applied in various fields. Recently, quantum technologies utilizing photons in the mid-infrared region have attracted much attention[1]. However, there are no single-photon detectors in the mid-infrared wavelengths. SNSPD is one of best candidate for high detection efficiency in the mid-infrared region.

In the mid-infrared region, the photon energy is smaller than in the near-infrared region, so the superconducting thin film used in the detector must be thinner and superconducting nanowire must be narrower. In addition, for highly efficient mid-infrared photon detection, the introduced light must be efficiently absorbed by the superconducting nanowire. We employ an approach to enhancing the optical absorptance at target wavelength is integrating the nanowire with the dielectric multilayer cavity[2]. In this study, superconducting nanowire were fabricated on a dielectric multilayer of Ta₂O₅ and Si films designed to maximize light absorption in the mid-infrared region and evaluated.

We cooled down the fabricated detector by a sorption refrigerator capable of cooling down to 0.8 K and evaluate the optical properties using a QCL light source (wavelength $\sim 4.3 \mu\text{m}$) in the mid-infrared region. We reduced optical efficiency between the fiber and the superconducting nanowire for the evaluation of internal efficiency because of the intensity of blackbody radiation in the mid-infrared region. The figure 1 shows the dependence of the internal efficiency of the superconducting nanowire on the bias current measured at different intensities of the mid-infrared light source. We also evaluated the optical efficiency of the same superconducting nanowire in the near-infrared region (1300 nm to 1600 nm) and confirmed that the spectra are consistent with the design.

Acknowledgment

This work was supported by MEXT Q-LEAP Grant Number JPMXS0118067634.

Reference

¹R. H. Hadfield, *Nat. Photon.*, **3**, 696–705 (2009).

²T. Yamashita, K. Waki, S. Miki, R. A. Kirkwood, R. H. Hadfield, H. Terai, *Sci rep.*, **6**, 35240 (2016).

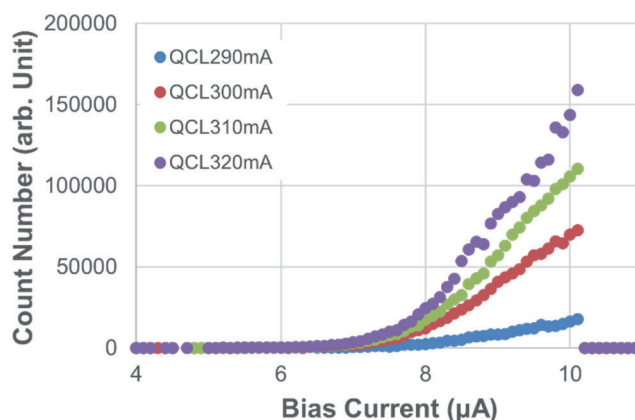


Fig 1. Comparison of the intensity dependence of the internal efficiency in the mid-infrared.

Efficient superconducting nanostrip single-photon detectors for 2 μm wavelength

Fumihiko China¹, Satoru Mima¹, Shigehito Miki^{1,2}, Masahiro Yabuno¹, Shigeyuki Miyajima¹ and Hirotaka Terai¹

¹ Advanced ICT Research Institute, National Institute of Information and Communications Technology

² Graduate School of Engineering, Kobe University

f-china@nict.go.jp

Introduction

In recent years, single-photon detection technology in the mid-infrared wavelength region has attracted attention. In particular, at the 2 μm wavelength band, highly efficient single-photon detectors are required for various applications such as light detection and ranging (LIDAR), satellite-based quantum communications, and silicon-based quantum optics. However, semiconductor avalanche photodiodes and photomultiplier tubes are limited to a sensitive wavelength of approximately 1.8 μm by the energy gap of the semiconductor. On the other hand, superconducting nanostrip single-photon detectors (SNSPDs) are promising detectors because of their wideband sensitivity including the mid-infrared region [1]. To obtain high system detection efficiency (SDE) using SNSPDs, the following three factors should be maximized: optical coupling efficiency, optical absorptance, and internal detection efficiency. The optical coupling efficiency can be maximized by increasing the active area of the SNSPD, and the optical absorptance of superconducting nanostrips is improved by implementing an optical cavity in the SNSPD. The internal detection efficiency can be improved by optimizing nanostrip parameters such as nanostrip width and thickness. In this study, we developed SNSPDs with a dielectric multilayer cavity (DMC) and attempted to maximize the three factors to achieve high SDE in the 2 μm wavelength.

Device design and experimental results

We developed NbTiN-SNSPDs with a DMC. Figure 1 shows the schematic of designed SNSPDs with a DMC comprised of 11 periodic SiO_2/Si bilayers on a Si wafer. Each dielectric layer of DMC is one-quarter of the optical thickness for the 2 μm wavelength. The DMC enhances the optical absorptance by concentrating the electric field of incident photons on the nanostrips. In the simulation results by finite element analysis, we confirmed that the optical absorptance at the 2 μm wavelength reaches over 99%. Based on the SNSPD designs, we fabricated NbTiN-nanostrips with a line width of approximately 110 nm on the DMC. The active area of the fabricated SNSPDs, 30 $\mu\text{m} \times 30 \mu\text{m}$, is enough larger than the mode field diameter of a single mode fiber for the 2 μm wavelength band. Subsequently, we tested the fabricated SNSPDs using a sorption-based cryocooler with an operating temperature of 0.77 K and an optical system composed of a laser source, a beam splitter, valuable optical attenuators (VOAs), neutral-density (ND) filters, a polarization controller, and power meters. We adjusted the optical input power to -110 dBm using three VOAs and two ND filters, and all five attenuators were carefully calibrated before SDE measurements. Figure 2 shows the measurement results of SDE and the dark count rate (DCR) of the SNSPD. We succeeded to demonstrate a high SDE of 79% at a 2 μm wavelength. In addition, we estimated the measurement uncertainty of SDE as $\pm 5.075\%$ by measuring all possible uncertainties of VOAs, ND filters, laser power, the count rate, DCR, and a power meter.

Acknowledgment

This work was supported by MEXT Q-LEAP Grant Number JPMXS0118067634.

Reference

¹F. Marsili et al., *Nano Lett.*, **12**, 4799-4804 (2012).

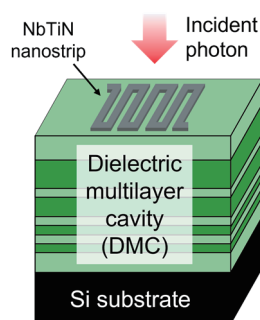


FIG. 1. Schematic of the device structure of an SNSPD with a DML.

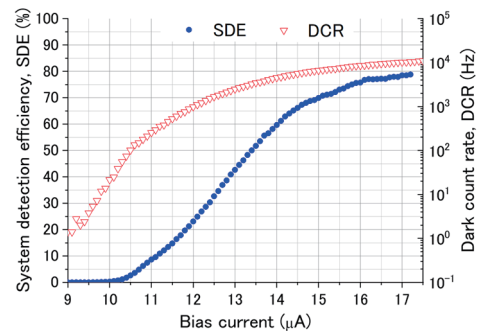


FIG. 2. Bias current dependences of system detection efficiency (SDE) and dark count rate (DCR).

Effect of pump laser linewidth on nonlinear quantum interferometric fringes

Jasleen Kaur¹, Yu Mukai¹, Ryo Okamoto¹ and Shigeki Takeuchi^{1*}

¹Department of Electronic Science and Engineering, Graduate School of Engineering, Kyoto University

*takeuchi@kuee.kyoto-u.ac.jp

Introduction

Infrared spectroscopy is a non-invasive technique used for the identification of materials by analyzing their infrared spectrum. This technique finds applications in chemical industries, environmental sensing, and life sciences, etc. However, conventional infrared spectroscopy techniques suffer from low directivity of infrared sources and thermal background noise deteriorating the sensitivity of IR detectors. Therefore, quantum infrared spectroscopy (QIRS) [1] is being widely investigated as this quantum sensing technology enables IR spectroscopy using a light source and detector in the visible region. In this technique, by utilizing the quantum correlation between visible and IR photon pairs and the quantum interference of their generation processes, we can extract the optical properties of the IR absorptive sample.

The generation of correlated photon pairs in QIRS relies on the spontaneous parametric down-conversion (SPDC) process. Since the current QIRS experiments have been demonstrated using a continuous wave (CW) laser [2,3], the probe photon flux generated is low, leading to an inferior signal-to-noise ratio (SNR) thus limiting the sensitivity of this technique. Achieving high generation efficiency of the PDC process can aid in increasing the SNR of the system. One of the possible ways is to use a short pulse pump laser as the excitation source. The temporal confinement of energy in a pulse laser helps in increasing the parametric gain of the PDC process. However, it is important to note that the pulse laser possesses a finite spectral linewidth which leads to a partial frequency correlation between the generated photon pairs, leading to increased distinguishability between the photons, thus lower interference contrast.

In this work, we report a quantitative analysis of how the pump laser linewidth affects the nonlinear quantum interferometer. As shown in fig.1, we excite a nonlinear quantum interferometer with both CW and pulse laser sources and compare the contrast of fringes using a dispersive spectrometer. We further derive the mathematical relationship between the interferometric pattern obtained by CW and pulse laser.

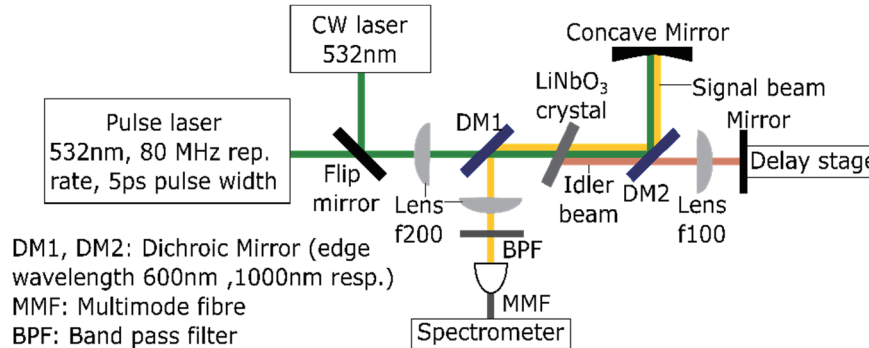


FIG. I. Schematic of the nonlinear quantum interferometer

Reference

- ¹D. A. Kalashnikov *et al.* Nat. Photonics, vol. 10, no. 2, p. 98–101 (2016)
- ²Y. Mukai *et al.* Phys. Rev. Appl., vol. 15, no. 3, p. 034019 (2021)
- ³P. Kaufmann *et al.* Opt. Express, vol. 30, no. 4, p. 5926 (2022)

Acknowledgment

This work was supported by MEXT Q-LEAP Grant Number JPMXS0118067634, JST-CREST Grant Number JPMJCR1674, JSPS KAKENHI Grant Number 21H04444, and WISE Program, MEXT

Highly efficient and ultra-broadband photon pair source using chirped quasi-phase matching slab waveguide

Bo Cao¹, Kyohei Hayama¹, Shun Suezawa¹, Mamoru Hisamitsu², Katsuhiko Tokuda²,
Sunao Kurimura³, Ryo Okamoto¹, and Shigeki Takeuchi¹

¹Department of Electronic Science and Engineering, Kyoto University

²Shimadzu Corporation

³National Institute for Materials Science (NIMS)

takeuchi@kuee.kyoto-u.ac.jp

Introduction

Entangled photon pairs with a broad spectral bandwidth are essential components in many quantum optical applications, such as quantum information, quantum communication and quantum sensing. One of the most rapidly developed technologies is quantum optical coherence tomography (QOCT) [1, 2]. To improve the performance for above applications, highly efficient ultra-broadband frequency correlated photon pair sources are required. In a previous work, we reported a demonstration of high efficiency and broadband frequency correlated photon pair collinear generation (photon are emitted into the same spatial mode) using a ridge-waveguide- based chirped quasi-phase matching (QPM) device [3]. However, two photon interference-based applications, like QOCT, cannot directly use collinearly emitted photon pairs. To solve this problem, here we report a scheme using a slab waveguide based chirped QPM device for the generation of highly efficient and ultra-broadband frequency correlated photon pairs under a non-collinear emission (emit photon pairs into separated spatial modes) condition. In experiments, we observed a generation efficiency of 8.2×10^5 pairs/(s· μ W) and a spectral bandwidth of 190 nm in full width half maximum (FWHM). In addition, we also used slab waveguides as photon pair sources in the two-photon interference experiments.

Experiments and results

The schematic view of this slab waveguide device is shown in Fig. 1. In this device, a layer of stoichiometric lithium tantalate (SLT) with a thickness of $\sim 3 \mu\text{m}$ is used as the waveguide core and resin is used as the cladding material. This waveguide is designed for the generation of photons with a central wavelength at 810 nm using 405 nm continuous wave (CW) pump light via a type-0 spontaneous parametric down conversion (SPDC) process.

We first measured the non-collinearly emitted photons spectra after single mode fiber coupling. In the case of using a non-chirped slab waveguide, we observed a spectrum with a bandwidth of 26 nm, and when using a 3% chirped QPM slab device, the spectral bandwidth expanded to 190 nm in FWHM. We also carried out a coincidence measurement using two single photon detectors (SPCMs) and time analyzer to estimate the generation efficiency. The generation efficiencies for the non-chirped device and the 3% chirped device are 2.4×10^6 pairs/(s· μ W) and 8.2×10^5 pairs/(s· μ W) respectively.

Finally, we performed Hong-Ou-Mandel (HOM) measurements using the non-collinearly emitted photon pairs generated from slab waveguides. The interference resulted a HOM dip with an FWHM width of $8.2 \mu\text{m}$ when using a non-chirped device, and a HOM dip with an FWHM width of $2 \mu\text{m}$ when using a 3% chirped device.

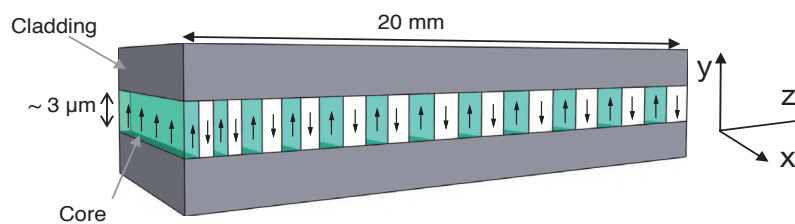


FIG. 1. The schematic view of a slab waveguide device.

This work was supported by JST-CREST (JPMJCR1674), MEXT Quantum Leap Flagship Program (JPMXS0118067634), JSPS KAKENHI (21H04444) and MEXT WISE Program.

Reference

¹A. F. Abouraddy, M. B. Nasr, B. E. A. Saleh, A. V. Sergienko, and M. C. Teich, Phys. Rev. A 65, 053817 (2002).

²K. Hayama, B. Cao, R. Okamoto, S. Suezawa, M. Okano, and S. Takeuchi, Opt. Lett. 47, 4949-4952 (2022).

³B. Cao, M. Hisamitsu, K. Tokuda, S. Kurimura, R. Okamoto, and S. Takeuchi, Opt. Express 29, 21615-21628 (2021).

Optical trapping and movement control of gold nanoparticles on an optical nanofiber

Rui Sun^{1,2}, Yining Xuan^{1,2}, Soyoung Baek¹, and Keiichi Edamatsu¹

¹Research Institute of Electrical Communication, Tohoku University

²Department of Electronic Engineering, Graduate School of Engineering, Tohoku University

sun.rui.p6@dc.tohoku.ac.jp

Introduction

Optical nanofiber has drawn lots of interests in past few years as a promising tool in quantum optics and quantum metrology for its unique properties^{1,2}. Our research focus on the single photon source based on quantum-dot-gold-nanoparticle coupled system on optical nanofiber³. With this experimental system, we have realized a single photon source which is much better than directly exciting the quantum dot with laser. For instance, significant Purcell enhancement of the single photon emission rate was observed⁴.

However, the current experimental system still has some drawbacks. The position of gold-nanoparticle on nanofiber is entirely random, which makes it difficult to quantitatively study the single-photon emission rate. Thus, we propose a non-contact method to control the position of a gold-nanoparticle on the nanofiber. In the past research, we have realized to control the motion of liposome particles in solution by changing the intensity of evanescent light field on the optical nanofiber surface⁵. Here, following a similar approach, we report on a protocol to achieve the control of gold nanoparticles on an optical nanofiber to further improve the properties of single photon source. As shown in Figure 2, the optical nanofiber is immersed in the solution containing gold nanoparticles, and 785 nm laser and 530 nm laser are injected at both ends of the nanofiber respectively. 785 nm laser is used to generate evanescent light field, and 530 nm laser is used to detect the movement of the gold nanoparticles on the surface of optical nanofiber. By adjusting the laser intensity, we can control the movement of the gold nanoparticles on the nanofiber surface. We will introduce optical tweezer to this system to achieve more precise position control of gold nanoparticles.

This work is supported by MEXT Q-LEAP Grant Number JPMXS0118067581.

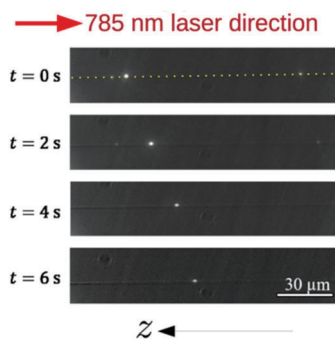


FIG. 1. The movement of a liposome along the nanofiber⁵.

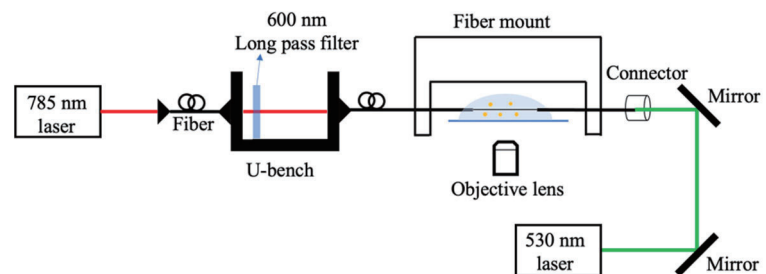


FIG. 2. The scheme of experimental setup.

Reference

- ¹ M. Joos, A. Bramati, and Q. Glorieux, *Opt. Express*, **27**, 18818-18830 (2019).
- ² C. Lee, M. A. Buyukkaya, S. Harper, S. Aghaeimeibodi, C. J. K. Richardson, and E. Waks, *Nano Letters*, **21**, 323-329 (2021).
- ³ M. Sadgrove, M. Sugawara, Y. Mitsumori and K. Edamatsu, *Sci Rep*, **7**, 17085 (2017).
- ⁴ M. Sugawara, Y. Xuan, Y. Mitsumori, K. Edamatsu and M. Sadgrove, *Phys. Rev. Research*, (in press) (2022).
- ⁵ T. Yoshino, D. Yamaura, M. Komiya, M. Sugawara, Y. Mitsumori, M. Niwano, A. Hirano-Iwata, K. Edamatsu, and M. Sadgrove, *Opt. Express*, **28**, 38527-38538 (2020).

Electromagnetic-field analysis of the plasmon-enhanced single photon emitters on an optical nanofiber

Yining Xuan^{1,2}, Rui Sun^{1,2}, Soyoung Baek¹, and Keiichi Edamatsu¹

¹Research Institute of Electrical Communication, Tohoku University

²Department of Electronic Engineering, Graduate School of Engineering, Tohoku University

xuan.yining.t8@dc.tohoku.ac.jp

Single photon emitter has many applications in quantum information, communication, and metrology. Therefore, bright single photon emitters with enhanced quantum efficiency are very important for practical quantum applications and have been studied using various systems [1]. To achieve an enhanced, polarized single photon source that can be coupled into the fiber network directly, we studied on a gold nanoparticle-quantum-dot (GNP-QD) coupled system [2,4], as shown in Fig.1. The single photon source in this research is based on a semiconductor quantum dot (QD) with the emission wavelength around 800 nm. The surface plasmon resonance of gold nanoparticles (GNP) provide large Purcell enhancement relative to conventional cavities and can also provide enhancement of degree-of-polarization (DOP) depending on the type of nanoparticle. In addition, optical nanofibers have the advantages of low optical loss when coupling to conventional fiber networks, and low cost as they can be fabricated from standard single mode optical fibers. Furthermore, through the evanescent field of the nanofiber, photons from QDs can be coupled directly into the nanofiber and hence an optical fiber network.

To understand the distribution of electric field and the impact of incident light on gold nanoparticles on the nanofiber, we carried out electromagnetic-field analysis (FDTD: Finite-difference time-domain method). We analyze the background field distribution, reflection coefficient, absorption and scattering cross section of gold nanoparticles on the fiber surface at various incident angles. Through the analysis of electric field distribution and localized surface plasmon response of gold nanoparticles in Fig.2, the performance of gold nanoparticles on the surface of nanofiber is obtained and discussed. The single photon source with GNP-QD structure can enhance the luminous efficiency of quantum dot due to the Purcell effect. We plan to add a quantum dot in the vicinity of the gold nanoparticle and perform the simulation.

This work was supported by MEXT Q-LEAP Grant Number JPMXS0118067581.

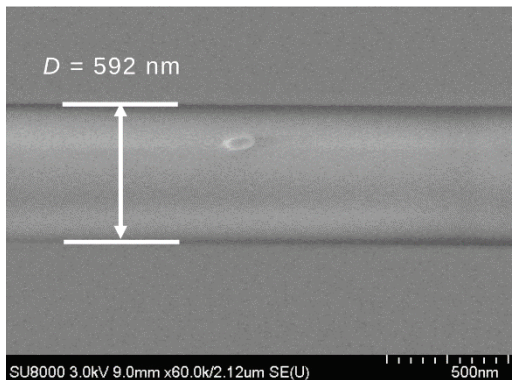


FIG. 1. SEM image of the quantum-dot-gold-nanorod coupled system on an optical nanofiber.

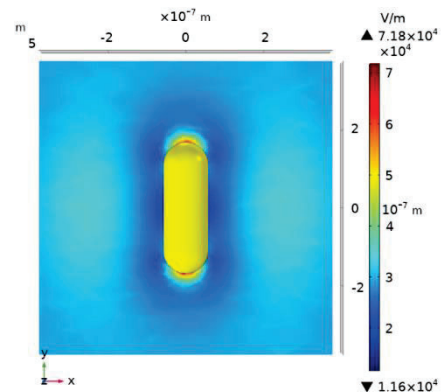


FIG. 2. Localized plasmon resonance of gold nanorod using FDTD simulation.

Reference

¹H. J. Kimble, Nature, 453, 7198 (2008).

²M. Sadgrove, M. Sugawara, Y. Mitsumori, and K. Edamatsu, Sci. Rep., 7, 17085 (2017).

³M. Sugawara, Y. Mitsumori, K. Edamatsu, and M. Sadgrove, Opt. Express, 28, 18938 (2020).

⁴M. Sugawara, Y. Xuan, Y. Mitsumori, K. Edamatsu, M. Sadgrove, Phys. Rev. Research, (in press) (2022).

Ultrafast measurement of biphoton wave packets using optical Kerr gating

Takahisa Kuwana¹, Masahiro Yabuno², Fumihiro China², Shigehito Miki², Hirota Terai²,
Peter J. Mosley³, Rui-Bo Jin⁴ and Ryosuke Shimizu¹

¹The University of Electro-Communications, 1-5-1 Chofugaoka, Chofu, Tokyo, Japan

²Advanced ICT Research Institute, National Institute of Information and Communications Technology,
588-2 Iwaoka, Nishi-ku, Kobe 651-2492, Japan

³Centre for Photonics and Photonic Materials, Department of Physics, University of Bath, Bath, BA2 7AY, UK

⁴Hubei Key Laboratory of Optical Information and Pattern Recognition, Wuhan Institute of Technology, Wuhan 430205, China
k2133039@gl.cc.uec.ac.jp

Introduction

Single-photon detection is of importance for quantum information and sensing technologies. Improving the temporal resolution in single-photon detection is essential for the further development of quantum technologies. Currently, a superconducting nanowire single-photon detector has achieved ~ 3 ps temporal resolution, which is the best temporal resolution as far as we know. However, there is a trade-off between detection efficiency and temporal resolution. Thus, extending into the femtosecond range is challenging without a catastrophic reduction in detector efficiency. On the other hand, optical gating with ultrafast laser pulses can efficiently detect photons with high temporal resolution. Up to now, we developed an ultrafast single-photon detector using an optical Kerr gating (OKG) and demonstrated the single-photon detection with 224 ± 9 fs temporal resolution under low-gating power consumption (~ 20 mW)¹. However, no demonstration of a two-photon detection by the OKG has been reported. In this work, we present the development of our OKG system to a two-photon detection toward joint temporal intensity (JTI) measurements.

Experiment

Figure 1 shows the schematic diagram of the experimental setup. Our PCF was specially designed to minimize the group velocity difference between the photons with the center wavelength of 1584 nm and the gating pulse with the wavelength of 792 nm for efficient cross-phase modulation. Ultrafast pulses from a mode-locked Ti:sapphire laser operating at the wavelength of 792 nm were divided by a polarization beam splitter. One is sent to a periodically poled KTP (PPKTP) crystal to generate biphotons in a type-II phase-matching condition and the other is used for gating pulses of the OKG system. Biphotons generated via PPKTP crystal were led to the OKG system with the Sagnac interferometer configuration. Photons were propagated in either clockwise (CW) or counterclockwise (CCW) directions. Only the photon wave packet in the CW propagation was copropagated with the gating pulse. Then, a nonlinear phase shift by the optical Kerr effect was added to the photon overlapped with the gating pulse in the PCF. In the case that the phase difference between CW and CCW propagation of the Sagnac interferometer is not zero, a portion of the photons are outputted to the detection port. Eventually, we can measure the envelope of the wave packet by sweeping the relative delay between the photon and the gating pulses. With the help of polarization multiplexing, we developed our system to the two-photon detection. We reconstruct the JTI from coincidence counts of our Kerr gating system.

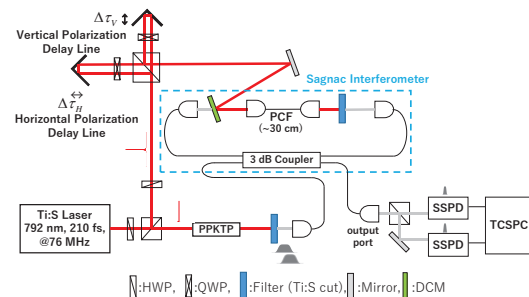


FIG. 1. JTI measured our OKG system

Results and discussion

Figure 2 shows the measured JTI. We can clearly see the two-photon temporal distribution with a negative correlation. This is the first experimental observation of the JTI by the OKG. We achieved the maximum signal-to-noise ratio with a gating power of 50 mW, meaning that the order-of-magnitude improvement of the gating power consumption compared to the up-conversion method².

Acknowledgment

This work was supported by MEXT Q-LEAP Grant Number JPMXS011806924.

Reference

- ¹ M. Yabuno, R. Shimizu, *et al.*, Opt. Express **30**, 4999-5007 (2022).
- ² R.-B. Jin, R. Shimizu, *et al.* Phys. Rev. Appl. **10**, 034011/1-11 (2018).

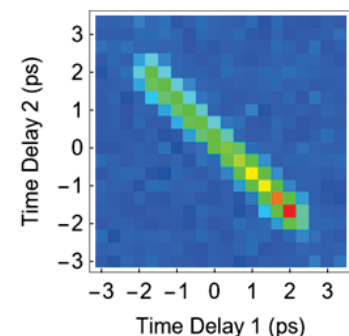


FIG. 2. JTI measured our OKG system

Growth of thick CVD diamond films containing aligned nitrogen-vacancy centers for high-sensitivity quantum sensors

Takeyuki Tsuji¹, Takayuki Iwasaki¹, and Mutsuko Hatano¹

¹Department of Electrical and Electronics Engineering, School of Engineering, Tokyo Institute of Technology

tsuji.t.ac@m.titech.ac.jp

A large volume of CVD diamond films containing aligned nitrogen-vacancy (NV) centers lead to highly sensitive quantum sensors. To form perfectly aligned NV centers, diamonds need to be grown using lateral growth in the $[1\bar{1}2]$ direction.[1] It is necessary to cut and polish the diamond substrate at a misorientation angle (θ_{mis}) to create the steps, as shown in Fig. 1. Geometrically, as θ_{mis} increases, the maximum thickness of the diamond film increases, as shown in Fig. 1. For example, if a 1 mm² diamond substrate is polished at $\theta_{mis}=10^\circ$, the maximum film thickness is $1\text{ mm} \times \sin(10^\circ) \approx 170\ \mu\text{m}$, while at $\theta_{mis}=0.5^\circ$, the maximum film thickness is $1\text{ mm} \times \sin(0.5^\circ) \approx 7\ \mu\text{m}$. Therefore, θ_{mis} is a key parameter in determining the thickness of the diamond films. In this study, the dependence of the growth rate and NV center properties on θ_{mis} ($= 0.4^\circ\text{--}9.9^\circ$) was investigated for synthesizing a thick diamond film containing aligned NV centers.

Diamond films containing NV centers were grown on Ib (111) diamond substrates (1 mm \times 1 mm \times 0.3 mm). The surfaces of the diamond (111) substrates were polished in the $[1\bar{1}2]$ direction at θ_{mis} of 0.4(1)°, 2.7(1)°, 3.7(1)°, 5.0(1)°, and 9.9(1)°, which were measured using X-ray diffraction. We used a high-power density MPCVD where the microwave plasma was reflectively concentrated above the diamond substrates by a spherical chamber.[2] Hydrogen, methane, and nitrogen gases flowed in the setup at 500, 0.5, and 0.01 sccm, respectively. The pressure, microwave power, and temperature were set to 30 kPa, 2.1 kW, and 800 °C, respectively. The thickness and nitrogen density of the diamond films were measured using secondary ion mass spectrometry (SIMS). The fluorescence of the NV centers was measured using a home-built confocal microscope.

The growth rate increased from 1.8 $\mu\text{m}/\text{h}$ to 5.3 $\mu\text{m}/\text{h}$ when θ_{mis} increased from 0.4° to 5.0°, and it was 4.4 $\mu\text{m}/\text{h}$ at 9.9°. (Fig.2. (a)) This was discussed by the relationship between a migration length of carbon precursors and a terrace width. With increased θ_{mis} , the NV yield, a fraction of the NV center density in the nitrogen density, increased from 0.4% to 1.1%. (Fig.2. (b)) Finally, a diamond film was synthesized for 30 h to obtain a thick diamond film using the 1 mm² diamond substrate with $\theta_{mis}=9.9^\circ$. Figure 2(c) shows a cross-sectional image of the CVD diamond film. Considering the refractive index of diamond (2.41) and immersion oil (1.52) and the numerical aperture (NA) of the objective lens (1.42), the distance of the detection point moved in the CVD diamond film was 1.71 times the distance the objective lens moved.[3] Thus, the film thickness was calculated as approximately 70 μm (CVD film thickness seen by an X-Zscan) \times 1.72 \approx 120 μm . Figure 2(d) shows the CW-ODMR spectra of the film at different positions shown in Fig. 5(g). Only two CW-ODMR peaks were observed, which confirmed the formation of perfectly aligned NV centers throughout the thick diamond film. This study is useful to design high-sensitivity diamond films using NV centers.

Acknowledgment This work was supported by MEXT Q-LEAP Grant Number JPMXS0118067395. and conducted at (NanofabPF, Tokyo Tech), supported by "Nanotechnology Platform Program" of the Ministry of Education, Culture, Sports, Science and Technology (MEXT), Japan, Grant Number JPMXP09F-21-IT-014.

Reference [1] T. Miyazaki, et al., Appl. Phys. Lett. 105, 261601 (2014).[2] T. Tsuji, H. Ishiwata, T. Sekiguchi, T. Iwasaki and M. Hatano, Diam. Relat. Mater. [108840], 108840 (2022). [3] E. E. Diel, J. W. Lichtman and D. S. Richardson, Nat. Protoc. 15 [9], 2773 (2020).

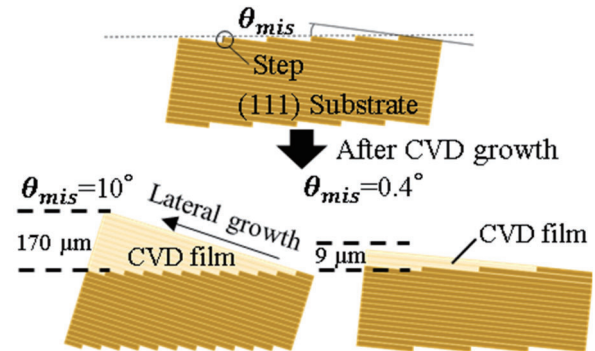


Fig.1. Differences in the maximum film thicknesses for different misorientation angles (θ_{mis}).

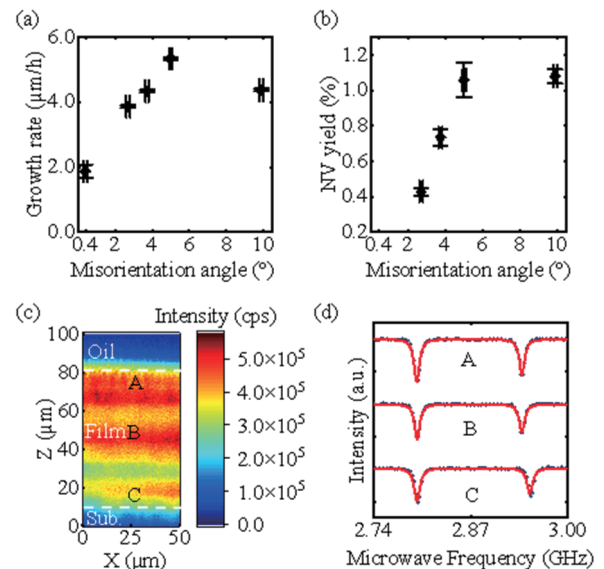


Fig.2. (a)–(b) Dependence of the growth rate and NV yield on misorientation angles, respectively. (c) Cross-sectional image of the CVD diamond film using the confocal microscope. (d) CW-ODMR spectra of the CVD diamond film at different positions shown in (c).

Enhancement of fluorescence collection efficiency using angle-shaped diamonds for compact magnetic sensor

Yuta Shigenobu¹, Yuta Kainuma¹, Yuji Hatano¹, Takayuki Shibata²

Akimichi Nakazono³, Takeshi Ohshima⁴, Mutsuko Hatano^{1,4}, Takayuki Iwasaki¹

¹Department of Electrical and Electronics Engineering, Tokyo Institute of Technology

²DENSO CORPORATION,

³YAZAKI CORPORATION,

⁴National Institutes for Quantum Science and Technology

shigenobu.y.aa@m.titech.ac.jp

Introduction

Nitrogen-vacancy (NV) centers in diamond work as highly sensitive magnetic field sensors with a wide dynamic range, a wide operating temperature range, and the ability to simultaneously measure magnetic field and temperature, which are suitable for applications of battery monitoring¹ and biomedical sensing². In order to improve the magnetic field sensitivity, it is important to develop a method to collect red fluorescence emitted from NV centers in a diamond sensor with high efficiency. A Compound Parabolic Concentrator (CPC) lens³ has been utilized to increase the collection efficiency. In this study, we propose a new method, which can be combined with the CPC lens, for the enhancement of the collection efficiency using a three-sided-angle-shaped diamond. We found that the efficiency can be more than doubled with a side angle of 30° or higher.

Method

The sensor head used in the experiment and simulation model is shown in Fig.1, where the distance (t) between the CPC lens and the Photo Detector (PD) light-receiving surface is variable from 1.75 mm to 11.75 mm. First, we used light path analysis software (LightTools) to simulate the fluorescence collection efficiency (β_{sim}) when the diamond side shaping angle θ was increased from 0° to 50° with a step size of 10°. Experimentally, a green laser (wavelength: 532 nm) was irradiated to be perpendicular to the (111) plane of the diamond sensor, and PD current was measured. The diamond sensors used were HPHT-grown Ib (111) substrates (2.0×2.0×0.6 mm³). The NV centers were formed by irradiating with an electron beam with a fluence of 1.0×10¹⁸ cm⁻² and subsequently annealing at 1000 °C for 2 hours. Then, the sidewalls of the samples were angle-polished.

Result

Figure 2(a) shows the simulated β_{sim} while changing the side-angle and distance between the CPC lens and light-receiving surface of PD. β_{sim} decreases as increasing the distance. Thus, we investigated the dependence of β_{sim} on the grinding angle at a short distance of 1.75 mm. The inset of Fig. 2(a) shows that β_{sim} increased in the range from 0° to 20°, while it remained approximately constant from 20° to 40°. The comparison between 0° and 30° polishing shows the increase in β_{sim} by a factor of about 2. The further increase in the angle above 40° again makes β_{sim} higher. Then, we performed the experiments using two samples of 0° and 30° shaping. Figure 2(b) depicts the measured PD current as a function of the green laser power. The PD current of the 30° polished sample becomes 2.4 times higher compared to the 0° sample, which agrees with the simulation.

This work was supported by MEXT Q-LEAP Grant Number JPMXS0118067395.

References

- [1] Y. Hatano et al., Sci. Rep. 12, 13991 (2022) [2] K. Arai et al, Commun Phys 5, 200 (2022)
[3] T. Wolf et al., Phys. Rev. X 5, 041001 (2015).

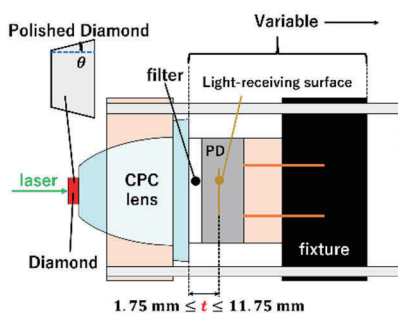


Fig.1 Sensor head structure

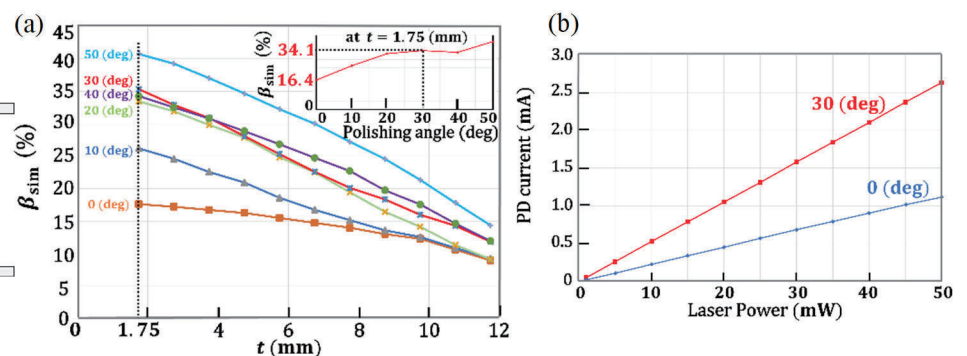


Fig.2 (a) Simulation of β_{sim} . depending on the polishing angle and PD position. (b) Experimentally obtained PD current for the 0° and 30° samples.

Transfer-printing-based integration of SiN grating structure on diamond toward highly sensitive quantum sensor

Ryota Katsumi^{1,2}, Takeshi Hizawa¹, Akihiro Kuwahata^{2,3}, Shun Naruse¹, Yuji Hatano⁴, Takayuki Iwasaki⁴, Mutsuko Hatano⁴, Fedor Jelezko⁵, Shinobu Onoda⁶, Takeshi Ohshima⁶, Masaki Sekino², and Takashi Yatsui^{1,2}

¹ Graduate School of Engineering, Toyohashi University of Technology

² Graduate School of Engineering, The University of Tokyo

³ Graduate School of Engineering, Tohoku University

⁴ School of Engineering, Tokyo Institute of Technology

⁵ Institute of Quantum Optics, Ulm University

⁶ National Institutes for Quantum Science and Technology

katsumi.ryota.ti@tut.jp

Introduction

A nitrogen-vacancy (NV) center in diamond is one of the promising candidates for quantum sensing, especially sensitive magnetic sensing thanks to their excellent spin property^{1,2}. However, their demonstrated magnetic field sensitivity is far beyond that based on conventional magnetometers including superconducting quantum-interference devices. One of the critical issues is the poor extraction efficiency of the emitted photons from the diamond NV substrate³. This can be overcome by implementing the nanostructure on diamond including gratings, but the fabrication of such structure on diamond has the technical difficulty.

Method and Result

In this work, we demonstrate the hybrid integration of a silicon nitride (SiN) circular grating structure on a single-crystal diamond NV substrate toward sensitive magnetometers. Figure 1(a) displays an SEM image of the grating based on SiN, which is transparent for the NV emission wavelength of ~ 700 nm. To pick them up, we employed the air-bridged structure for the grating. By using the pick-and-place transfer printing⁴ [Fig. 1(b)], the SiN grating was integrated on the diamond NV substrate. Figure 1(c) displays an optical microscope image of the fabricated device. The SiN grating is bonded with the diamond NV substrate.

The fabricated device was characterized using micro-photoluminescence (μ PL) spectroscopy. The NV centers were excited with a 532 nm-CW laser. The red curve in Fig. 1(d) shows a PL spectrum measured for the sample with the SiN grating at an input laser power of 12 mW. For comparison, we measured the PL spectrum for the bare region of the diamond NV substrate near the SiN grating (blue curve in Fig. 1(d)). The collected photon counts are increased by a factor of up to 1.6 with the SiN grating structure. We also evaluated the magnetic sensitivity of the fabricated device. Figure 1(e) shows the lock-in voltage detected by the lock-in detection system² as a function of the magnetic field strength B . The detected voltages with the grating are higher than those in the bare region, which is consistent with the results of Fig. 1(d) and demonstrating the improvement of the magnetic sensitivity in the fabricated device.

Acknowledgement

This work was supported by MEXT Q-LEAP Grant Number JPMXS0118067395 and Kakenhi (20H02197, 20H05091, 20K21118, 21K20428, 22H01525, and 22K14289).

References

- ¹J. M. Taylor, *et al.*, Nat. Phys. **4**, 810 (2008).
- ²A. Kuwahata, *et al.*, Sci Rep **10**, 2483 (2020).
- ³D. Le Sage, *et al.*, Physical Review B **85**, 121202 (2012).
- ⁴R. Katsumi, *et al.*, Optica **5**, 691 (2018).

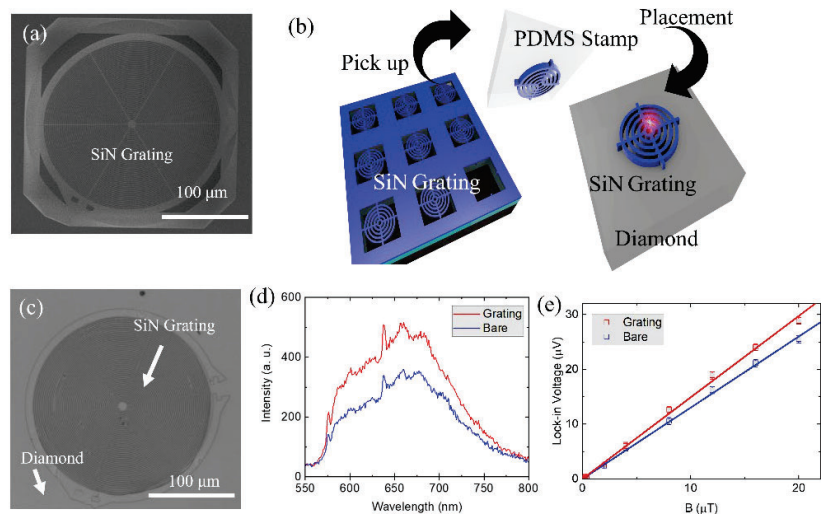


FIG. 1. (a) SEM image of the fabricated SiN grating. (b) Schematics of transfer printing of SiN grating on diamond. (c) Optical microscope image of the fabricated device. (d) Measured PL spectra (red: SiN grating, blue: bare region). (e) Lock-in voltage detected by the lock-in detection system as a function of magnetic field strength (B).

NVC-SPM System to Inspect Electric Devices

Teruo Kohashi¹, Masanari Koguchi¹, Akehito Shiotake² and Satoshi Ono²

¹Hitachi, Ltd., Research & Development Group, Hatoyama, Saitama, 350-0395 Japan

²The Graduate School of Informatics and Engineering, The University of Electro-Communications, Choufu, Tokyo, 182-8585, Japan

teruo.kohashi.fc@hitachi.com

Introduction

A scanning probe microscope using nitrogen-vacancy color centers in diamond (NVC) as a probe (NVC-SPM) has been developed [1,2], taking advantage of excellent characteristics of NVC, such as high sensitivity for magnetic field detection in three dimensions and high spatial resolutions. For now, this technique is mainly used to study fundamental physical phenomena. On the other hand, we are developing an NVC-SPM to inspect electric devices by evaluating magnetic fields generated from a tiny electric wiring. In this paper, we report the development of a new system including a compact microwave antenna and mini-mirror, which makes it possible to inspect the predetermined electric circuit in a wide circuit board.

Results

It is important to set the microwave antenna as close as fifty μm to the probe in NVC-SPM, referring to the previously published example [2]. In order to detect magnetic field generated around a minute wiring between the pads, the microwave antenna should be inserted between the two electrical pads, which are positioned in the distance of less than 1mm. Moreover, irradiation and detection light are performed with a confocal microscope with a working distance of 4.5 mm. It means that the antenna and the probe should be set above the predetermined electric circuit in the space of 4.5mm. We need to set these components precisely in the measurement; therefore, it is desired to confirm the position of each component in the vertical direction from the sample surface. However, the field of view is very narrow through the objective lens (e.g., several hundred μm) because the lens center diameter is very small. A new function for precise position adjustment among these components was required in our SPM system.

Our new NVC-SPM is summarized in Fig. 1. We designed the microwave antenna with very tiny coil with diameter of $500\mu\text{m}$, and mini-mirror to confirm the position of each component from vertical direction using a camera. We developed the above-mentioned system as shown in Fig. 2, and confirmed that this system works properly. As a next challenge, we will inspect the actual electric circuit using this NVC-SPM system.

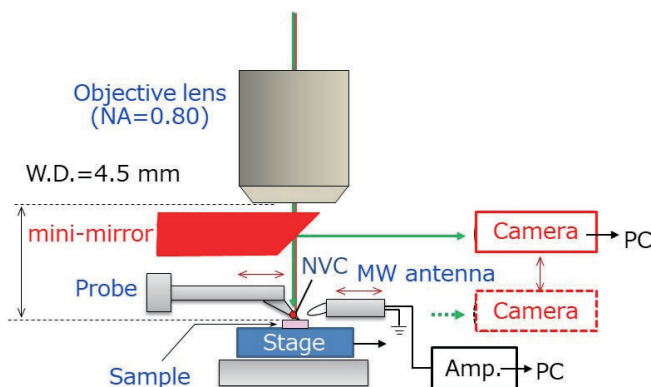


FIG. 1. Newly developed NVC-SPM system with mini-mirror.

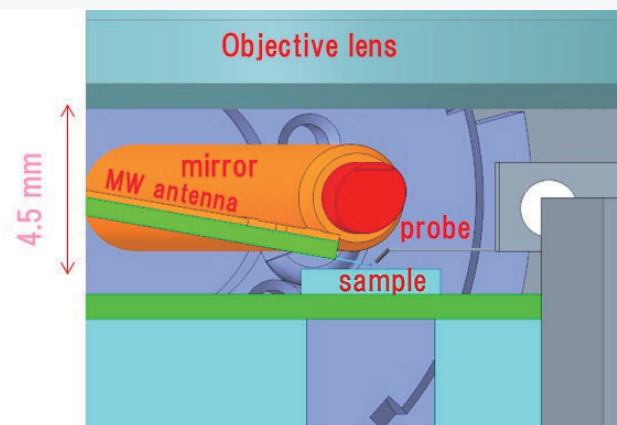


FIG. 2 3D-CAD image of set up around the sample.

This work was supported by MEXT Q-LEAP Grant Number JPMXS0118067395.

Reference

- [1] J. M. Taylor, P. Cappellaro, L. Childress, L. Jiang, D. Budker, P. R. Hemmer, A. Yacoby, R. Walsworth, M. D. Lukin, Nat. Phys. **4**, 810 (2008).
- [2] T. X. Zhou, R. J. Stohr and A. Yacoby, Appl. Phys. Lett **111**, 163106(2017).

Enhancing sensitivity with entanglement in coupled nitrogen vacancy centres

Ernst David Herbschleb¹, Riku Kawase¹, Hiroyuki Kawashima¹, Hiromitsu Kato², Toshiharu Makino², Satoshi Yamasaki³, Shinobu Onoda⁴, Hiroshi Abe⁴, Takeshi Ohshima⁴, Norikazu Mizuochi¹

¹Institute for Chemical Research, Kyoto University

²National Institute of Advanced Industrial Science and Technology (AIST)

³Nanomaterials Research Institute, Kanazawa University

⁴National Institutes for Quantum Science and Technology (QST)

herbschleb@dia.kuicr.kyoto-u.ac.jp

Introduction

Quantum sensing has great potential for applications that require ultra-high sensitivities. The nitrogen-vacancy (NV) centre is an important example of a quantum sensor, since it works under ambient conditions, enables high spatial resolution, and several physical quantities can be measured. Coherence is a quantum resource that is already utilised in many quantum sensing protocols. However, the ultimate quantum resource, entanglement, has yet to see use. This could enhance the sensitivity significantly, but it is far from straightforward.

Method

In our research, to create NV centres that have a high chance to be coupled, we implant molecules with multiple nitrogen atoms into diamond samples, such that the distance between potential NV centres is dictated by straggling only [1]. By choosing phosphorus-doped diamond ([P] $\approx 5 \times 10^{15} \text{ cm}^{-3}$, created via CVD with enriched ^{12}C [2]), we expect to have a higher yield [3], and hence a higher chance to find NV centres with a strong coupling. Moreover, the coherence time is potentially longer [3], which is important for various quantum protocols.

We compare results between intrinsic diamond and phosphorus-doped diamond, for which initial results show an increase in yield (Fig. 1). Moreover, the number of spots with more than one NV centre is consistent with the yield per nitrogen atom; an example ODMR spectrum is shown in Fig. 1. Double electron–electron resonance experiments give the coupling strength between NV centres, which needs to be sufficiently strong to attempt to utilise a couple for enhanced sensing.

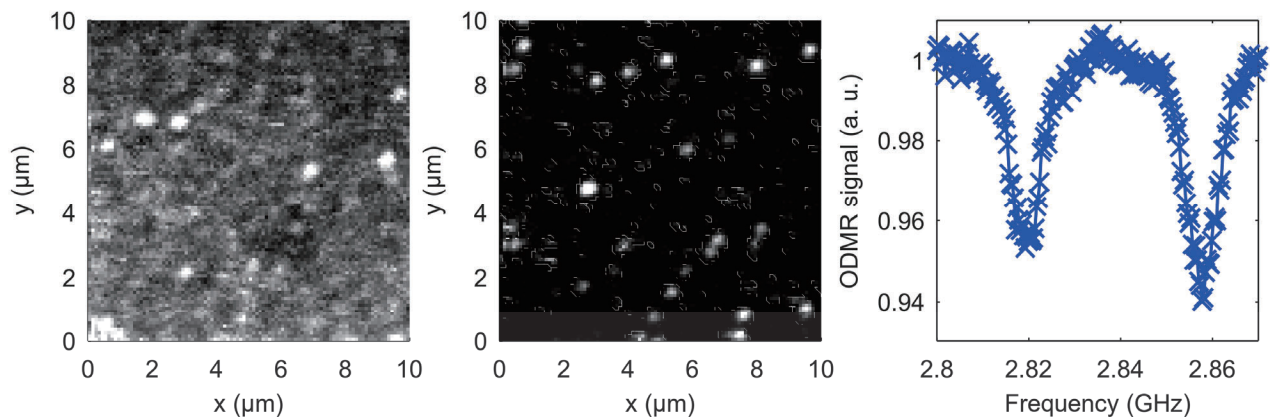


FIG. 1. (Left) Confocal microscope image for intrinsic diamond, showing less than 10 spots with NV centres. (Middle) Confocal microscope image for phosphorus-doped diamond implanted with the same parameters as intrinsic diamond. There are over 20 spots with NV centres. Moreover, the photon count per NV centre is higher compared to the intrinsic sample. (Right) Optically detected magnetic resonance (ODMR) image for a spot with two NV centres with a different orientation.

Acknowledgement

This work was supported by MEXT Q-LEAP Grant Number JPMXS0118067395.

References

- ¹Haruyama et al., Nature Communications 10, 2664 (2019).
- ²E. D. Herbschleb et al., Nature Communications 10, 3766 (2019).
- ³A. Watanabe et al., Carbon 178, 294–300 (2021).

Frequency-bin generation of entangled photons via quantum optical synthesis

Takeru Naito¹, Masahiro Yabuno², Fumihiro China², Shigehito Miki², Hiroataka Terai²,
and Ryosuke Shimizu¹

¹ *The University of Electro-Communications, 1-5-1 Chofugaoka, Chofu, Tokyo, Japan*

² *Advanced ICT Research Institute, National Institute of Information and Communication Technology, 588-2 Iwaoka, Nishi-ku, Kobe Japan
n2133076@uec.ac.jp*

Introduction

Entangled photons in high-dimensional Hilbert space are expected to increase information capacity. Although there are several approaches to realize such a high-dimensional state of the entangled photons, frequency-bin encoding is suitable for optical-fiber-based communication systems with wavelength multiplexing technologies. Up to now, frequency-bin state generation has been reported in some physical systems; Micro-ring resonators [1] and domain structure engineering of quasi-phase-matched devices [2]. However, most of the physical characteristics of the frequency-bin state are determined by the designed device structures. Therefore, it may be difficult to precisely adjust the frequency-bin state to the communication system. On the other hand, we reported manipulating the time-domain structure of a biphoton wave packet via Fourier optical synthesis in the frequency domain and realized an ultrafast time-bin state of the biphoton wave packet in several pico-second ranges [3]. Since the Fourier optical approach is independent of the device structure, it would provide better flexibility in manipulating the time-frequency structure of the biphoton wave packet. In this study, we present a proof-of-concept experiment of a two-photon spectral modulation with Fourier optical synthesis (FOS) toward the frequency-bin state generation with high flexibility.

Experimental results

In this experiment, photon pairs are generated by spontaneous parametric down-conversion using a periodically poled MgO-doped stoichiometric LiTaO₃ (PPMgSLT) crystal. In the earlier experiment with the PPMgSLT, broadband joint spectral intensity (JSI) distribution with negative correlation was reported even under a type-II phase-matching condition. Based on this scheme, we develop a spectral manipulation technique by Fourier optical synthesis in the time domain. Since discrete joint temporal intensity (JTI) distributions are needed for our synthesis, we adopt a bidirectional pumping scheme to the PPMgSLT crystal by reflecting the pump pulse by a concave mirror. As a result, a sequential JTI distribution with positive temporal correlation is created. For further manipulation, we placed a dichroic mirror between the PPMgSLT and the concave mirror to separate the biphoton wave packet, created by the first pumping, from the pump pulse. Adjusting a mirror position for the biphoton wave packet, we can control the temporal separation of the two biphoton wave packets along anti-diagonal direction. Photon pairs from the bidirectional pumped source were collected into a polarization-maintaining fiber and were sent to a fiber-based spectrometer. We reconstructed JSIs from the arrival time of photons after passing through the spectrometer. Photons were detected by superconducting single-photon detectors.

Figure 1 represents the resultant JSI when the two JTIs are distributed parallel to each other to the diagonal direction defined by $\Delta\tau_s = -\Delta t_i$. We can see the JSI is modulated along the anti-diagonal direction defined by $\Delta\nu_s = -\Delta\nu_i$ and it forms a frequency-bin state. The product of these modulation periods of each bin and interval of the two JTI is $\Delta t_- \cdot \Delta\nu_- \cong 1.3$, meaning successful demonstration of the FOS in the time domain.

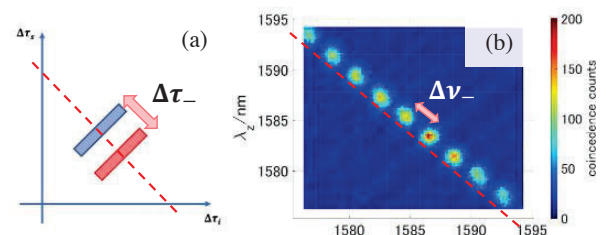


FIG.1. (a)Expected JTI (b) Measured JSI formed the frequency-bin state.

Acknowledgement

This work was supported by MEXT Q-LEAP Grant Number JPMXS011806924.

Reference

- [1] C. Joshi, A. Farsi, A. Dutt, B.Y.Kim, X. Ji, Y. Zhao, A.M. Bishop, M. Lipson, and A.L. Gaeta, "Frequency-Domain Quantum Interference with Correlated Photons from an Integrated Microresonator," *Phys. Rev. Lett.* **124**, 143601/1-7 (2020).
- [2] C.L. Morrison, F. Graffitti, P. Barrow, A. Pickston, J. Ho, and A. Fedrizzi, "Frequency-bin entanglement from domain-engineered down-conversion" *APL Photonics* **7**, 066102 (2022).
- [3] R.B. Jin, K. Tazawa, N. Asamura, M. Yabuno, S. Miki, F. China, H. Terai, K. Minoshima, and R. Shimizu, "Quantum optical synthesis in 2D time-frequency space," *APL Photonics* **6**, 086104/1-7 (2021).

SE-03A-a2-07

Development of highly sensitive gravimeter based on atom interferometry using hybrid system for field applications

Takeshi Hojo, Kaito Takamura, and Ken'ichi Nakagawa

Institute for Laser Science

University of Electro-Communication

t_houjo@ils.uec.ac.jp

Introduction

Transportable gravimeters with the sensitivity of about few micro Gal (10^{-9} g) are required in the fields of geophysics and geodesy. As the atom gravimeters have favorable features for these fields such as high sensitivity and no moving elements, they will contribute to these fields. We have developed a transportable gravimeter for these fields. Our experimental setup is shown in Fig.1. In our experiment, using retro-reflected three-beam MOT, about 10^7 laser cooled ^{87}Rb atoms are loaded in a glass cell. One of problems to limit the sensitivity of the atom gravimeters is the vibrational noise from the floor through the retro-reflecting mirror of Raman beams (Fig. 1). Therefore, the low frequency (< 10 Hz) vibrational noise of the mirror should be suppressed by using passive or active vibrational systems to achieve the target sensitivity of the gravity measurement. In our gravimeter system, we use a commercial passive isolation system with a resonance frequency of about 0.5 Hz, and we can improve the signal to noise ratio of the interference fringe (Fig. 2). Without a vibrational isolator, we could not clearly observe the interference signal for the interaction time longer than 30 ms. By employing a vibrational isolator, we could observe the interference signal for the interaction time up to 45 ms, and the sensitivity of $\Delta g/g = 7.2 \times 10^{-8}$ was realized. However, a residual vibrational noise limits the sensitivity and we could not further improve the sensitivity. To improve the sensitivity further, we consider a hybrid approach in which both the atom gravimeter and the mechanical accelerometer are employed to improve the sensitivity [1]. To realize this hybrid system, we first examined the correlation between the signals from the atom gravimeter and the mechanical accelerometer. The phase shift of the observed interference signal and the shift estimated from the accelerometer are plotted in Fig. 3, and we could observe the correlation between both signals. Using the high correlation between both signals, the phase of the interference signal is compensated by the phase shift estimated from the mechanical accelerometer signal, and we will be able to further improve the sensitivity of the gravity measurement.

Acknowledgement

This work was supported by MEXT Q-LEAP
Grant Number JPMXS0118069452

Reference

[1] Aopeng Xu, "vibration compensation of an atom gravimeter", Chinese Optics Letters Vol. 17, Issue 7, 070201(2019)

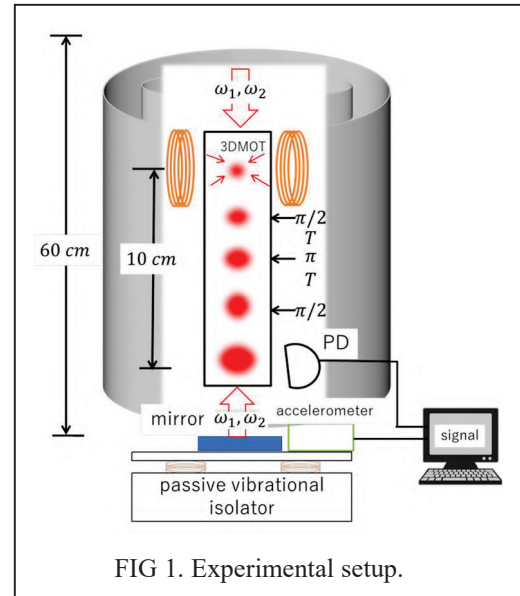


FIG 1. Experimental setup.

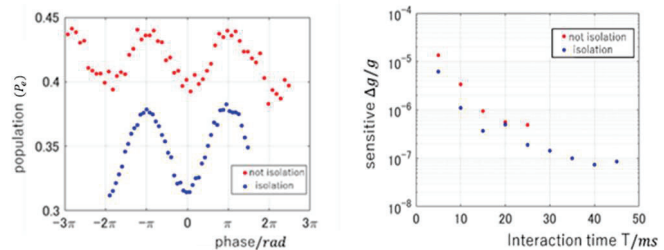


FIG 2. Interference signals without (red) and with vibrational isolation (blue)

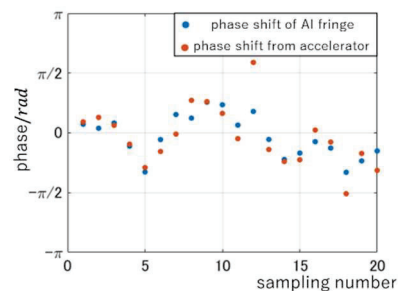


FIG3. Phase shifts of the interference signal (blue) and the accelerometer (orange)

Implementation of Double Quantum Magnetometry to Continuously Excited Ramsey Method

Yuta Araki¹, Ikuya Fujisaki¹, Yuji Hatano¹, Takeharu Sekiguchi¹, Takayuki Shibata²,
Takayuki Iwasaki and Mutsuko Hatano¹

¹Department of Electrical and Electronics Engineering, School of Engineering, Tokyo Institute of Technology

²DENSO Corporation

araki.y.aj@m.titech.ac.jp

Introduction

NV centers, spin qubits in diamond, have been studied for magnetic sensing applications. The continuously excited (CE)-Ramsey method reported high sensitivity of $17\text{pT}/\sqrt{\text{Hz}}$ for DC magnetometry¹. However, for the measurement of magneto-encephalo-graphy (MEG) in humans, which is our measurement target, further improvement in sensitivity is needed. The double quantum magnetometry (DQ) is a method to improve the DC field sensitivity². Applying DQ to the conventional Ramsey measurement not only effectively doubles the NV gyromagnetic ratio, but also improves T_2^* due to common-mode noise rejection. We report the development of a measurement protocol in which DQ is applied to the CE-Ramsey method to improve the sensitivity of the DC magnetic field.

Method

The diamond sample was 110- μm -thick ^{12}C CVD layer deposited on a type IIa substrate, and was irradiated with electron beams of $5 \times 10^{17}\text{cm}^{-2}$ and annealed. P1 and NV center concentrations were estimated to be approximately 8 ppm and 0.8 ppm. The static magnetic field of 10 mT was aligned parallel to the NV axis. A 532 nm laser was irradiated from the side of the sample. The fluorescence was focused by a CPC lens and read by a photodetector. To implement DQ, we applied the MW frequencies resonant to the low-frequency $m_s = 0 \leftrightarrow -1$ transition and the high-frequency $m_s = 0 \leftrightarrow +1$ transition simultaneously. The single-quantum (SQ) Rabi frequencies for the two transitions were matched.

Result

CE-SQ-2-Ramsey and CE-DQ-4-Ramsey were performed to confirm the effect of DQ in the CE protocol. Compared to SQ, twice the frequency of oscillation was obtained in DQ [see Fig.1 (a)], confirming that a doubling of the NV gyromagnetic ratio was achieved. Dephasing time T_2^* , fitted values, were similar for SQ and DQ, confirming that common-mode noise rejection was achieved [see Fig.1 (a)]. Next, to confirm the effect of DQ on sensitivity enhancement, we compared the measurements of sweeping of detuning, which corresponds to an external magnetic field, between SQ and DQ. The results confirmed that the slope was improved by the application of DQ [see Fig.1 (b)].

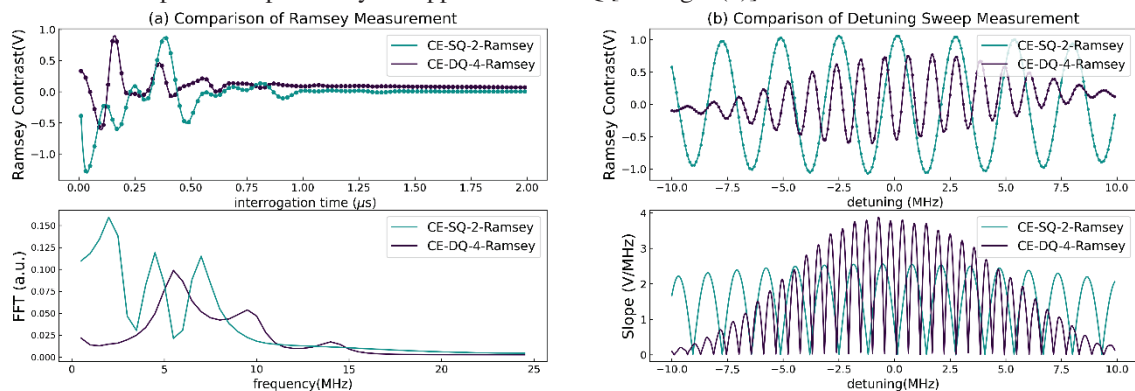


FIG. 1. (a) Comparisons of NV Ramsey measurements (Upper) and Discrete Fourier transform (Lower). (b) Comparisons of Detuning sweep measurements of SQ and DQ (Upper) and their calculated Slopes (Lower).

Acknowledgements

This work was supported by MEXT Q-LEAP Grant Number JPMXS0118067395.

We thank Dr. Hiromitsu Kato (AIST) and Dr. Shinobu Onoda, Dr. Takeshi Ohshima (QST) for supplying diamond samples.

Reference

¹C. Zhang, *et al*, *Phys Rev Appl*, **15**, 1 (2021)

²E. Bauch *et al.*, *Phys Rev X*, **8**, 31025 (2018)

Development of highly sensitive compact quantum sensor with NV center in ^{12}C -enriched CVD diamond for bio-medical and industrial application

Yuta Kainuma¹, Yuta Shigenobu¹, Yuji Hatano¹, Takayuki Shibata², Akimitchi Nakazono³, Hiromitsu Kato⁴, Takeshi Ohshima⁵, Takayuki Iwasaki¹, and Mutsuko Hatano^{1,5}

¹Department of Electrical and Electronics Engineering, School of Engineering, Tokyo Institute of Technology

²DENSO CORPORATION

³YAZAKI CORPORATION

⁴National Institute of Advanced Industrial Science and technology

⁵National Institutes for Quantum Science and Technology

kainuma.y.aa@m.titech.ac.jp

Introduction

Magnetometers based on the ensemble nitrogen-vacancy (NV) centers have high magnetic sensitivity and have monitored not only rat's cardiac magnetism¹ but also battery current over a wide dynamic range². For these applications, especially, magnetoencephalography have required high magnetic sensitivity and multiple sensors. Thus, the development of a compact quantum sensor is important to be implemented in the system with sufficient spatial resolution. However, these sensors have not achieved the magnetic sensitivity required to detect magnetoencephalography.

We investigated the magnetic sensitivity of the quantum sensor head by lateral laser irradiation using ^{12}C -enriched chemical vapor deposition (CVD) growth diamond, which is suitable for NV centers and scalable device fabrication.

Method

Figure 1(a) shows the construction of the quantum sensor head, the inside of the dashed line is an NV diamond; The NV centers in ^{12}C -enriched CVD diamond were formed by electron-beam irradiation (5.0×10^{17} e/cm²) and high-temperature annealing after it. The excitation green laser (wavelength: 532 nm) was focused on the side of the NV diamond by a lens (focal length: 200mm). The photoluminescence from the NV center collected by compound parabolic concentrator (CPC) lens and split laser by the beamsplitter in the optical line are detected by a photodiode (PD1) and PD2 as shown in Fig.1(a). A laser-noise compensation is performed by an auto-balance (AB) circuit and the output signal is modulated by a lock-in amplifier (LIA) with the modulation frequency ($f_{\text{mod}} = 7.03$ kHz). The magnetic field was adjusted to be parallel to the NV quantum axis. The resonance frequency of the lock-in optically detected magnetic resonance (ODMR) spectra was locked by the output microwave frequency updated. The optical setup was assembled in the magnetic shield.

Result and discussion

The measured signal spectra are shown in Fig.1(b). the floor noise of on- and off-resonance was estimated less than 60 pT/Hz^{0.5} and 40 pT/Hz^{0.5}, however, electronic noise matched the off-resonance noise at 1 Hz. We confirmed that floor-noise attenuation in the on-resonance spectra at low frequencies seems that the feedback circuit captures the resonance frequency of ODMR. From the long-measured magnetic signal, the minimum detectable magnetic field (MDF) was extracted with Allan variance, reaching approximately 260 fT. MDF can be improved by faster feedback circuit and NV diamond quality; the use of preferentially-aligned NV center CVD diamond improves the magnetic field sensitivity by a factor of about 3 or more³.

Acknowledgments This work was supported in part by MEXT Q-LEAP Grant Number JPMXS0118067395.

References [1] K. Arai et al., Commun. Phys. **5**, 200 (2022), [2] Y. Hatano et al., Sci. Rep. **12**, 13991 (2022),

[3] C. Osterkamp et al., Sci. Rep. **9**, 5786 (2019)

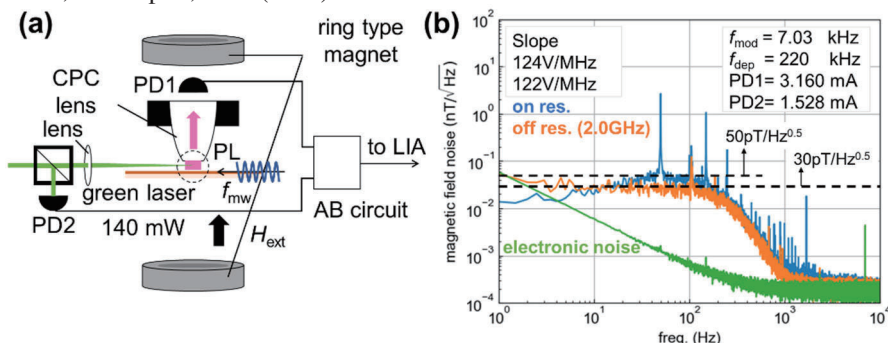


Fig. 1 (a) A schematic of the construction of quantum sensor head: dashed line indicates NV diamond sensor. The diamond was glued to the apex of the CPC lens by optical adhesives. (b) Measured FFT spectrum of magnetic sensitivity. The off-resonance was measured with a microwave ($f_{\text{mw}} = 2.0$ GHz) applied. Electronic noise was measured without a laser.

Development of a Nonmagnetic Helical Sensor Drive Multipoint Measuring Mechanism for Magnetocardiography in Animals

Wenyu Shang¹, Motofumi Fushimi¹, Shinichi Chikaki¹, Masaki Sekino¹

¹Graduate School of Engineering, The University of Tokyo

Shangwenyu720@g.ecc.u-tokyo.ac.jp

Introduction

In the clinic, electrocardiography (ECG) and magnetocardiography (MCG) are widely known as common techniques to observe the electrophysiological activity of the heart. Because the magnetic permeability is more uniform than the conductivity in the organism, to obtain more accurate cardiac electrical information, MCG usually shows higher accuracy and specificity than ECG. (for some diseases) [1]. This study will focus on MCG technology. By introducing a new type of helical nonmagnetic measurement device, taking animals as the measurement target, we can obtain all-around magnetic field information to complete the depth measurement of the cardiac current source and realize 3D reconstruction.[2]

Methods

In this study, we proposed a new sensor array for MCG measurement in animal to obtain more depth information about current sources. Unlike conventional devices, we used a ring-shaped sensor array instead of a flat plane sensor array. We designed a mechanism to realize multipoint MCG measurement and assembled it with nonmagnetic material, as shown in Figure 1. With this mechanism, MCG data were measured using 3 OPMs.

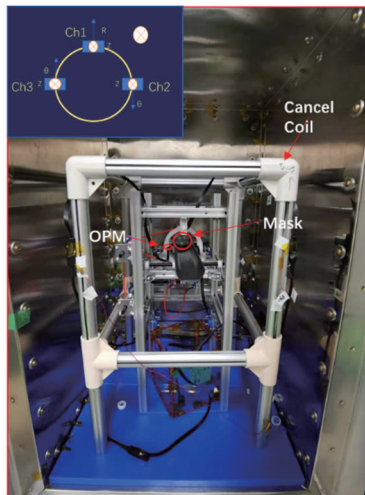


Figure 1. Multipoint MCG measurement mechanism

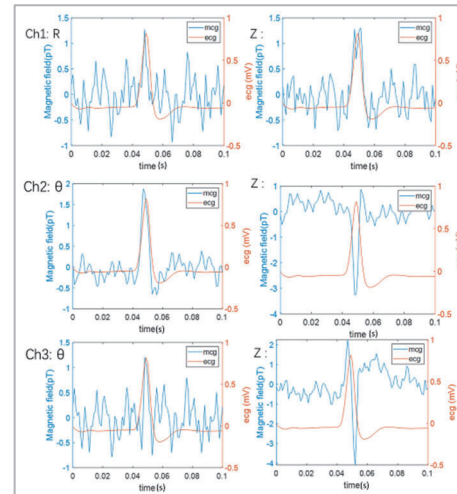


Figure 2. Result of MCG measurement in rat

Results and discussion

Figure 2 shows the results of MCG measurement. 3 OPMs with six channels were used to measure the rat's MCG. The two channels of OPM respectively detected the r and θ direction of ring. The result of additive averaging based on the simultaneously acquired ECGs shows that the R wave can be clearly captured from directions other than the anterior chest plane. However, its signal strength is weak (about 2 pT), and the design of the mechanism needs to be improved to obtain a signal with a higher signal-to-noise ratio.

Acknowledgments

This work was supported by MEXT Q-LEAP Grant Number JPMXS0118067395.

Reference

- [1] Shin, et al. (2019). *Clinical Hemorheology and Microcirculation*, 73(2), 283-291.
- [2] R. Fenici, *Expert Rev. Mol. Diagn.*, vol. 5, no. 3, pp. 291–313, May 2005.

Ensemble NV⁻ center in diamond for quantum sensing created by high fluence electron beam irradiation

Shuya Ishii^{1,2}, Seiichi Saiki¹, Shinobu Onoda^{1,2}, Yuta Masuyama¹, Hiroshi Abe^{1,2}, Takeshi Ohshima^{1,2}

¹Takasaki Advanced Radiation Research Institute, National Institutes for Quantum Science and Technology, 1233 Watanuki, Takasaki, Gunma 370-1292, Japan, ²Institute for Quantum Life Science, National Institutes for Quantum Science and Technology, 4-9-1 Ana-gawa, Inage-ku, Chiba 263-8555, Japan
ISHII.shuya@qst.go.jp

Introduction

NV⁻ center has been paid attention as a quantum sensor for highly sensitive detection of magnetic field, electric field, temperature and strain, etc. [1]. Electron beam irradiation followed by subsequent thermal annealing is known as the effective procedures to create NV⁻ center in diamond. The electron irradiation generates vacancies in diamond and the annealing enables vacancies to diffuse in the lattice. Then diffused vacancies are captured by nitrogen atoms, and as a result, NV centers are created. In addition, substitutional nitrogen atom at a lattice site (P1 center) also acts as a donor for NV center, the charge state of NV centers changes from neutral (NV⁰) to NV⁻. Creation high concentration of ensemble NV⁻ centers is needed to achieve high sensitively sensing [1]. The magnetic sensitivity is proportional to the reciprocal of the number of NV centers and T₂ (spin coherence time), i.e., high concentration NV⁻ centers with long T₂ increase the sensitivity. P1 center has an important role for being a component of NV⁻ centers and acting as donor to the NV center. But it also plays a role as decoherence source (decrease in magnetic field sensitivity) [1]. Therefore, it is important to create high concentration of NV⁻ centers considering the amount of P1 centers.

In current study, we investigate irradiation fluence dependence of the creation behavior of NV centers in type-Ib diamonds by using electron spin resonance (ESR) and photo-luminescence (PL) to understand the creation mechanism of NV⁻ center. The values of T₂ are also evaluated by Hahn-echo measurement, since it is one of the key parameters for highly sensitive magnetometry [1]. Then, we discuss the creation mechanism of NV centers based on concentrations of defects.

Method

The commercial diamonds synthesized by High Pressure and High Temperature (HPHT) were used. The initial P1 concentrations ([P1]_{initial}) for the samples were measured by ESR, 80, 72, 52, and 46 ppm, respectively. 2 MeV electrons were irradiated with fluences up to 8.0×10^{18} e/cm² at room temperature. Then, the samples were annealed at 1000°C for 2 hours to create NV centers. The concentration of P1 (number of electron spins) was measured by ESR. The initial concentration of P1 was in the range from 50 ppm to 100 ppm. The ratio of NV⁻ to NV⁰ was evaluated from PL spectrum. All these measurements were performed at room temperature. The values of T₂ of NV⁻ center ensembles were measured using a home-built fluorescent microscope with a microwave system.

Results & Discussion

We studied the creation behavior of NV center in type-Ib diamonds with high [P1]_{initial} under relatively high irradiation fluences. The decrease rate of P1 centers as a function of irradiation fluence shows similar tendencies for all type-Ib diamond samples, regardless of the initial P1 concentration in the low fluence range ($\sim 4.0 \times 10^{18}$ e/cm²). The reduction rate of P1 centers suggests that P1 centers are consumed by recombination with introduced vacancies. However, the decrease rate of P1 became lower in the high fluence ranges from 6.0×10^{18} e/cm² to 8.0×10^{18} e/cm², especially when [P1]_{initial} is smaller, in spite that [P1] still exists even after irradiation at 8.0×10^{18} e/cm². The process of P1 center consumption seems to shift depending on the residual P1 centers. Furthermore, the P1 center consumption and NV⁻ center creation were compared and as a result, it is concluded that some amounts of the P1 centers were consumed by other defects. The conversion efficiency from [P1]_{initial} to the [NV⁻] reached $\sim 19\%$ at 8.0×10^{18} e/cm² and the value confirms the usefulness of electron beam irradiation for high concentration of NV⁻ centers in type-Ib diamonds, whereas results in this study suggests that not all P1 centers converted to NV⁻ center and the residual defects might leads to a cause of decoherence..

Acknowledgement

This work was supported by Quantum Leap Flagship Program (Q-LEAP; JPMXS 0118067395 and JPMXS0118068379) of MEXT.

Reference

[1] J. F. Barry, J. M. Schloss, E. Bauch, M. J. Turner, C. A. Hart, L. M. Pham and R. L. Walsworth. Rev. Mod. Phys., **92**, No.1, 015004 (2020)

Synthesis of n-type diamond using *tert*-butyl phosphine for high sensitivity of the NV sensor

Riku Kawase¹, Hiroyuki Kawashima^{1,2}, Hiromitsu Kato², Norio Tokuda³, Satoshi Yamasaki³, Mikihiro Kubota¹, Masahiko Ogura², Toshiharu Makino², Norikazu Mizuochi^{1,4}

¹Institute for Chemical Research, Kyoto University, Gokasho, Uji, Kyoto 611-0011, Japan

²National Institute of Advanced Industrial Science and Technology (AIST), Tsukuba, Ibaraki 305-8568, Japan

³Graduate School of Natural Science and Technology, Kanazawa University, Kanazawa, Ishikawa 920-1192, Japan

kawase.riku.87n@st.kyoto-u.ac.jp

Introduction

Recently, ultra-long spin coherence time ($T_2 \approx 2.4$ ms) of the single nitrogen-vacancy (NV) center in P-doped n-type diamond was obtained¹. The spin coherence time was the longest in room-temperature among solid-state systems. In addition to the long T_2 , as a negative charge state of the NV center is stable². Furthermore, it also reported that creation yield of shallow NV centers formed by ion-implantation was improved in addition to longer T_2 and improved charge stability³. Due to such reports, P-doping methods for n-type diamond synthesis is getting more important.

Phosphine is usually used for P-doped diamond synthesis by chemical vapor deposition (CVD). However, phosphine has high explosibility and toxicity, so it threatens safety of experimenters and expensive exclusion equipment was required. Therefore, we synthesized P-doped n-type diamond with *tert*-butyl phosphine (TBP) whose explosibility and toxicity were lower than phosphine's ones⁴, and we confirmed that the synthesized sample shows relatively long T_2 (1620 ± 100 μ s, FIG. 1). We also confirmed perfect alignment of NV axis which is also important for high sensitivity of NV quantum sensor.

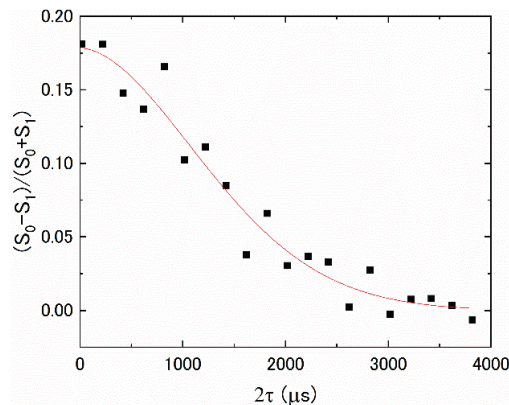


FIG. 1. Result of Hahn-echo measurement

Reference

- ¹E. D. Herbschleb, H. Kato, Y. Maruyama, T. Danjo, T. Makino, S. Yamasaki, I. Ohki, K. Hayashi, H. Morishita, M. Fujiwara, N. Mizuochi, *Nature Communications*, **10**, 3766 (2019).
- ²Y. Doi, T. Fukui, H. Kato, T. Makino, S. Yamasaki, T. Tashima, H. Morishita, S. Miwa, F. Jelezko, Y. Suzuki, N. Mizuochi, *Physical Review B*, **93**, 081203(R) (2016).
- ³A. Watanabe, T. Nishikawa, H. Kato, M. Fujie, M. Fujiwara, T. Makino, S. Yamasaki, E. D. Herbschleb, N. Mizuochi, *Carbon*, **178**, 294-300 (2021).
- ⁴H. Kato, S. Yamasaki, and H. Okushi, *phys. stat. sol. (a)* **202**, 2122–2128 (2005).

This work was supported by MEXT Q-LEAP Grant Number JPMXS0118067395

Decoherence Phenomena in Nitrogen-Vacancy Diamond

Aulden Jones¹, Tokuyuki Teraji², Chikara Shinei², and Yuta Masuyama³

¹*School of Physics, Georgia Institute of Technology*

²*Research Center for Functional Materials, National Institute for Materials Science*

³*National Institutes for Quantum and Radiological Science and Technology*

Introduction

Nitrogen vacancy (NV) centers in diamond are atom-sized spin defects whose unique properties enable their use as robust quantum sensors. Recent research efforts have focused on NV magnetometry, where both single and ensemble NVs are used for highly sensitive magnetic field detection with nanoscale spatial resolution. While NV sensors have been successfully applied to fields ranging from neuroscience to condensed matter physics, ensemble NV diamonds are still below the sensitivity threshold needed for many more potential applications¹. Presented here is an attempt to investigate the relationship between large crystallographic strain features and the spin coherence time T_2^* in NV-diamonds grown by chemical vapor deposition (CVD). A better understanding of this relationship can provide valuable input for improving diamond growth methods and eventually extending T_2^* .

*This work was supported under the NSF Global Quantum Leap Program under Grant No. OISE-2020174.

Reference

¹J. F. Barry, J. M. Schloss, E. Bauch, M. J. Turner, C. A. Hart, L. M. Pham, and R. L. Walsworth, Rev. Mod. Phys. 92, 015004 (2020).

Improvement in the long-term stability of the interferometer gyroscope using slow and continuous atomic beams

Naoki Nishimura¹, Takuya Kawasaki², Tomoya Sato², Ryotaro Inoue², Mikio Kozuma^{1,2}

¹ Department of Physics, School of Science, Tokyo Institute of Technology

² Institute of Innovative Research, Tokyo Institute of Technology

nishimura.n.ae@m.titech.ac.jp

Introduction

Gyroscopes consisting of an atom interferometer can measure angular velocity. Since their expected sensitivity is higher than that of optical interferometers [1], many studies have paid much attention to the application of atom gyroscopes, for example, precision measurement of physical constants [2] and inertial navigation of ships and aircraft [3]. We are developing a matter-wave gyroscope using Raman transitions for a cold and continuous Rb atomic beam. A deadtime-free measurement and long-stability obtained by a continuous atom beam interferometer benefit the non-GPS type of inertial navigation. In our previous study, we successfully measured the rotation of the Earth with our gyroscope with continuous and cold atomic beam of Rb [4]. Currently, we are aiming to improve the accuracy of the gyroscope for the level required for inertial navigation.

Method

In the atom interferometer using Raman transitions, three pairs of counter-propagating Raman beams construct a $\pi/2$ - π - $\pi/2$ Mach-Zehnder type interferometer [5]. The phase in the interference signal, which reflects the Sagnac effect, is measured as the population ratio between the ground-state hyperfine states $F=1$ and $F=2$ of ^{87}Rb atom. The constant frequency shift Δf in the π Raman beams induces a sinusoidal change in the ratio of the population with the frequency of $2\Delta f$. We create a reference signal of the frequency $2\Delta f$ based on the signal of the frequency Δf by a synthesizer. We estimate the phase of the fluorescence signal by the lock-in detection with the reference signal.

If drift occurs in the relative phase of Raman beams, it worsens the long-term stability of the interferometer. To eliminate the spurious phase shift caused by the drift in the relative phase of Raman beams, a simultaneous measurement of interferometers with counter-propagating atomic beams that share Raman beams is employed. The sign of the Sagnac phase shift induced by the rotation depends on the velocity vector, while that induced by other drifts such as acceleration, movement of optical elements, and imperfections in the equipment is the same for the interferometers. Thus, the common-mode phase drifts are canceled by taking the difference between the output phase shifts in two interferometers while enhancing the phase shift originating from the system's rotation. Although the common-mode rejection is a powerful method to improve long-term stability, the common-mode rejection ratio is limited in the actual system. It is desirable to suppress the relative phase drift itself as much as possible. One of the most significant sources of long-term drift in the output phase of our interferometer is the imperfectness in the relative phase locking of Raman beams. The relative phase of counter-propagating Raman beams is measured as the optical beat note between Raman beams. The locking of the relative phase is achieved by stabilizing the beat note to the external RF reference using the PID feedback loop. The performance of the feedback circuit, which consists of discrete electronic components, is vulnerable to changes in operational conditions, such as temperature. We newly introduce the feedback circuit consisting of a field programmable gate array (FPGA). The full-digitalized feedback system is free from the instability stemming from the change in the environmental conditions where the gyroscope is operated. As a result, the performance of the stabilization of the relative phase of Raman beams is improved.

Result

The stability of the interferometer as a gyroscope is evaluated by calculating the Allan deviation of the output phase of the interferometer. The performance of the gyroscope with FPGA-based stabilization for the relative phase of Raman beams will be reported. In addition, the changes in the response of the interferometer to the variations in the environmental condition will be presented.

Reference

¹T. L. Gustavson, P. Bouyer, and M. A. Kasevich, *Phys. Rev. Lett.*, **78**, 2046 (1997)

²G. Rosi, F. Sorrentino, L. C. Acciapiuti, M. P. Revedelli, G. M. Tino. *Nature*, **510**, 518-521 (2014)

³J.C. Fang and J. Qin *Sensors*, **12**, 6331-6346 (2012)

⁴T. Sato, R. Inoue and M. Kozuma, short presentation in 4th IFQMS, SE-03A-61-05, 7-9 Dec. 2021

⁵M. Kasevich and S. Chu, *Phys. Rev. Lett.*, **67**, 181 (1991).

Bragg interferometer using slow and continuous atomic beam with sub-recoil transverse momentum width

Tomoya Sato¹, Toshiyuki Hosoya^{2,3}, Ryotaro Inoue¹ and Mikio Kozuma^{1,3}

¹ Institute of Innovative Research, Tokyo Institute of Technology

² Japan Aviation Electronics Industry, Ltd.

³ Department of Physics, School of Science, Tokyo Institute of Technology
sato@qnav.iir.titech.ac.jp

Introduction

A gyroscope based on interferometry using a continuous atomic beam is one of the most promising candidates for next-generation inertial navigation to complement navigation with external references such as GPS because of their high sensitivity, deadtime-free detection, and long-term stability. In recent years, alkaline earth-like atoms have attracted attention to improving the sensitivity and stability of interferometers [1]. In contrast to alkali atoms, which are widely used in atom interferometry [2], alkaline earth-like atoms do not possess electron spin in their ground state, making them less susceptible to effects of environmental magnetic fields. An interferometer with Bragg diffraction, which uses only the ground state, can benefit from this advantage. In addition, higher-order Bragg diffraction increases the area of the interferometer, thus the sensitivity of the gyroscope will be improved.

In atomic interferometry with Bragg diffraction, the interference signal is evaluated by measuring the number of atoms in different momentum states of the same internal state. Therefore, an atomic beam whose initial momentum width is narrower than the recoil momentum of the Bragg beam is essential for high-precision measurement. In our recent paper, we propose a new technique to obtain the high-flux atomic beam of ytterbium (Yb) with sub-recoil momentum width [3]. The interferometer with such type of atomic beam will pave the way to the high-end gyroscope for inertial navigation.

Method

By applying two-dimensional cooling using 1S_0 - 3P_1 intercombination transition to a slow atomic beam of ^{171}Yb produced by dipolar-allowed transition, we have successfully compressed the transverse momentum width of the atomic beam to below $4\hbar k$, where $\hbar k$ is the recoil momentum of the Bragg beam (dipolar-allowed 1S_0 - 1P_1 transition). For further reduction of momentum width, we applied a momentum filtering technique to our atomic beam using an ultra-narrow transition between the ground state and long-lived metastable state 3P_2 . The atomic beam orthogonally passes the laser light resonant on the ultra-narrow transition (507nm). With our experimental condition, the spectral linewidth associated with the transverse momentum width of the atomic beam is determined by the transit time broadening rather than the lifetime of the metastable state. Since the transition time broadening is adjusted to correspond to the momentum width of less than $\hbar k$, atoms can be excited to the metastable state in a momentum-selective manner. After blowing up the remaining atoms in the ground state, which have unwanted momentum components, one can obtain ground state atoms within the narrow momentum width by transporting the atoms from the metastable state to the ground state in the same momentum-selective manner.

The momentum-filtered atomic beam is introduced into the interferometer region, where three pairs of counter-propagating Bragg beams construct the $\pi/2$ - π - $\pi/2$ Mach-Zehnder type interferometer. The Sagnac effect causes the sinusoidal variation between populations of momentum states $0\hbar k$ and $2n\hbar k$ as a function of the acceleration and angular velocity on the Sagnac loop, where n is the order of the Bragg diffraction. For the momentum-resolved detection, the third 507nm light, tuned to excite the $2n\hbar k$ state, is introduced just after the interferometer. The change in the population of the $2n\hbar k$ momentum state can be detected as the change in the loss of the atoms in the ground state.

Results

We successfully generate an atomic beam of ^{171}Yb whose momentum width is $0.20(8)\hbar k$ by the momentum filtering. The higher order Bragg diffraction, up to the 10th, is observed. With the obtained atomic beam with narrow momentum width, the construction of the Bragg interferometer is ongoing. The present status of the development will be reported.

This work was supported by JST-Mirai Program, Grant Number JPMJMI17A3 and COI-NEXT, Grant Number JPMJPF2015.

Reference

- ¹T. Mazzoni et al., *Phys. Rev. A*, 92, 053619 (2015).
- ²D. Sayoie et al., *Sci. Adv.* 4, eaau7945 (2018).
- ³T. Hosoya et al., *Opt. Commun.*, 528, 129048 (2023).

Development of a cryogenic suspension system for TOrsion-Bar Antennae (TOBA)

Ching Pin Ooi¹, Satoru Takano¹, Yuka Oshima¹, Kentaro Komori², Yuta Michimura^{2,3} and Masaki Ando^{1,2}

¹Department of Physics, The University of Tokyo

²RESCEU, The University of Tokyo

³LIGO Laboratory, California Institute of Technology

ooichingpin@g.ecc.u-tokyo.ac.jp

Introduction

TOrsion-Bar Antennae (TOBA), is a proposed gravitational wave antenna¹, targeted at observing intermediate mass black hole mergers with peak sensitivity in the range 0.1 – 10 Hz, but can also be used for early earthquake warnings via measuring transient gravitational perturbations². TOBA phase III is currently being built, with a target sensitivity that would make it useful for early earthquake warnings. To that end, a cryogenic suspension system is being developed to achieve the low thermal suspension noise requirements. TOBA, as its name suggests, uses torsion bars for sensing. Thus, this work focuses on quantifying and reducing suspension thermal noise of torsion pendulums, with two key technologies, cryogenic temperatures and crystalline fibres.

Method

Our setup consists of a copper beryllium torsion pendulum, suspended by a 1 mm thick sapphire fibre, and is cooled in a cryogenic chamber to near 4 K. The Q value, a parameter which characterizes the thermal noise of the suspension, is measured off the setup via an optical lever. Coil-coil actuators were used to excite the torsion pendulum to start off the ringdown for Q value measurements.

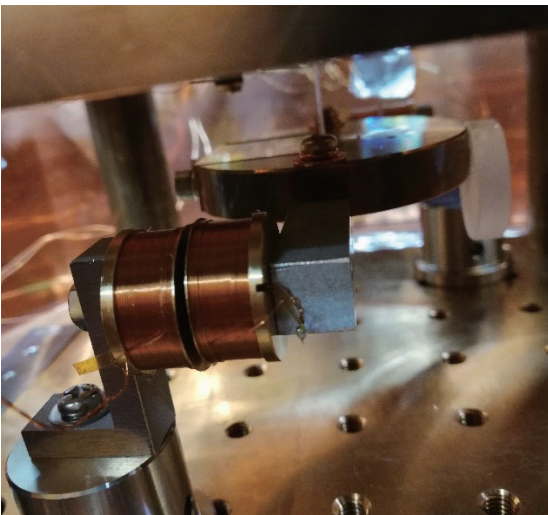


Fig. 1. Torsion pendulum suspended by 1 mm sapphire fibre, in a cryogenic chamber. Coil-coil actuators provide the initial excitation for ringdown.

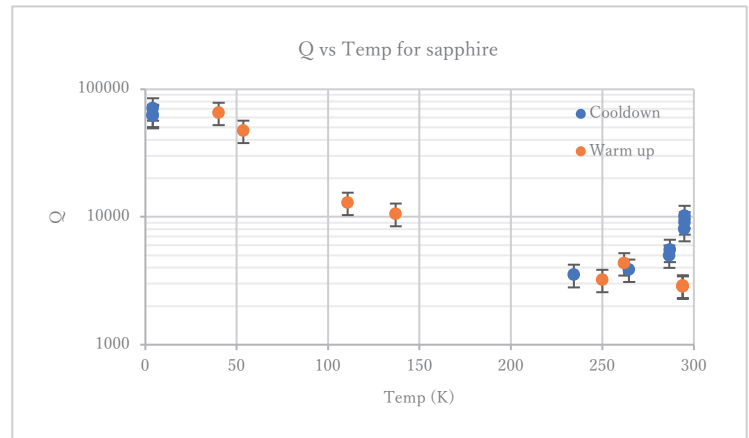


Fig. 2. Range of Q values with temperature of the cryogenic chamber. This ranges from 3000 – 70 000 across the temperatures, and we note here that the highest values are when it is coldest.

Acknowledgments

We would like to thank the Shigemi Otsuka and Togo Shimozawa for manufacturing the mechanical parts used. This work is supported by MEXT Q-LEAP Grant Number JPMXS0118070351.

Reference

¹M. Ando *et al.*, *Phys. Rev. Lett.*, 105, 161101 (2010)

²J. Harms *et al.*, *Geophys. J. Int.*, 201, 1416-1425 (2015)

Torsion-Bar Antenna for Early Earthquake Alert

Yuka Oshima¹, Satoru Takano¹, Ching Pin Ooi¹,
Kentaro Komori², Yuta Michimura^{2,3}, and Masaki Ando^{1,2}

¹Department of Physics, University of Tokyo

²RESCEU, University of Tokyo

³LIGO Laboratory, California Institute of Technology

yuka.oshima@phys.s.u-tokyo.ac.jp

Introduction

Torsion-Bar Antenna (TOBA) is a highly sensitive gravity gradient sensor using torsion pendulums [1]. We use test masses suspended horizontally and aim to detect the torsional rotation caused by tidal forces as shown in FIG. 1. The resonant frequency of torsional motion is ~ 1 mHz, therefore TOBA has good design sensitivity in low frequencies (0.1 - 10 Hz). TOBA is useful for gravity-based earthquake early warning [2], and the observation of Newtonian noise and gravitational waves. A prototype detector Phase-III TOBA with a 35 cm-scale pendulum is under development [3]. The target sensitivity is set to 10^{-15} $1/\sqrt{\text{Hz}}$ at 0.1 Hz. Phase-III TOBA can detect earthquakes with a magnitude 7 or larger within 10 seconds from a 100 km distance [3].

Method

For Phase-III TOBA, we operate torsion pendulums at cryogenic temperatures to reduce thermal noise. We have successfully demonstrated cooling down test masses at 6 K [4]. Now, torsion pendulums are under development to achieve our target sensitivity. Differential Fabry-Perot cavities are used to read out the rotational angle to the pendulums. We finished designing the parameters of Fabry-Perot cavities and the mechanical parts for the pendulums.

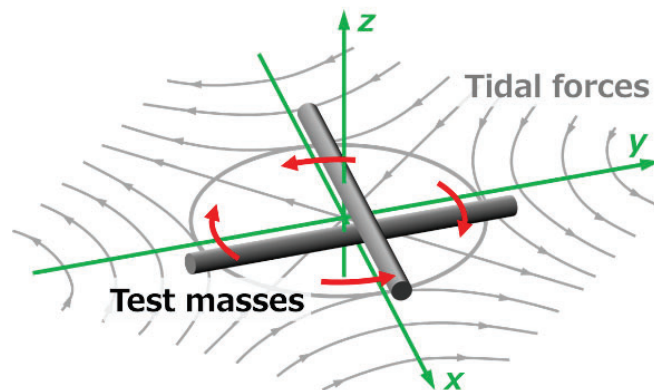


FIG. 1. the schematic of TOBA. Test masses are suspended horizontally in the x-y plane and a suspension wire is stretched in the z-axis. Grey lines represent tidal forces, red arrows show the rotational motion of the pendulums.

Acknowledgments

We would like to thank Shigemi Otsuka and Togo Shimozaawa for manufacturing the mechanical parts used. This work was supported by MEXT Quantum LEAP Flagship Program (MEXT Q-LEAP) Grant Number JPMXS0118070351. Y.O. was supported by JSPS KAKENHI Grant Number JP22J21087 and JSR Fellowship, the University of Tokyo.

Reference

- ¹M. Ando *et al.*, *Phys. Rev. Lett.*, 105, 161101 (2010).
- ²J. Harms *et al.*, *Geophys. J. Int.*, 201, 1416 (2015).
- ³T. Shimoda *et al.*, *International Journal of Modern Physics D*, 29, 1940003 (2020).
- ⁴T. Shimoda, PhD thesis, The University of Tokyo (2019).

Optimized Design of Quasi-phase-matched crystal for Spectrally-Pure-State Generation at MIR Wavelengths Using Metaheuristic Algorithm

Wu-Hao Cai,^{1,2,*} Fumihiro Kaneda,¹ Keiichi Edamatsu,¹ and Rui-Bo Jin^{2,*}

¹Research Institute of Electrical Communication, Tohoku University, 2-1-1 Katahira, Sendai, 980-8577, Japan

²Hubei Key Laboratory of Optical Information and Pattern Recognition, Wuhan Institute of Technology, Wuhan 430205, China

*E-mail: cai@quantum.riec.tohoku.ac.jp; jin@wit.edu.cn

Introduction

Quantum light sources in the mid-infrared (MIR) band play an important role in many applications, such as quantum sensing, quantum imaging, and quantum communication. However, there is still a great demand for high-quality quantum light sources in the MIR band, such as the spectrally pure single-photon source. In this work, the generation of a spectrally-pure state in an optimized poled lithium niobate crystal using a metaheuristic algorithm is presented. In particular, the particle swarm optimization algorithm is adopted to optimize the duty cycle of the poling period of the lithium niobate crystal. With this approach, the spectral purity can be improved from 0.820 to 0.998 under the third group-velocity-matched condition, and the wavelength-tunable range from 3.0 to 4.0 μm for the degenerate case and 3.0 to 3.7 μm for the nondegenerate case. This work paves the way for developing quantum photonic technologies at the MIR wavelength band [1-4].

Tables and Figures

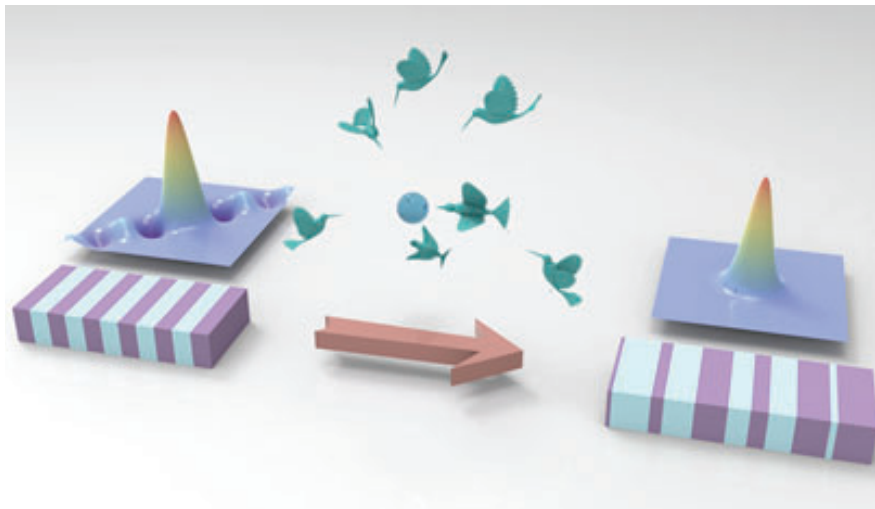


FIG. 1. The concept figure of optimized design of the lithium niobate crystal by using particle swarm optimization (PSO) algorithm. Left: In a standard periodically poled lithium niobate crystal, side lobes in the joint spectral amplitude (JSA) profile of biphoton degraded the purity. Right: In an optimized poled LN (OPLN) crystal which is designed using a PSO algorithm, the side lobes can be eliminated after optimization, the spectral purity of JSA can be improved obviously.

Reference

¹W.-H. Cai, Y. Tian, S. Wang, Q. Zhou, C. You*, and R.-B. Jin*, *Adv. Quantum Technol.*, **5**, 2200028 (2022) **Selected the front cover of the journal for the July issue**

²B. Wei, W.-H. Cai, C. Ding, G.-W. Deng, R. Shimizu, Q. Zhou, R.-B. Jin, *Opt. Express*, **29**, 256 (2021).

³P. B. Dixon, J. H. Shapiro, F. N. C. Wong, *Opt. Express*, **21**, 5879 (2013).

⁴C. Cui, R. Arian, S. Guha, N. Peyghambarian, Q. Zhuang, Z. Zhang, *Phys. Rev. Appl.*, **12**, 034059 (2019)

Experimental generalized measurement of qubits using a quantum computer

Tingrui DONG^{1,2}, Binho LE³, Fumihiko KANEDA¹, Soyoung BAEK¹ and Keiichi EDAMATSU¹

¹Research Institute of Electrical Communication, Tohoku University

²School of Engineering, Tohoku University

³Frontier Research Institute for Interdisciplinary Sciences, Tohoku University

dong.tingrui.r7@dc.tohoku.ac.jp

Introduction

Quantum computers, which provide the ability to surpass classical computers, are also able to carry out some fundamental experiments in quantum mechanics. For example, generalized quantum measurement protocols and their uncertainty relations¹ [1] can be realized and tested in a quantum computer. Here, we propose the implementation of generalized quantum measurement of qubits in a noisy intermediate-scale quantum computer (NISQ). First, we demonstrate the variable-strength measurement of a single qubit, which was once studied by photon polarization qubits², using an NISQ (IBM-Q). The performance of the measurement is quantified and discussed in terms of the characteristics of the noise and error of the NISQ. We also implement the nonlocal, variable strength parity measurement of a pair of qubits we recently proposed³. The circuit we build will also be a part of deterministic, complete Bell state measurement with arbitrary precision. To date, we made a demonstration of the strongest measurement situation by using the 7-qubit quantum computer (ibm-perth). The performance of the measurement strategy is limited due to the noise and error in present NISQ.

This work is supported by MEXT Q-LEAP (JPMXS0118067581) and JST, the establishment of university fellowships towards the creation of science technology innovation (JPMJFS2102).

Figures

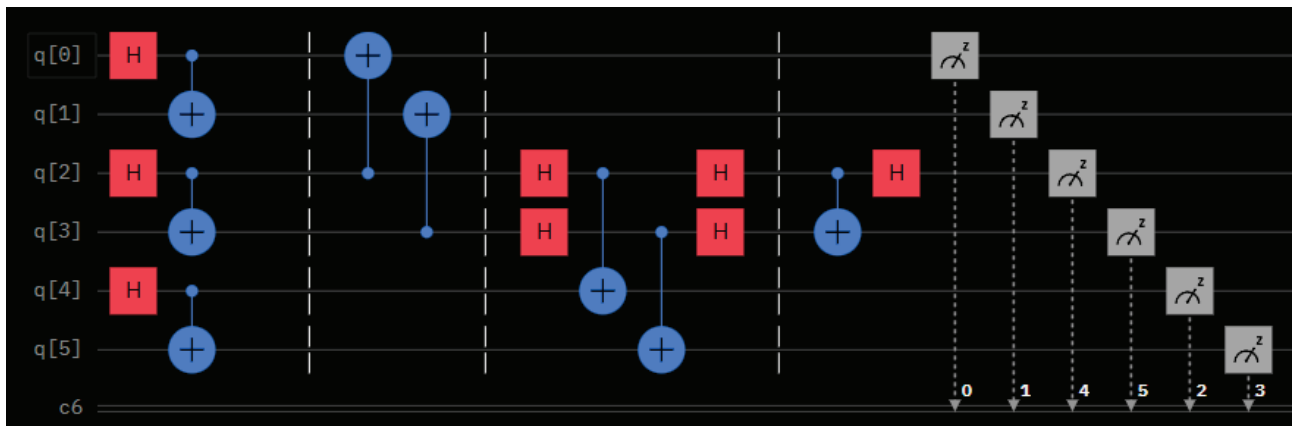


Fig.1 The measurement circuit of measuring a pair of qubits. The qubit 0 and 1 perform as meter 1 for measurement parity information. The qubit 2 and 3 perform the entangled system. The qubit 4 and 5 perform as the other meter for checking the phase information. The system pair is coupled with two meters by CNOT gate. Finally, the Bell-state measurement are done on the system qubits, and the meters are projected on the calculational basis.

Reference

- ¹M. Ozawa, Phys. Rev. A, 67, 042105 (2003).
- ²F. Kaneda, S.-Y. Baek, M. Ozawa, and K. Edamatsu, Phy. Rev. Lett. 112, 020402 (2014).
- ³P. Vidil and K. Edamatsu, New J. Phys. 23, 043004 (2021).

5th IFQMS

The 5th International Forum
on Quantum Metrology and Sensing

PROCEEDINGS

Short Presentation Session for Young Scientists
Part 2: SE-03B

29 November, 2022
Online Conference (Zoom)

Joint Program Session with Quantum Innovation 2022

Proc. 5th IFQMS (The 5th International Forum on Quantum Metrology and Sensing)

Quantum Sensing Track : Short Presentations by Young Researchers

SE-03B. Short Presentations by Young Researchers on SE-01, 04, 06, 07 Topics [5th IFQMS]

*Note: Depending on the program, the order of presentations may change within the same group

All the times in the program are Japan Standard time (GMT+9)

Nov 29 (Tue.)	Session / Presentation	Mentor Chair Co-chair / Presenter	Affiliation	Abstract ID
13:10-14:30	SE-03B-α1. Break-out Session 1			
	Chair	Noriaki Yahata	QST	
	Co-chair	Hidetoshi Kono	QST	
	Structural dynamics of the Mn4CaO5 cluster during the S2-S3 transition in photosystem II	Hongjie Li	Okayama U	SE-03B-α1-01
	Visualization of hydrogen in Photosystem II by high-resolution Cryo-EM analysis	Fusamichi Akita	Okayama U	SE-03B-α1-02
	Pulsed-EPR study for radical reactions with biological antioxidants utilizing quantum effect of electron spin	Hiroki Hirano	Kanagawa U	SE-03B-α1-03
	Coherent control of radical pair by local optimization theory	Akihiro Tateno	Saitama U	SE-03B-α1-04
	Probing the coherent spin dynamics of radical pairs in weak magnetic field using nanoseconds field switching technique	Ryusei Nozawa	Saitama U	SE-03B-α1-05
	Role of a tyrosine radical in the photoreaction of chicken Cryptochrome 4, a magnetoreceptor candidate molecule	Hiroaki Otsuka	Waseda U	SE-03B-α1-06
	Cavity ring-down measurements by continuous pulse trains for magnetic field effects on transient radical species.	Tsubasa Kimura	Saitama U	SE-03B-α1-07
	Germanium vacancy defects in detonation nanodiamonds for temperature sensing	Fu Haining	Kyoto U	SE-03B-α1-08
	Evaluation of the surface-modified nanodiamond probes by in vivo fluorescence imaging	Koki Okamoto	Tokyo Tech	SE-03B-α1-09
	Detection of heat generation from biological system using double quantum thermometry	Hitoshi Ishiwata	QST	SE-03B-α1-10
	The Anomalous Formation of Irradiation Induced Nitrogen-Vacancy Centers in 5-Nanometer-Sized Detonation Nanodiamonds	Frederick Tze Kit SO	Kyoto U	SE-03B-α1-11
	Microwave antenna architecture for quantitative prediction of ODMR signals	Keisuke Oshimi	Okayama U	SE-03B-α1-12
14:50-16:10	SE-03B-α2. Break-out Session 1			
	Chair	Yoichi Takakusagi	QST	
	Co-chair	Ryoko Araki	QST	
	An Artificial Intelligence Nanopore Platform Detects Omicron SARS-CoV-2 in clinical samples	Kaoru Murakami	Hokkaido U	SE-03B-α2-01
	Non-equilibrium ϕ_4 theory in a Hierarchy: Towards Manipulating Holograms in Quantum Brain Dynamics	Akihiro Nishiyama	Kobe U	SE-03B-α2-02
	Construction of dipeptide-based DNP-NMR molecular probe library focusing on kidney injury mouse model	Yuki Aketa	U Tokyo	SE-03B-α2-03
	Nuclear hyperpolarization of liquid water by using photoexcited triplet electrons in organic nanocrystals	Naoto Matsumoto	Kyushu U	SE-03B-α2-04
	Development of Polarizing Agent with Controlled Electronic Structure for Highly Efficient triplet-DNP	Keita Sakamoto	Kyushu U	SE-03B-α2-05
	DNP-NMR molecular probe for the detection of Dipeptidyl peptidase-4 activity in vivo	Akihito Goto	U Tokyo	SE-03B-α2-06
	Generation of polarized triplet electron spins at solid-liquid interfaces	Reiya Yabuki	Kyushu U	SE-03B-α2-07
	Photoreaction study of a primate blue-light sensitive photoreceptor using vibrational spectroscopy	Yosuke Mizuno	Nagoya Tech	SE-03B-α2-08
	Novel photoisomerization reaction in near-infrared light absorbing enzymerhodopsins	Masahiro Sugiura	Nagoya Tech	SE-03B-α2-09
	Development of a real-time 4D quantum temperature imaging system to measure intercellular thermal diffusivity	Haruka Maeoka	Hiroshima U	SE-03B-α2-10
	Bidirectional neural network and its application to image denoising, super-resolution, and image completion	Kei Majima	QST	SE-03B-α2-11
	Molecular insight into photoactivation mechanism of BLUF protein by QM/MM free energy simulation	Masahiko Taguchi	QST	SE-03B-α2-12

Structural dynamics of the Mn_4CaO_5 cluster during the S_2 - S_3 transition in photosystem II

Hongjie Li¹, Yoshiki Nakajima¹, Daichi Yamada², Kana Hashimoto¹, Minoru Kubo^{2,3}, So Iwata^{3,4}, Michihiro Suga¹ and Jian-Ren Shen¹

¹Research Institute for Interdisciplinary Science and Graduate School of Natural Science and Technology, Okayama University, Okayama, Japan

²Graduate School of Science, University of Hyogo, Hyogo, Japan,

³RIKEN SPring-8 Center, Hyogo, Japan

⁴Department of Cell Biology, Graduate School of Medicine, Kyoto University, Kyoto, Japan

Introduction

Photosystem II (PSII) catalyzes light-induced water oxidation through the S_i -state cycle at its oxygen-evolving catalyst, a Mn_4CaO_5 cluster. During this process, four electrons and four protons are released from two water molecules, and one di-oxygen molecule is evolved. Pump-probe time-resolved serial femtosecond crystallography (TR-SFX) has been used to capture several intermediate states of PSII, deepening our understanding of the water oxidation reaction. Significantly, a newly inserted oxygen O6 was observed in the vicinity of O5 in the S_3 -state before the di-oxygen formation^{1,2}. However, the origin of the O6 and the mechanism to incorporate it remain to be elucidated. To address this issue, we analyzed the structural dynamics of PSII during the onset of S_2 - S_3 state transition at various time points from nanoseconds to milliseconds after two flashes (2F) illumination using an X-ray free electron laser at SACLA, Japan.

Following the 2nd flash, no difference electron densities was observed within 20 ns. Instead, from 200 ns to 30 μs , paired positive and negative difference densities appeared in the area around Q165 and Y_Z , which was decreased at 200 μs and vanished at 5 ms following the 2nd flash (Fig. 1). Refined models demonstrate that Q165 and Y_Z move in the same direction during 200 ns to 30 μs and restore by 5 ms. These movements can be explained by the oxidation and re-reduction of Y_Z during the S_2 - S_3 state transition.

One positive density close to the Ca^{2+} ion, constructed with a water molecule and designated as O6*, appeared during 1 μs to 200 μs and vanished at 5 ms, with the concomitant increase of the O6 density from 30 μs to 5 ms (Fig. 1). We speculate that this water is the origin of O6 and is translocated via the Ca^{2+} ion binding site to the O6 site. Following the insertion of O6, Mn4 and Mn1 move apart from each other, opening the Mn_4CaO_5 cluster and presumably preparing for subsequent di-oxygen release in the next state transition.

These results provide important insights into the molecular mechanism of water oxidation in PSII.

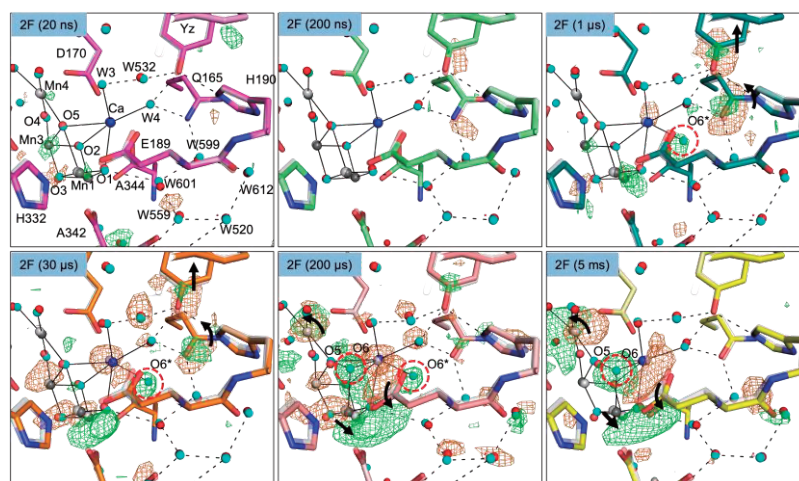


Fig. 1. Structural dynamics around the Mn_4CaO_5 cluster during the S_2 - S_3 transitions. Refined structures are superposed with $F^{\text{obs}}_{(2\text{F})} - F^{\text{obs}}_{(1\text{F})}$ difference density maps contoured at +3.5 (green) and -3.5 (orange) from 20 ns to 5 ms. The 1F structure is in grey and the 2F intermediate structure is colored. Black dot lines depict hydrogen bonds. Black arrows represent structural changes.

Reference

¹Suga, M. *et al.*, *Nature* **543**, 131-135 (2017)

²Suga, M. *et al.*, *Science* **366**, 334-338 (2019)

Visualization of hydrogen atoms in Photosystem II by high-resolution Cryo-EM analysis

Fusamichi Akita¹, Radostin Danev^{2,3}, Yoshiki Nakajima¹, Huaxin Yu⁴, Koji Kato⁵, Naoyuki Miyazaki⁶, and Jian-Ren Shen¹

¹Research Institute for interdisciplinary Science, Okayama University

²Graduate School of Medicine, The University of Tokyo

³PRESTO, Japan Science and Technology Agency

⁴Microbial Sciences Institute, Department of Microbial Pathogenesis, Yale University

⁵Structural Biology Division, Japan Synchrotron Radiation Research Institute

⁶Osaka Research Center for Drug Discovery, Otsuka Pharmaceutical Co., Ltd.

fusamichi_a@okayama-u.ac.jp

Introduction

Photosystem II (PSII) is a membrane protein supercomplex and functions to catalyze light-induced water-splitting, leading to the generation of electrons, protons, and molecular oxygen. PSII consists of 20 protein subunits and several cofactors, chlorophylls, carotenoids, and the oxygen-evolving center (OEC) responsible for splitting water through five intermediate states, S₀, S₁, S₂, S₃, and S₄. The structure of PSII at 1.9 Å resolution was solved in 2011, which revealed that the OEC has a “distorted chair” shape with a Mn₄CaO₅ composition¹. The structure of PSII without radiation damage at the S₁ state was determined at 1.95 Å resolution using femtosecond X-ray free electron lasers (XFEL)². Subsequently, the S₃ state was analyzed using a time-resolved serial XFEL³, and the structural transition from S₂ to S₃ was determined using fixed-target XFEL⁴. These studies showed the insertion of an oxygen atom (O6) into the vicinity of O5 in the Mn₄CaO₅ cluster, giving rise to a mechanism of O-O bond formation between O5 and O6. However, there has been little discussion on the protonation states of residues and water molecules as well as hydrogen release pathways, which require high-resolution structural analysis. Recent innovations in cryo-electron microscopy (Cryo-EM) technology have made it possible to achieve high resolutions that may show hydrogen atoms. Here, we analyzed the structure of PSII at 1.45 Å resolution using Cryo-EM. The difference map obtained showed peaks arising from hydrogen atoms around amino acid residues and water molecules. In this presentation, I will discuss the structural analysis of PSII by high-resolution cryo-EM, the protonation states of OEC and the hydrogen atom network.

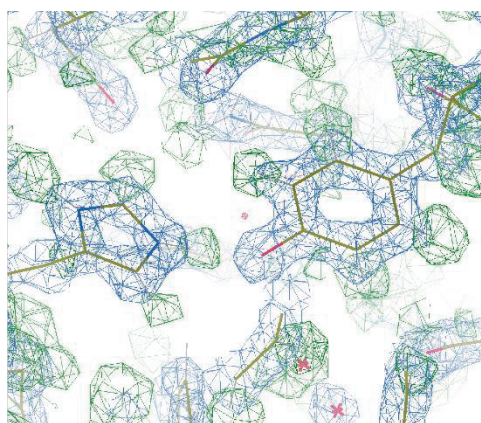


Fig. The Cryo-EM map of PSII at 1.45 Å resolution. The blue and green maps indicate the original Cryo-EM map and the calculated difference map, respectively.

Reference

1. Umena Y., Kawakami K., Shen J.-R., Kamiya N., Crystal structure of oxygen-evolving photosystem II at a resolution of 1.9 Å. *Nature*, **473**, 55-60 (2011).
2. Suga M. et al., Native structure of photosystem II at 1.95 Å resolution viewed by femtosecond X-ray pulses. *Nature*, **517**, 99-103 (2015).
3. Suga M. et al., Light-induced structural changes and the site of O=O bond formation in PSII caught by XFEL. *Nature*, **543**, 131-135 (2017).
4. Suga M. et al., An open-cubane oxyl/oxo mechanism for O=O bond formation in PSII revealed by XFEL. *Science*, **366**, 334-338 (2019).

Pulsed-EPR study for radical reactions with biological antioxidants utilizing quantum effect of electron spin

Hiroki Hirano¹, Kaito Marumo¹, Ikuo Nakanishi², Akio Kawai¹,

¹Graduated School of Science, Kanagawa university

²Institute for Quantum Life Science, Quantum Life and Medical Science Directorate, National Institutes for Quantum Science and Technology

r201503326@jindai.jp

Introduction

Radicals are important species that are highly reactive and play an important role in biological reactions. Usually, aging and disease of living body are caused by radicals. To protect these problems, there are many biological antioxidants in vivo. The biological antioxidants work to eliminate highly reactive radicals by reacting with them and transform themselves into stable radical species. A large number of studies have been made to determine radical reaction rate constants of biological antioxidants to evaluate radical trapping abilities¹. What seems to be lacking, however, is the observation in elementary reaction process, particularly in reactions with carbon-centered radicals. For understanding of the radical reactions, it is necessary to discuss them in terms of the kinetics of the elementary reaction process observations.

We have been investigating radical addition reaction mechanisms and rate constants by utilizing time-resolved (TR-) EPR and pulsed-EPR². These methods can observe elementary reaction process owing to their high time resolutions of several 10 ~ 100 ns. The radical reaction rate constants are obtained by measuring the electron spin echo (ESE) decay utilizing pulsed-EPR. The ESE signal is given by the spin wave packet of radicals that are in coherent state. Therefore, the radicals can be selectively observed. In this study, we aim to investigate radical reactions of biological antioxidants by identifying the reaction product radicals and determine radical rate constant of biological antioxidants utilizing these techniques.

Experimental method

TR-EPR measurement was performed to identify the intermediate radicals formed by radical reactions of antioxidants. Radical reaction rate constants of antioxidants were determined by ESE decay measurements. The radicals were generated by photolysis of radical sources such as aromatic ketone compounds. As for the antioxidants, α -tocopherol (α -Toch) and *tert*-butylphenol (TTBP) were used.

Results and Discussion

Fig.1 shows the ESE decays of 2-hydroxypropyl (2Hy-Pr) radical under different α -Toch concentrations. The ESE of the radicals was generated by a conventional Hahn echo pulse sequence with a $\pi/2$ pulse and a τ -delayed π pulse, which was initiated at t ns after the laser flash (laser flash – t – $\pi/2$ – τ – π – τ – ESE). The decay was obtained by monitoring the ESE signal intensity, $S(\tau)$, for series of τ values. The top line is the ESE decay of the 2Hy-Pr radical without antioxidants. The ESE decay rate, $1/T_M^*$, was determined by the exponential decay fitting procedure of the $S(\tau)$ profile on the basis of the equation,

$$S(\tau) = S_0 \exp\left(\frac{2\tau}{T_M^*}\right)$$

with S_0 (initial ESE amplitude) and T_M^* as a fitting parameter. Then, the ESE decay measurements were performed with different concentrations of α -Toch (Fig.1). It was found that the $1/T_M^*$ was faster depending on the α -Toch concentration. This is due to the elimination of 2Hy-Pr by the reaction with α -Toch. $1/T_M^*$ of these decays were also determined and the results were plotted against the concentration of α -Toch (Fig.2). The liner relationship was obtained and therefore, the radical reaction rate constant, k , was determined by the liner fitting following the equation,

$$\frac{1}{T_M^*} = \frac{1}{T_M} + k [\alpha\text{-Toch}]$$

where $1/T_M$ is the α -Toch -independent the ESE decay rate. The determined k value was $(3.2 \pm 0.2) \times 10^6 \text{ M}^{-1} \text{ s}^{-1}$. At the conference, we will discuss the reactivity of α -Toch by comparing the rate constant of TTBP.

Reference

¹ Packer, J. E., Slater, T. F., and Willson, R. L., *Nature*, 278, 737–738 (1979)

² H. Hirano, H. Takahashi, A. Kawai, *J. Phys. Chem. B*, 126, 6074–6082. (2022)

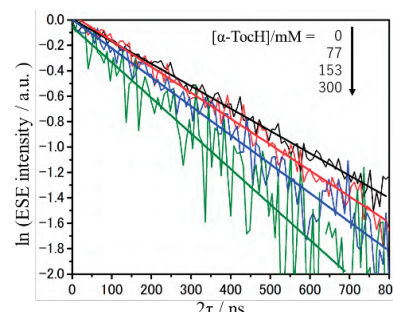


Fig.1 Time profiles of ESE intensity, $S(\tau)$, of 2Hy-Pr radical under various α -Toch concentrations.

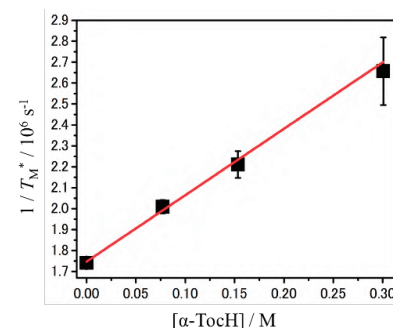


Fig.2 Stern-Volmer type analysis of $1/T_M^*$ of 2Hy-Pr radical versus $[\alpha\text{-Toch}]$.

Coherent control of radical species by local optimization theory

Akihiro Tateno¹, Kenta Masuzawa¹, Hiroki Nagashima¹, Michihiko Sugawara², and Kiminori Maeda¹

¹Graduate School of Science and Engineering, Saitama University

²Keio Quantum Computing Center, Keio University

a.tateno.275@ms.saitama-u.ac.jp

Introduction

Design of laser waveforms optimized for reaction control has attracted theoretical and experimental attention¹. However, it is not easy to realize the designed laser field. In contrast, recent progress of arbitrary wave generator (AWG) enables us to produce the designed radio wave field (RF). Recently, we have shown that it is possible to control the recombination reaction of a radical pair (RP) in high field using radio wave magnetic resonance designed based on the local optimization theory^{1,2}. As an example of coherent control, here we show the spin multiplicity control of RP at low fields and the design of optimized AWG pulse that induce selective spin echoes.

Coherent control in local optimization targets a transient state $|f\rangle_L$ that is non-eigenstate of the Hamiltonian at a specific time t_f . In order to produce $|f\rangle_L$ at t_f , it is necessary to calculate the moving target $|\rho_f\rangle_L$ that time-evolves to $|f\rangle_L$. $|\rho_f\rangle_L$ can be calculated by the time reverse Liouville operator as shown by

$$|\rho_f\rangle_L = \exp\{i\hat{L}_0(t_f - t)\}|f\rangle_L$$

We have chosen the singlet state and the S_y+S_z states as $|f\rangle_L$ for the reaction control of RPs and the selective spin echo measurement, respectively.

The calculation for the spin multiplicity control was done in a model RP system having one nuclear spin (HFC $A=0.5$ mT). In low magnetic field, almost all spin states are mixing coherently. We calculated an RF field with the aim of controlling a singlet born RP to singlet state after 1 μ s. The FIG.1a shows time-evolutions of the singlet probability in presence and absence of designed RF field. The RF irradiation change the singlet probability at 1 μ s after the production of RP from 39 % to 96 %.

As a model system for selective control of spin systems, we used a mixed system of TEMPO (solution) and BDPA (solid) whose stick diagram of the resonance lines is shown in FIG. 1b. In this system, we designed the RF waveform so that the electron spin of TEMPO radical transitions to the S_y state for three hyperfine lines at $t=200$ ns keeping the electron spin of BDPA in the S_z state. FIG 1c shows that the calculated RF provides the FT-EPR spectrum of selectively excited TEMPO radicals (solid line) whereas the spectrum obtained by composite pulse of three colour RF pulses contains the signal of undesired the other radical (broken line).

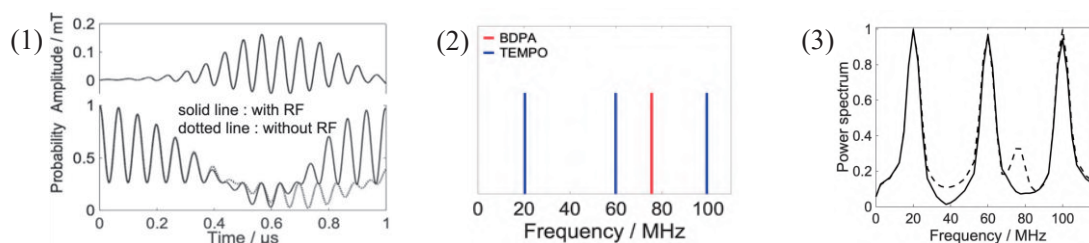


FIG. 1) Upper: Calculated RF, Lower: Time-evolution of singlet probability. 2) Model system 3) Calculated spin echo after optimised pulse (solid line) and after multi-colour pulse (dotted line)

References

¹M. Sugawara, *J. Chem. Phys.* **118**(15), 6784-6800 (2003).

²K. Masuzawa, M. Sato, M. Sugawara, and K. Maeda, *J. Chem. Phys.* **152**, 014301 (2020)

Probing the coherent spin dynamics of radical pairs in weak magnetic field using nanoseconds field switching technique

Ryusei Nozawa¹, Taisuke Matuo¹, Hiroki Nagashima¹, Kiminori Maeda¹

¹Department of Chemistry, Graduate School of Science and Technology, Saitama University.

r.nozawa.939@ms.saitama-u.ac.jp

Introduction

Recent discussions of the mechanism of magnetic sensitivity in animals have focused attention on the spin dynamics of radical pairs in the low-field region and the effects of the magnetic field. The existence of low-field effects in radical pairs is easy to confirm, since the magnetic field effects in radical pairs are in the opposite direction of those in the usual hyperfine coupling and relaxation mechanisms, but there are many theoretical models that are believed to be responsible for the magnetic field effects.[1] Matsuo et al. used nanosecond magnetic field switching techniques for the xanthone-DABCO system in SDS micelle solutions to analyze the behavior of radical pairs at weak magnetic fields and found the decay time of the transient absorption change was extremely short only when the external magnetic field was changed from the peak magnetic field of the low-field effect to zero field.[2] This result suggests that the origin of the low-field effect in this system is not pseudo-normal spin mixing, but coherent due to the breaking of the degenerate electron-nuclear spin state. We also thought we could observe a time equivalent to coherent low-field effect generation by applying nanosecond magnetic field switching techniques. Based on these, the nanosecond magnetic field switching technique was further applied in this study to four more magnetic fields exhibiting low-field effects to zero field to probe the coherent low-field effect generation process.

Method • Result

MARY spectra in the low-field region obtained in SDS micellar solutions of xanthone and DABCO are shown in FIG 1[a]. Transient absorption changes associated with magnetic field switching from four low magnetic fields(1.5, 1.1, 0.7, 0.4 mT) to zero magnetic field were monitored and their post-laser delay time dependence plotted. Experimental results on the curve of $t \approx h/2g\mu_B B_0$ as shown FIG1[b]. Comparing this result with the time evolution of the Singlet-like magnetic field effect by the one-nucleus spin model, it reflects the most prominent time of the coherent onset of the low-field effect due to the breaking of the degeneracy of the electron-nucleus spin state by the Zeeman energy. This indicates that the present method captures the generation of the low-field effect due to the breaking of the degeneracy in time. However, some other systems do not exhibit such ideal behavior and don't reflect the coherent rise time. This indicates the possibility of the influence of decoherence of spin systems, mechanisms of low-field effects other than degenerate breaking, and so on.

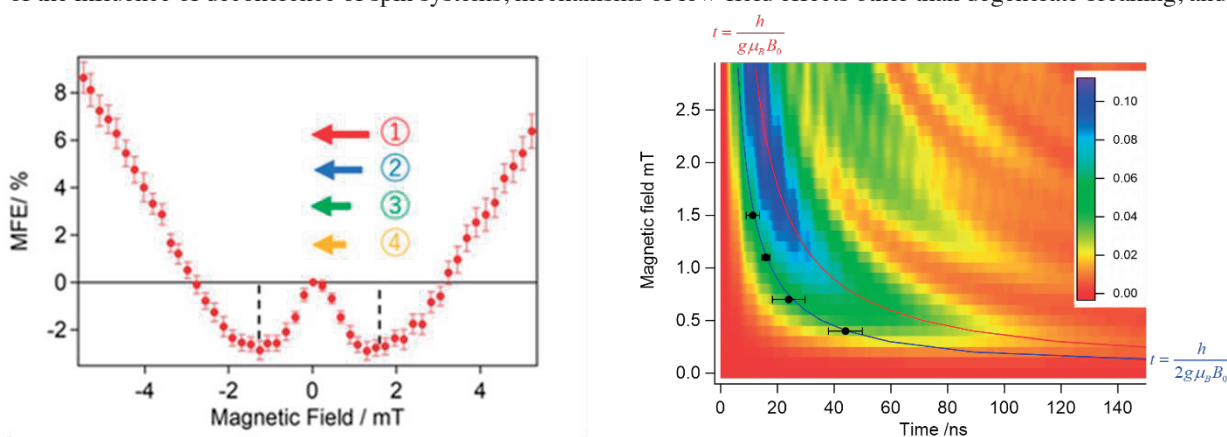


FIG.1. [a] Experimental results of MARY spectra of the Xanthone-DABCO system and the scheme for changing the magnetic field. [b] Calculation results magnetic field effects of Singlet in the one-nucleus spin, and the result of inverse field switching.

Reference

- [1] ¹Maeda, K. et al., *Nature*, 452,387-390(2008).
 [2] ¹Matuo.T., *Master thesis*(2018).

Role of a tyrosine radical in the photoreaction of chicken Cryptochrome 4, a magnetoreceptor candidate molecule

Hiroaki Otsuka¹, Ryosuke Miyake¹, Keiko Okano¹, Yasushi Imamoto², and Toshiyuki Okano¹

¹Department of Electrical Engineering and Bioscience, School of Advanced Science and Engineering, Waseda University

²Department of Biophysics, Graduate School of Science, Kyoto University
o1.2t5.8tt21.tf@ruri.waseda.jp

Introduction

Some animals have the ability of magnetoreception [1]. Interestingly, the magnetoreception of birds and insects is driven by light. As a possible mechanism of the light-dependent magnetoreception, “Radical pair mechanism (RPM)” has been proposed, in which the magnetosensitive bifurcation of reaction of two entangled radicals (radical pair) formed by photoexcitation is used [2]. The magnetic sensor in RPM would have the light-sensitivity and the ability of radical formation, and cryptochromes (CRYs) are considered to be candidates for the magnetoreceptor. Our previous study revealed the ability of photoreception via flavin adenine dinucleotide chromophore (FAD) and radical formation of CRY4 in the chick retina [3–5]. The spectroscopic analysis of the transient reaction of chicken CRY4 (cCRY4) identified a formation of FAD anion radical (FAD^{•-}) upon light absorption, which was reacted into bifurcated reaction of oxidation or protonation. Interestingly, a neutral tyrosine radical (Tyr-O[•]) like spectrum was detected with the formation of FAD^{•-} and it decayed along with the protonation of FAD^{•-} [6]. According to RPM, magnetosensitive reaction of bifurcation to reduction and oxidation is expected to a key step. Although the detail role and the site of Tyr-O[•] formation are unknown, Tyr-O[•] could play an important role in the bifurcation.

In this study, we aim to identify the site of Tyr-O[•] formation and elucidate the role of Tyr-O[•] in the photoreaction of cCRY4 by comparing the photoreaction of cCRY4 tyrosine mutant with that of wild-type cCRY4.

Method

Tyr319 is an amino acid locating near the fourth tryptophan that constitutes a putative electron-transfer pathway called Trp-tetrad in cCRY4, and it was mutated to phenylalanine (F). Wild-type and Y319F mutant of recombinant cCRY4 were expressed by yeast expression system and purified by GST-tag-based purification system. Steady-state photoreactions and their efficiencies were analyzed using double beam spectroscopy (UV-2450). Transient reactions of each sample were measured by laboratory-built, time-resolved spectrophotometry system.

Results and discussion

The chromophore FAD in the dark-state of cCRY4 is oxidized (FAD_{OX}). Blue light irradiation reduces the FAD_{OX} to FAD^{•-}, a part of which is immediately (subsecond order) protonated to a neutral radical form (FADH[•]). Quantum yield of FAD_{OX} → FADH[•] in cCRY4 WT was 16%, while that in cCRY4 Y319F decreased to 6.0%. As reported previously, cCRY4 WT showed FAD^{•-} formation immediately after photoexcitation (< 0.5 ms), followed by bifurcation to fast (≈ 100 ms) oxidation (FAD^{•-} → FAD_{OX}) and slow (≈ 400 ms) protonation (FAD^{•-} → FADH[•]), the former of which was accompanied by decay of Tyr-O[•] (FIG. 1A). In contrast, most of the FAD^{•-} was oxidized in cCRY4 Y319F, and noticeably, spectra resembling tryptophan neutral radicals (Trp[•]) instead of Tyr-O[•] were observed (FIG. 1B).

The observation of Trp[•]-like spectra in cCRY4 Y319F is consistent with the idea that Tyr319 donates electron to FAD via Trp tetrad. The suppression of the FAD^{•-} protonation in cCRY4 Y319F suggests a possible role of Tyr-O[•] in the protonation.

Reference

¹R. Wiltshcko and W. Wiltshcko, *Adv. Exp. Med. Biol.* **739**, 126 (2012); ²T. Ritz, S. Adem, and K. Schulten, *Biophys. J.* **78**, 707 (2000); ³Y. Kubo, M. Akiyama, Y. Fukada, and T. Okano, *J. Neurochem.* **97**, 1155 (2006); ⁴R. Watari, C. Yamaguchi, W. Zemba, Y. Kubo, K. Okano, and T. Okano, *J. Biol. Chem.* **287**, 42634 (2012); ⁵H. Mitsui, T. Maeda, C. Yamaguchi, Y. Tsuji, R. Watari, Y. Kubo, K. Okano, and T. Okano, *Biochemistry* **54**, 1908 (2015). ⁶H. Otsuka, H. Mitsui, K. Miura, K. Okano, Y. Imamoto, and T. Okano, *Biochemistry* **59**, 3615 (2020).

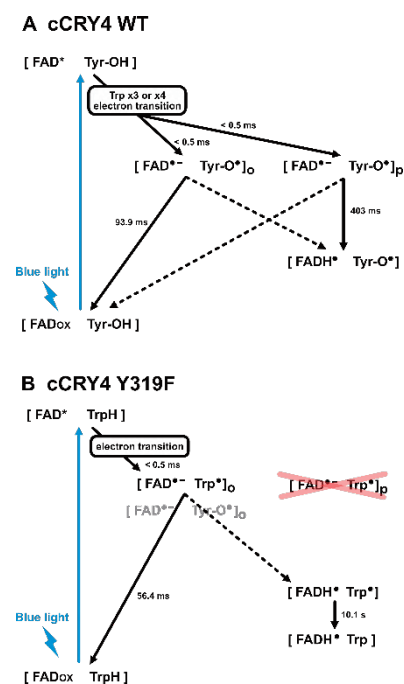


FIG. 1. Reaction model of cCRY4 WT and cCRY4 Y319F (A) FAD^{•-} binding cCRY4 is bifurcated into oxidation form and protonation form. Tyr-O[•] decays as FAD^{•-} oxidizes. (B) Almost FAD^{•-} oxidizes in cCRY4 Y319F, and Trp[•] is formed instead of Tyr-O[•].

SE-03B- α 1-07

Cavity ring-down measurements by continuous pulse trains for magnetic field effects on transient radical species.

Tsubasa Kimura¹ and Kiminori Maeda¹¹Department of Chemistry, Graduated school of Science and Engineering, Saitama University

t.kimura.485@ms.saitama-u.ac.jp

Introduction

The magnetic field effect (MFE) measurements of photo-generated radical pairs in photochemical reactions fundamentally need very high sensitivity and long acquisition with many light pulse irradiations. The degradation due to the multiple pump pulse irradiations is a difficult concern when we apply to precious biological samples. Previously, the sensitivity problem was solved with pump-probe type cavity ringdown (CRDS) method [1], which boosts the effective optical path length using optical cavity. If we compared the CRDS with the cavity enhanced absorption spectroscopy (CEAS) [2], the CRDS on transient absorption (TA) measurements has advantageous aspects: 1) free from correction of the wavelength dependent cavity enhancement, 2) free from the fluctuations of the probe beam, 3) clear estimation of the time resolution.

Here we developed a new CRDS technique named super-CRDS (SCRDS) [3], which is sequential CRDS measurements using a pulse train of a super continuum source (SC source). SCRDS allows us to measure the absorptions at many delay times with 200 ns interval (5 MHz). Therefore, we can get the transient absorption (TA) time trace by a single excitation simultaneously. This fact dramatically reduces the number of excitation light irradiations, keeping the sensitivity as same as pump-probe CRDS.

Method

The TA at 500~600 nm and its magnetic field effect were measured by SCRDS technique. The mixed aqueous solution of FMN 50 μ M and HEWL 200 μ M, 40 mL was flown from a syringe pump to a sample cell (200 μ L volume and 1 mm optical length). The CRDS signal is penetrated from the back side of the cavity mirror and monitored by a photomultiplier tube. The CRD signals are fit by a single exponential function for every delay times. The transient absorbances ΔA per single pass of the probe light can be calculated by the lifetime of the signal τ and that at the negative delay time τ_0 . The TA was measured in the field range from 0 to 20 mT. Pulsed magnetic fields, whose duration is 1.8 ms, were synchronized with the excitation pulse laser. The flat region of the magnetic field in time was used for the TA measurements. In the MFE measurement, the absorption was measured while the magnetic field was varied by 2 mT, and the absorption from 10 to 90 μ s was averaged to obtain the magnetic field effect at each magnetic field. This process was repeated 200 times at each magnetic field.

Results

The intensity of the excitation light was adjusted to be comparable to that of Ref [1]. FIG. 1 is a plot of TA time profiles, and FIG. 2 is a plot of MFE measurement. SCRDS requires only one-tenth of the number of shots, (200 shots), to measure the TA for a single magnetic field intensity, and the error can be suppressed to ± 0.25 %.

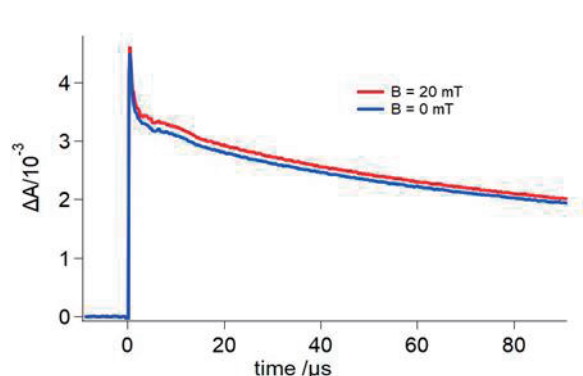


FIG. 1. Time-resolved transient absorption signal in the system of FMN 50 μ M and HEWL 200 μ M. The signal obtained by 100 shots laser excitation is averaged.

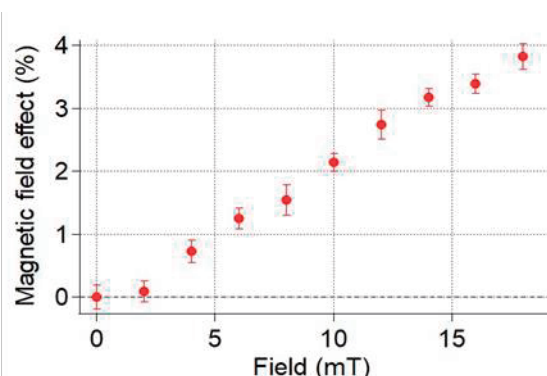


FIG. 2. Magnetic field effect using SCRDS in the system of FMN 50 μ M and HEWL 200 μ M. 200 shots averaged per points.

Acknowledgements: This work was supported by MEXT Q-LEAP Grant Number JPMXS0120330644

References: [1] Maeda, K *et al.*, *J. Am. Chem. Soc.*, **133**, 17807–17815 (2011).

[2] Neil, S. R. T *et al.* *J. Phys. Chem. B*, **118**, 4177–4184(2014).

[3] Japan Patent 2022- 7803.

Germanium Vacancy Defects in Detonation Nanodiamonds for Temperature Sensing

Haining Fu¹, Masanori Fujiwara¹, Izuru Ohki¹, Ming Liu², Akihiko Tsurui², Taro Yoshikawa², Masahiro Nishikawa², and Norikazu Mizuochi¹

¹Institute for Chemical Research, Kyoto University

²Daicel Cooperation

fu.haining.82r@st.kyoto-u.ac.jp

Introduction

Group IV color centers such as silicon-vacancy center (SiV) and germanium-vacancy center (GeV) in nanodiamonds (NDs) are promising candidates for all-optical nanoscale thermometry. Because these defects have sharp zero phonon lines (ZPLs) and the ZPL peak wavelength changes depending on local temperature. For live-cell application, NDs should be smaller than 30 nm to avoid non-invasive methods. However, the minimum size of NDs concluding group IV color centers as temperature sensors reported was 200 nm [1]. This motivated us to synthesize NDs by detonation method, which is suitable for the mass production of NDs in smaller size. In 2020, we reported the first synthesis of SiV-containing detonation nanodiamonds (SiV-DNDs) [2]. Then, we performed all-optical thermometry with SiV-DNDs in an average size of 20 nm. This is the smallest size applied for thermometry using color-center-containing NDs [3].

Compared to SiV center, GeV center shows higher quantum efficiency, and its ZPL peak wavelength is 100 nm shorter than SiV center, make it a good candidate for temperature sensing. GeV-containing detonation nanodiamonds (GeV-DNDs) has been synthesized successfully according to the recent report [4]. And in our current study, we focus on the temperature sensing of GeV-DNDs, evaluated their PL spectrum response according to temperature. GeV center combining SiV center is suitable for multi-color imaging application and local temperature measurements of live-cell organelles.

Methods & Results

After the detonation of explosives with Ge dopant, our sample was processed by purification, dispersion, surface modification, and ultracentrifugation. Supernatant and suspension were collected as different samples. In addition, the sediment was also collected and dispersed into pure water as another sample. Each sample was dropped on a coverslip, natural drying in the air atmosphere. A thermoplate is set to control the sample temperature. Each sample were observed and taken photoluminescence (PL) image by a homebuilt confocal microscope.

Both the supernatant and suspension samples showed weak GeV centers' ZPL signals at around 602 nm, and a strong PL background signal from DND itself has been observed. In the sediment sample, however, we found a strong ZPL signal from some bright spots in PL image (Fig. 1(a)). These bright spots may be GeV-DND aggregations or large GeV-DND particles. At these spots, we confirmed that the ZPL peak wavelength (λ) linearly red-shifted with increasing temperature (T) (Fig. 1(b)). The slope $\Delta\lambda/\Delta T$ is an indicator of the temperature response and the average value is 0.009 nm/K, which agrees with the GeV center ensemble in a bulk diamond (0.008 nm/K) [5]. The particle distribution is investigated by transmission electron microscope image. The average particle size is 20 nm, much smaller than the reported GeV-NDs for thermometry application (400 nm) [6]. Finally, we measured and calculated the temperature sensitivity (η_T), which defined as the temperature deviation (σ_T) per unit integration time (1s). As an example, a temperature sensitivity as 1.9 K Hz^{-1/2} measured at a bright spot shows in Fig. 1(c), means that a sub-Kelvin temperature change can be measured in 10 seconds.

This work is supported by MEXT Q-LEAP (No. JPMXS0120330644).

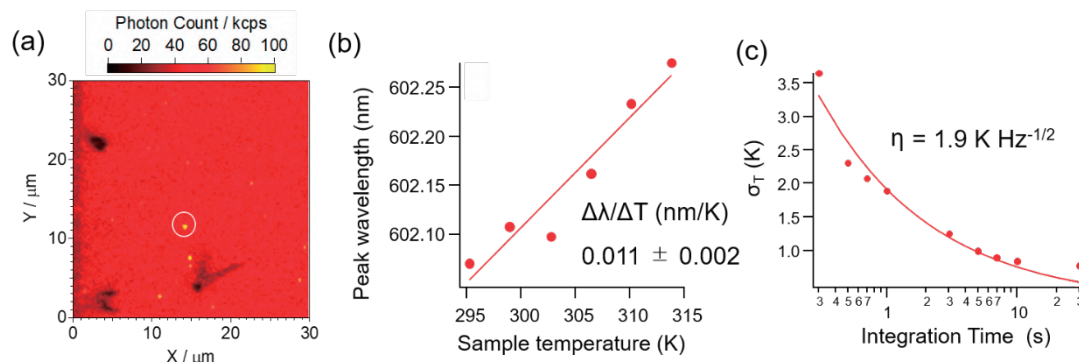


Figure 1 (a) PL image of the GeV-DND sediment sample. (b) and (c) Temperature dependence and temperature sensitivity measurements at the bright spot depicted in a white circle in (a).

Reference

- [1] C. T. Nguyen, et al., *Appl. Phys. Lett.* **112**, 203102 (2018). [2] Y. Makino, et al., *Diam. Relat. Mater.* **112**, 108248 (2021). [3] M. Fujiwara, et al., *Carbon*, **198**, 57 (2022). [4] Y. Makino, et al., *Diam. Relat. Mater.* **130**, 109493 (2022) [5] S. Blakley, et al., *ACS Photonics*, **6**, 1690 (2019). [6] T. T. Tran, et al., *Sci. Adv.* **5**, eaav9180 (2019)

Evaluation of the surface-modified nanodiamond probes by *in vivo* fluorescence imaging

Koki Okamoto¹, Masaya Muto¹, Tetsuya Kadonosono¹, Kiichi Kaminaga², Ryuji Igarashi², and Shinae Kizaka-Kondoh¹

¹*School of Life Science and Technology, Tokyo Institute of Technology*

²*Institute for Quantum Life Science, National Institutes for Quantum Science and Technology*
okamoto.k.am@m.titech.ac.jp

Introduction

In recent years, fluorescent nanodiamond have attracted attention as a novel *in vivo* imaging probe¹. Nitrogen-vacancy centers in nanodiamond have electrons whose quantum state (such as spin resonance frequencies) change according to changes in the surrounding environment. This variation of quantum state can be used to develop environmentally responsive sensor probes^{2, 3}. Tumors have a unique and complex microenvironment characterized by hypoxia⁴, which is closely associated with treatment resistance and malignant progression, making it important therapeutic targets. Early detection of tumor hypoxia is expected to contribute to the improvement of cancer treatment.

Our goal in this research is to develop nanodiamond imaging probes that can detect hypoxia in tumors with high sensitivity. Here, we take full advantage of the excellent photostability of fluorescent nanodiamonds, to perform fundamental *in vivo* evaluations of 50-100 nm surface-modified diamond nanoparticles, which are the basic for creating hypoxia probes. We evaluated their fluorescence sensitivity upon *in vivo* administration (intratumoral, subcutaneous, and intravenous) in mice.

Polyglycerol hydrophilically modified 100-nm nanodiamond particles were found to be the most sensitive for fluorescence detection among the particles evaluated, and thus will be used as a base material to create sensor probes that detects hypoxic cells using the cellular oxygen sensor function. Such probes are expected to contribute to early detection of hypoxic diseases including malignant tumors.

This work was supported by MEXT Q-LEAP Grant Number JPMXS0120330644.

Tables and Figures

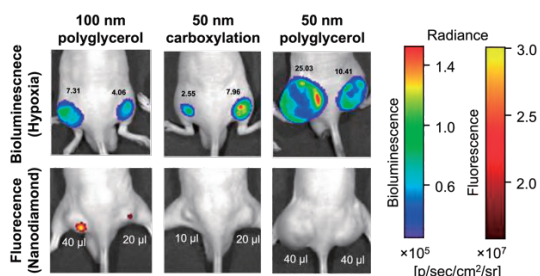


FIG. 1. Representative images of mice with hypoxic tumors (top: bioluminescence) and nanodiamond particles injected into tumor (bottom: fluorescence).

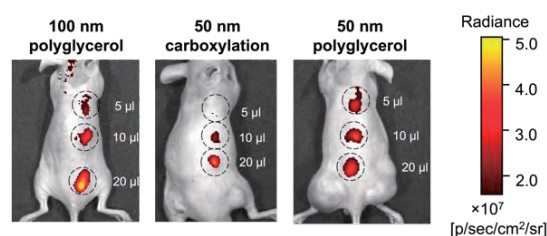


FIG. 2. *In vivo* fluorescence image of subcutaneously injected surface-modified nanodiamond particles.

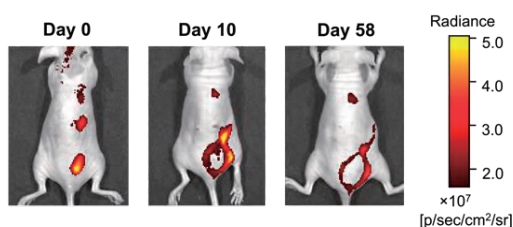


FIG. 3. *In vivo* fluorescence image of 100-nm nanodiamond particles with polyglycerol hydrophilic modification at the indicated time points after subcutaneous injection of the particles.

Reference

- ¹M. H. Alkahtani et al., *Nanophotonics*, **7**, 1423-1453 (2018)
- ²M. Fujiwara et al., *Sci. Adv.*, **6**, 37 (2020).
- ³T. Fujisaku et al., *ACS Nano*, **13**, 11726-11732 (2019)
- ⁴V. Petrova et al., *Oncogenesis*, **7**, 10 (2018)

SE-03B- α 1-11

5The Anomalous Formation of Irradiation Induced Nitrogen-Vacancy Centers in 5-Nanometer-Sized Detonation Nanodiamonds

Frederick T.-K. So^{1,2,3}, Alexander I. Shames⁴, Daiki Terada^{2,3}, Takuya Genjo^{2,3}, Hiroki Morishita¹, Izuru Ohki¹, Takeshi Ohshima⁵, Shinobu Onoda⁵, Hideaki Takashima⁶, Shigeki Takeuchi⁶, Norikazu Mizuochi¹, Ryuji Igarashi^{3,7}, Masahiro Shirakawa^{2,3*}, Takuya F. Segawa^{2,8*}

¹Institute for Chemical Research, Kyoto University

²Department of Molecular Engineering, Graduate School of Engineering, Kyoto University

³Institute for Quantum Life Science, National Institutes for Quantum and Radiological Science and Technology

⁴Department of Physics, Ben-Gurion University of the Negev, Israel

⁵Takasaki Advanced Radiation Research Institute, National Institutes for Quantum Science and Technology

⁶Department of Electronic Science and Engineering, Kyoto University

⁷National Institute for Radiological Sciences, National Institutes for Quantum Science and Technology

⁸Laboratory for Solid State Physics, ETH Zurich, Switzerland

so.kit.58a@st.kyoto-u.ac.jp

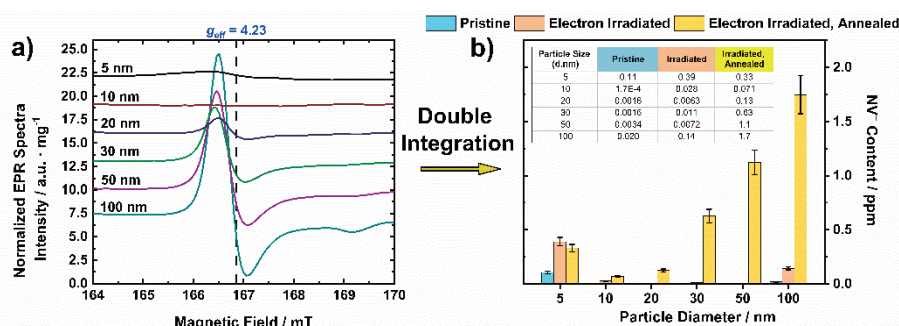
Introduction

Nanodiamonds containing negatively charged nitrogen-vacancy (NV⁻) centers are versatile room-temperature quantum sensors in a growing field of research. Yet, knowledge regarding the NV⁻ formation mechanism in very small particles is still limited. This study focuses on the formation of the smallest NV⁻-containing diamonds, 5 nm detonation nanodiamonds (DNDs). As a reliable method to quantify NV⁻ centers in nanodiamonds, half-field signals in electron paramagnetic resonance (EPR) spectroscopy are recorded. By comparing the NV⁻ concentration with a series of nanodiamonds from high-pressure high-temperature (HPHT) synthesis (10–100 nm), it is shown that the formation process in 5 nm DNDs is unique in several aspects. NV⁻ centers in DNDs are already formed at the stage of electron irradiation, without the need for high-temperature annealing, an effect related to the very small particle size. Also, the NV⁻ concentration (in atomic ratio) in 5 nm DNDs surpasses that of 20 nm-sized nanodiamonds, which contradicts the observation that the NV⁻ concentration generally increases with particle size. This can be explained by the 10 times higher concentration of substitutional nitrogen atoms in the studied DNDs ($[N_S \approx 1000 \text{ ppm}]$) compared to the HPHT nanodiamonds ($[N_S \approx 100 \text{ ppm}]$). Upon electron irradiation at a fluence of $1.5 \times 10^{19} \text{ e}^-/\text{cm}^2$, DNDs show a 12.5-fold increment in the NV⁻ concentration with no sign of saturation reaching 1 out of about 80 DNDs containing an NV⁻ center. These findings can be of interest for the creation of defects in other very small semiconductor nanoparticles beyond NV-nanodiamonds as quantum sensors.

This work was supported by MEXT Q-LEAP Grant Number JPMXS0120330644 & JPMXS0118067395, KAKENHI (Grants 20H00453, 18K19297 and 21H04444)

Method

Figure 1. (a) Continuous-wave HF EPR spectra ($\nu = 9.87^* \text{ GHz}$) of electron-irradiated (2 MeV , $5 \times 10^{18} \text{ e}^-/\text{cm}^2$) NDs with different particle sizes after high-temperature annealing. The double integral of the signal at $g_{\text{eff}} = 4.23$ provides the NV⁻ concentration. (b) A summary graph of NV⁻ content (ppm, in units of atomic ratio) in NDs of different sizes, measured via the HF EPR technique. Blue bars are the pristine NDs, orange bars are the electron-irradiated NDs, and yellow bars are the electron-irradiated and subsequently annealed NDs (derived from the $g_{\text{eff}} = 4.23$ signal in the EPR spectrum of panel a). Electron irradiation was conducted with 2 MeV electrons at a fluence of $5 \times 10^{18} \text{ e}^-/\text{cm}^2$. Annealing was performed at $800 \text{ }^\circ\text{C}$ in vacuum for 2 h. All samples were boiling acid treated at $130 \text{ }^\circ\text{C}$ for 3 days to remove Fe^{3+} impurities, which overlap with the HF EPR NV⁻ signal. Inset table shows the corresponding NV⁻ concentrations in ppm. Errors in NV⁻ concentration do not exceed $\pm 15\%$.



Electron irradiation was conducted with 2 MeV electrons at a fluence of $5 \times 10^{18} \text{ e}^-/\text{cm}^2$. Annealing was performed at $800 \text{ }^\circ\text{C}$ in vacuum for 2 h. All samples were boiling acid treated at $130 \text{ }^\circ\text{C}$ for 3 days to remove Fe^{3+} impurities, which overlap with the HF EPR NV⁻ signal. Inset table shows the corresponding NV⁻ concentrations in ppm. Errors in NV⁻ concentration do not exceed $\pm 15\%$.

Microwave antenna architecture for quantitative prediction of ODMR signals

Keisuke Oshimi^{1*}, Masazumi Fujiwara¹

¹Grad. Sch. Natural Science and Technology, Okayama University

*pcfw97je@s.okayama-u.ac.jp

Introduction

Quantum sensing with fluorescent nanodiamonds (NDs) containing nitrogen-vacancy (NV) centers is performed under the fluorescence microscope with microwave irradiation. It reads a modulation of optically detected magnetic resonance (ODMR) of electron spins of NV centers. This technique and the low cytotoxicity and biocompatibility of NDs enable to measure physical quantities inside biological samples, such as electric field, magnetic field, and temperature. So far, several antenna structures have been developed for microwave excitation and used in biological research [1-3]. Recently, we reported a glass-based antenna device having millimeter-scale area of microwave irradiation [4]. In this work, we demonstrate the quantitative prediction of the ODMR on our antenna devices, by thoroughly studying the relationship between the antenna properties and ODMR contrast.

Method

We quantitatively predict ODMR contrast on the glass surface of the antenna chip device developed for ODMR measurements in biological samples (FIG. 1(a)). As shown in FIG. 1(b), we first simulated the microwave magnetic field ($|B|$) in the ODMR measurable area (sample detection area) by numerical simulation based on the finite element method, considering the microwave reflection and transmission of chip devices and microwave components (cables, RF switches, and amplifier). We next converted the simulated $|B|$ to ODMR contrast of NDs using a theoretical equation based on rotational Bloch equations [5]. For the comparison of this theoretical ODMR with the experimental results, we overlaid the theoretical curve, as shown in FIG. 1(c). We found theoretical results closely matched the experimental results, which indicates experimental ODMR measurements are predictable by the numerical simulation at the stage of design development. In the presentation, we explain about the development methodology, and the future biological application of ND-based quantum sensing.

This work was supported by the Nanotechnology Platform Project (Nanotechnology Open Facilities in Osaka University) of MEXT (JPMXP09F21OS0055), JSPS-KAKENHI (19K21935, 20H00335, 20KK0317), AMED (JP21zf0127004), JST (JPMJMI21G1), the MEXT-LEADER program, the Mazda Foundation, and Osaka City University Strategic Research Grant 2017–2020, MEXT Quantum Leap Flagship Program (MEXT Q-LEAP, JPMXS0120330644).

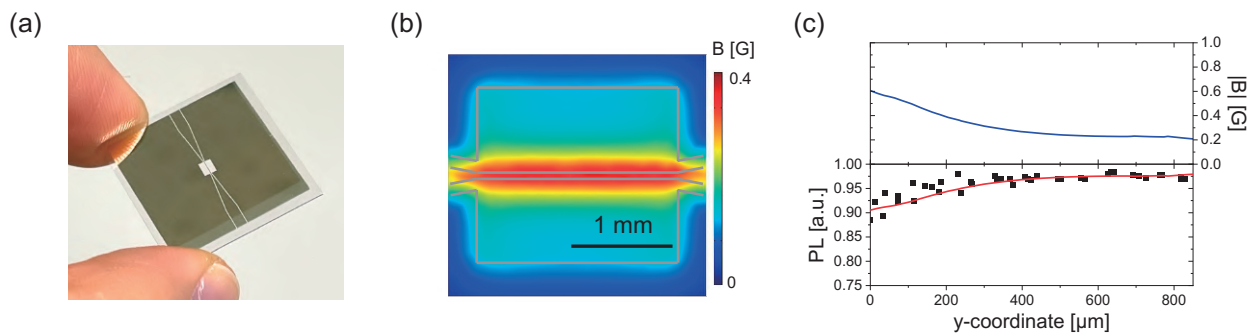


FIG. 1 (a) Photograph of an antenna chip device. (b) The computed spatial distribution of $|B|$ at 2.87 GHz on the chip surface. (c) Position dependence of the simulated $|B|$ (top; blue line) and measured ODMR depth (bottom; black squares) with the line calculated from the simulated $|B|$ (bottom; red line).

Reference

¹Yukawa et al., *Nanoscale Adv.*, **2**, 1859 (2020). ²J. Choi et al., *PNAS*, **117**, 14636 (2020). ³R. Igarashi et al., *J. Am. Chem. Soc.*, **142**, 7542 (2020). ⁴Oshimi, Nishimura, Matsubara, Tanaka, Shikoh, Zhao, Zou, Komatsu, Ikado, Takezawa, Kage-Nakadai, Izutsu, Yoshizato, Morita, Tokunaga, Yukawa, Baba, Teki and Fujiwara, *Lab Chip*, **22**, 2519 (2022). ⁵A. Dréau et al., *Phys. Rev. B*, **84**, 195204 (2011).

SE-03B- α 2-01

An Artificial Intelligence Nanopore Platform Detects Omicron SARS-CoV-2 in clinical samples

Kaoru Murakami^{1,2}, Shimpei Kubota^{1,2}, Keiichiro Akabane¹, Kumiko Tanaka¹, Rigel Suzuki³, Yuta Shinohara¹, Hiroyasu Takei⁴, Shigeru Hashimoto¹, Yuki Tanaka², Shintaro Hojyo^{1,2}, Kazuki Sato^{1,6}, Yuichi Kojima^{1,6}, Masateru Taniguchi^{5*}, and Masaaki Murakami^{1,2,12*}

1) Molecular Psychoimmunology, Institute for Genetic Medicine, Graduate School of Medicine, Hokkaido University, Sapporo 060-0815, Japan

2) Group of Quantum immunology, Institute for Quantum Life Science, National Institute for Quantum and Radiological Science and Technology (QST), Chiba 263-8555, Japan

3) Department of Microbiology and Immunology, Graduate School of Medicine, Hokkaido University, Sapporo, 060-0815, Japan.

4) Aipore Inc., 26-1 Sakuragaokacho, Shibuya, Tokyo 150-8512, Japan.

5) The Institute of Scientific and Industrial Research, Osaka University, Ibaraki, 567-0047, Osaka, Japan.

6) Department of Hematology, Faculty of Medicine, Hokkaido University, Sapporo, 060-8638, Japan

Abstract

We recently reported a highly accurate, cost-effective artificial intelligence nanopore platform (AI-nanopore platform) to detect coronaviruses, including Wuhan SARS-CoV-2 within five minutes.

We here show that this platform can further distinguish SARS-CoV-2 alfa, beta, gamma, delta, and omicron variants. Moreover, it identified mutated Wuhan SARS-CoV-2 expressing the spike proteins of the delta and omicron variants. Furthermore, we identified the omicron variant with a sensitivity of 100% and specificity of over 94% in saliva specimens isolated from COVID-19 patients, which is the similar and/or better values to RT-PCR. Importantly, AI-nanopore platform can identify even low concentrations of omicron variants with both sensitivity and specificity of over 95% in saliva specimens, which had more than 30 Ct values of RT-PCR analysis and are hard to be evaluated by RT-PCR, suggesting that the platform has an advantage over RT-PCR analysis. Thus, this AI-nanopore platform may be an effective diagnostic tool for emerging infectious pathogens including SARS-CoV-2 in clinical situation.

Rationale:

We recently reported an artificial intelligence (AI)-nanopore platform that enables testing for Wuhan SARS-CoV-2 with high sensitivity and specificity. However, which parts of SARS-CoV-2, whether mutated SARS-CoV-2 variants, or clinical samples with low concentration of virus are recognized by the AI-nanopore platform are unknown.

Objectives:

To investigate these three questions.

Methods:

We analyzed cultured SARS-CoV-2 alpha, beta, gamma, delta, and omicron variants using an improved AI-nanopore platform. To identify the specific SARS-CoV-2 structures detected by the platform, we prepared mutated Wuhan variant SARS-CoV-2 expressing the spike proteins of the delta or omicron variants. Additionally, we analyzed 241 saliva samples with omicron variants collected from 132 infected and 109 uninfected people based on RT-PCR results using the platform.

Measurements and Main Results:

The platform distinguished cultured SARS-CoV-2 the five variants and the mutated Wuhan variant, suggesting the platform's sensitivity for the spike protein. Furthermore, it identified omicron SARS-CoV-2 with a sensitivity of over 100% and specificity of over 94% from saliva specimens isolated from COVID-19 patients. Moreover, the platform can identify even low concentrations of omicron variants with both sensitivity and specificity of over 95% in saliva specimens, which are hard to be evaluated by RT-PCR.

Conclusions:

The AI-nanopore platform is an effective diagnostic tool for SARS-CoV-2 variants in clinical samples even with low concentration virus.

Keywords: COVID-19 diagnosis, AI-nanopore, SARS-CoV-2 variants

SE-03B-α2-02

Non-equilibrium ϕ^4 theory in a Hierarchy: Towards Manipulating Holograms in Quantum Brain Dynamics

Akihiro Nishiyama¹, Shigenori Tanaka¹ and Jack A. Tuszynski²

¹Graduate School of System Informatics, Kobe University, 1-1 Rokkodai, Nada-ku, Kobe, 657-8501, Japan

²Department of Oncology, University of Alberta, Cross Cancer Institute, Edmonton, Alberta, Canada T6G 1Z2

anishiyama@people.kobe-u.ac.jp

Introduction

We describe non-equilibrium ϕ^4 theory in a hierarchical manner in order to develop a method for manipulating coherent fields as a toy model of introducing control into Quantum Field Theory (QFT) of the brain, which is called Quantum Brain Dynamics (QBD). We begin with the Lagrangian density of ϕ^4 model, and derive the Klein–Gordon equation of coherent fields with a damping term as an input–output equation proposed in areas of morphological computation or reservoir computing. Our analysis is extended to QFT in a hierarchy representing multiple layers covering cortex in a brain. We find that the desired target function is achieved via time-evolution in the Klein–Gordon Eqs. in a hierarchy of numerical simulations when a signal in both the input and output prevails over noise in the intermediate layers. Our approach will be applied to control coherent fields in the systems (in a hierarchy) described in the QFT framework, with potential applications allowing to manipulate quantum fields, especially holograms in QBD.

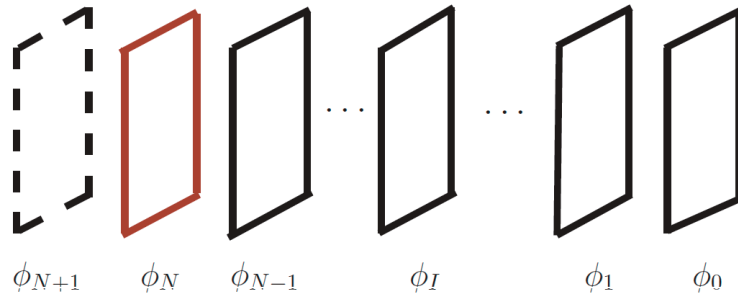


FIG. 1. Quantum field $\phi(x)$ in a hierarchy.

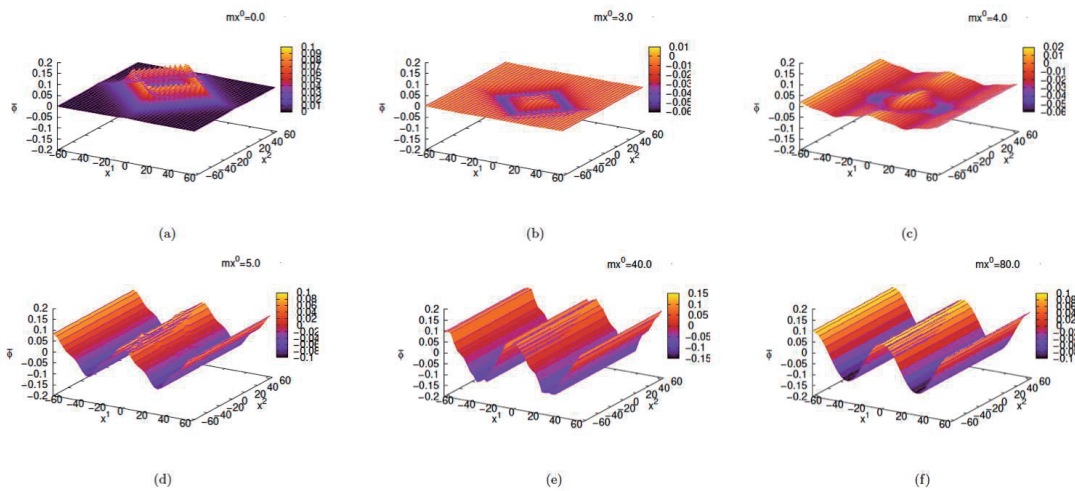


FIG. 2. Distribution of evolving coherent field $\phi(x)$.

Acknowledgement

The present work was supported also by MEXT Quantum Leap Flagship Program (MEXT QLEAP) Grant Number JPMXS0120330644.

Reference

- ¹ Akihiro Nishiyama, Shigenori Tanaka, and Jack A. Tuszynski. Non-equilibrium Quantum Brain Dynamics II: Formulation in 3+1 dimensions. *Physica A: Statistical Mechanics and its Applications*, 567:125706, 2021.
- ² Akihiro Nishiyama, Shigenori Tanaka, and Jack A. Tuszynski. Quantum Brain Dynamics and Holography. *Dynamics* 2.2: 187-218, 2022.

Construction of dipeptide-based DNP-NMR molecular probe library focusing on kidney injury mouse model

Yuki Aketa¹, Yutaro Saito¹, Fuminori Hyodo², Masayuki Matsuo³ and Shinsuke Sando^{1,4}

¹Department of Chemistry and Biotechnology, Graduate School of Engineering, The University of Tokyo, Japan

²Department of Radiology, Frontier Science for Imaging, School of Medicine, Gifu University, Japan

³Department of Radiology, School of Medicine, Gifu University, Japan

⁴Department of Bioengineering, Graduate School of Engineering, The University of Tokyo, Japan

Introduction

Dissolution dynamic nuclear polarization (dDNP) is a powerful technique that dramatically enhances the sensitivity of molecular probes in nuclear magnetic resonance imaging (NMR/MRI), which allows non-invasive detection of NMR/MRI signals in a deep site of the body with high sensitivity^{1,2}. Molecular probes hyperpolarized with dDNP have been successfully applied for metabolic imaging *in vivo* and have been expected to have medical applications such as disease diagnosis and assessment of drug treatment^{2,3}. Although various DNP-NMR molecular probes have been developed⁴, a limited number of biomarkers, usually well-studied enzymes, have been targeted despite the enormous number of potentially targetable enzymes expressed *in vivo*. This situation is mainly due to the paucity of enzymes known to be associated with diseases. In addition, it is unclear which enzymatic activity is applicable to the diagnosis of diseases by DNP-MRI even if the enzymatic activity can be detected in the biosamples. To expand the utility of DNP-NMR, it is desired to devise a new approach to discover biomarker enzymes applicable to the disease diagnosis by DNP-NMR. To this end, we envisioned that it would be an effective strategy to compare the metabolic activity of diseased and healthy tissues for a compound library and discover molecules with disease-specific activity. We focused on exopeptidase which cleaves *N*- or *C*-terminus peptide bonds in peptides because they are known to be related to disease progression,⁵⁻⁷ and we selected dipeptides for the library because they could be recognized from two types of exopeptidases, aminopeptidase and carboxypeptidase, at least.

In the present study, we designed dipeptide libraries targeting aminopeptidases and carboxypeptidases respectively and prepared 180 compounds of the dipeptide libraries in total. Finally, we carried out a screening assay with the dipeptide libraries in the kidney injury mouse model. In this presentation, we will show the design strategy for the dipeptide libraries and the screening results.

Tables and Figures

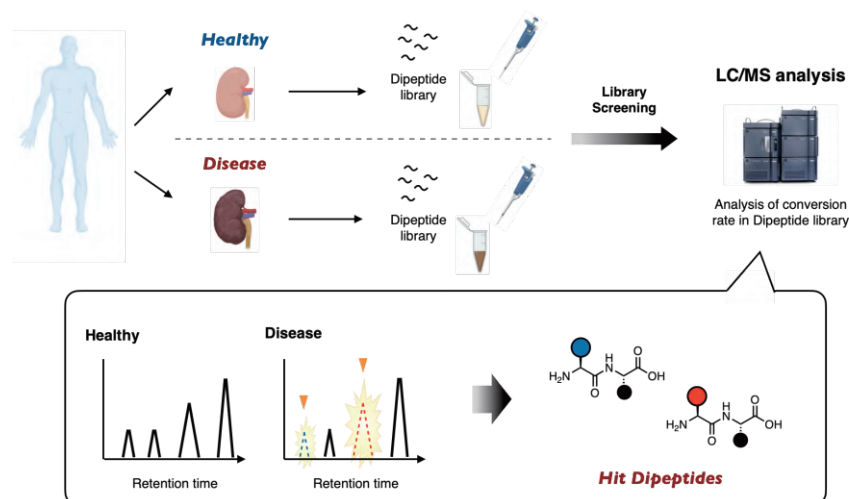


Figure 1. Strategy for discovering new biomarkers in this study.

Reference

- ¹J. H. Ardenkjær-Larsen *et al.*, *Proc. Natl. Acad. Sci. U. S. A.* **100**, 10158–10163 (2003).
- ²K. Golman *et al.*, *Proc. Natl. Acad. Sci. U. S. A.* **103**, 11270–11275 (2006).
- ³S. E. Day *et al.*, *Nat. Med.* **13**, 1382–1387 (2007).
- ⁴Y. Kondo *et al.*, *Angew. Chem. Int. Ed.* **60**, 2–23 (2021).
- ⁵L. Guzman-Rojas *et al.*, *Proc. Natl. Acad. Sci. U. S. A.* **109**, 1637–1642 (2012).
- ⁶D. A. Silver *et al.*, *Clin. Cancer Res.* **3**, 81–85 (1997).
- ⁷P. Selvakumar *et al.*, *Clin. Cancer Res.* **10**, 2771–2775 (2004).

This work was supported by MEXT Quantum Leap Flagship Program (MEXT Q-LEAP) Grant Number JPMXS0120330644.

SE-03B- α 2-04

Nuclear hyperpolarization of liquid water by using photoexcited triplet electrons in organic nanocrystals

Naoto Matsumoto¹, Koki Nishimura¹, Nobuo Kimizuka¹, Yusuke Nishiyama^{2,3}, Kenichiro Tateishi⁴, Tomohiro Uesaka⁴, Nobuhiro Yanai^{1,5}

¹Department of Applied Chemistry, Graduate School of Engineering, Center for Molecular Systems, Kyushu University,

²NanoCrystallography Unit, RIKEN-JEOL Collaboration Center; ³JEOL RESONANCE Inc.,

⁴Cluster for Pioneering Research, RIKEN, RIKEN Nishina Center for Accelerator-Based Science,

⁵FOREST, JST

yanai@mail.cstm.kyushu-u.ac.jp

Introduction

Nuclear magnetic resonance (NMR) and magnetic resonance imaging (MRI) are powerful methods to analyze molecular structures and diagnose diseases. However, the sensitivity of NMR/MRI is quite low because of the low nuclear spin polarization. Dynamic nuclear polarization (DNP) can improve the sensitivity of NMR/MRI by transferring highly polarized electron spins to nuclear spins. On the other hand, the DNP using radical electrons uses electron polarization in thermal equilibrium, which requires cryogenic temperatures (~ 4 K) to obtain high polarization.

Recently, DNP using photoexcited triplet electrons (triplet-DNP) has attracted much attention (FIG. 1).¹ In triplet-DNP, the use of non-equilibrium electron polarization allows nuclear hyperpolarization even at room temperature. However, polarizable targets have been limited to solid samples because polarization transfer from electrons to nuclei requires strong dipole interactions.² Towards the biological application, the hyperpolarization of liquid water has remained an important challenge. In this work, we demonstrated the first hyperpolarization of liquid water by triplet-DNP.³

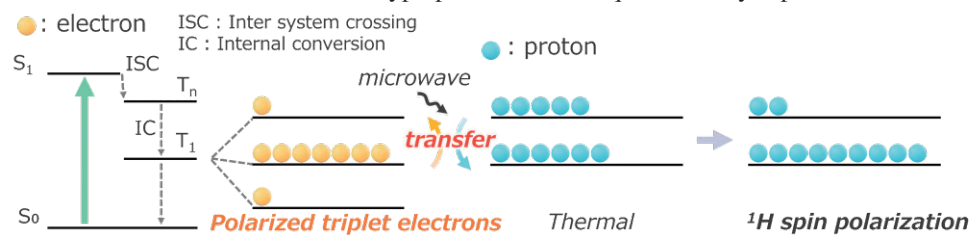


FIG. 1. Schematic representation of triplet-DNP.

Results and discussion

The hyperpolarization of liquid water in triplet-DNP requires polarization transfer from crystals to water, and it is important to increase the surface area of crystals. We prepared 3 sizes of nanocrystals, 390, 270, and 170 nm, respectively, by reprecipitation method and each sample was named NC₃₉₀, NC₂₇₀, and NC₁₇₀, respectively. Triplet-DNP experiments with mixtures of nanocrystals and water showed ¹H-NMR signal enhancement not only crystals but also water (FIG. 2a). ¹H-NMR enhancement of water was increased by decreasing the size of nanocrystals, indicating that hyperpolarization of water was derived from nanocrystals (FIG. 2b). Some control experiments and simulations revealed a scenario of water hyperpolarization in which polarization of photoexcited triplet electron was transferred to nuclear spins in the nanocrystals, and then transferred to liquid water at the nanocrystals-water interfaces.

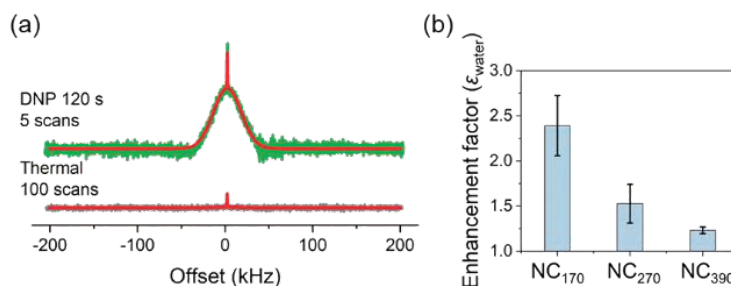


FIG. 2. (a) ¹H-NMR spectra of thermal (black) and after triplet-DNP for 120 s (green) at 28.2 MHz. (b) Nanocrystal size dependent ¹H-NMR enhancement of water.

Reference

¹A. Henstra *et al.*, *Chem. Phys. Lett.*, **165**, 6 (1990).

²K. Nishimura *et al.*, *Chem. Commun.*, **56**, 7217 (2020)

³N. Matsumoto *et al.*, *J. Am. Chem. Soc.*, **144**, 18023 (2022)

SE-03B- α 2-05

Development of Polarizing Agent with Controlled Electronic Structure for Highly Efficient triplet-DNP

Keita Sakamoto¹, Tomoyuki Hamachi¹, Kenichiro Tateishi², Tomohiro Uesaka²,
Nobuo Kimizuka^{1,3}, Nobuhiro Yanai^{1,3,4}

¹Department of Applied Chemistry, Graduate School of Engineering, Kyushu University

²RIKEN Nishina Center for Accelerator-Based Science

³Center for Molecular Systems (CMS) Kyushu University

⁴FOREST, Japan Science and Technology Agency

yanai@mail.cstm.kyushu-u.ac.jp

Introduction

Dynamic nuclear polarization using photo-excited triplet electron (triplet-DNP) achieves the nuclear hyperpolarization by transferring polarization from triplet electron spins to nuclear spins. However, it has remained difficult to attain large nuclear polarization in amorphous materials of practical importance. This is due to the broadening of ESR spectra of the triplet state by the random orientation of the polarizing agents and the anisotropic interaction of the electron spins. While the ESR spectra can be sharpened by controlling the orientation of the polarizing agents within a single crystal,^{1,2} the target molecules cannot be incorporated into the single crystal. Therefore, instead of such "orientation control", this study aims to sharpen the ESR spectra and improve the DNP efficiency by "molecular design" focusing on the electronic structure of polarizing agents.

Method

The shape of the ESR spectra is determined by the zero-field splitting parameters (D , E), which reflect the electronic structure of the excited triplet state. When the electrons are symmetrically delocalized, the values of $|D|$ and $|E|$ become smaller and the ESR spectrum becomes sharper. In order to obtain such delocalized electronic structures, we have synthesized 6,13-di(thiophen-2-yl)pentacene (DTP) by introducing a thienyl group, a five-membered ring with small steric hindrance, into pentacene, and evaluated its electronic structure and polarization performance (FIG 1).

Time-resolved ESR measurements of pentacene and DTP were conducted in a β -estradiol glass matrix. Compared to pentacene, DTP showed more intense and sharper ESR signal thanks to their smaller $|D|$ and $|E|$ values (FIG. 2a).

The triplet-DNP experiment was conducted with an integrated solid effect sequence. *o*-Terphenyl (OTPh) was employed as the amorphous matrix. FIG. 2b shows the buildup curve of ¹H NMR signal intensity after triplet DNP at 120 K. For triplet-DNP with DTP, the final polarization after 5 min reached 0.83%, about three times higher than that with pentacene. Triplet-DNP of partially deuterated OTP ([D₁₄]OTP : OTP = 90 : 10 wt% (OTPd)) with DTP resulted in the polarization of 7.5%, which was much higher than the previous highest value of 1.5%.³

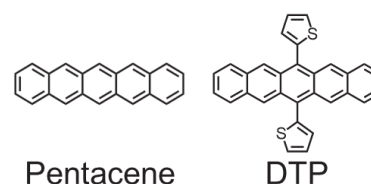


FIG. 1 Chemical structures of pentacene and DTP

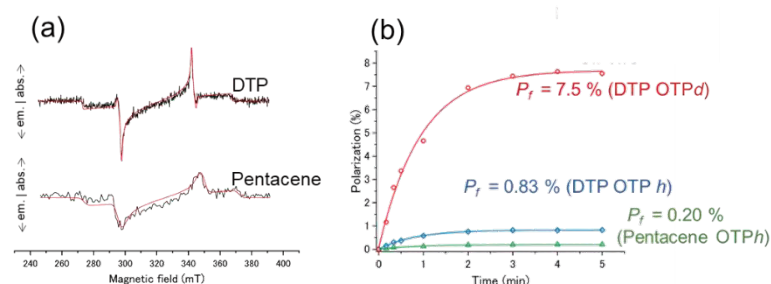


FIG. 2 (a) ESR spectra and, (b) buildup curve of ¹H NMR signal Intensity.

Reference

- ¹Takeda, K., *Triplet State Dynamic Nuclear Polarization* (VDM, Saarbrücken, Germany, 2009).
- ²Tateishi, K., et al., *Proc. Natl. Acad. Sci. U. S. A.*, 111, 7527–7530 (2014).
- ³Tateishi, K., et al., *Angew. Chem. Int. Ed.*, 52, 13307–13310 (2013).

DNP-NMR molecular probe for the detection of Dipeptidyl peptidase-4 activity *in vivo*

Akihito Goto¹, Hiroyuki Yatabe¹, Kazutoshi Yamamoto², Murali C. Krishna², Yutaro Saito¹, and Shinsuke Sando¹

¹Department of Chemistry and Biotechnology, Graduate School of Engineering, The University of Tokyo

²National Institute of Health, USA

goto-akihito0528@g.ecc.u-tokyo.ac.jp

Introduction

Dipeptidyl peptidase-4 (DPP-4) is a peptidase that cleaves peptides at the second residues from the N-terminal terminus, preferentially when the second residue is proline or alanine (Figure 1). Because DPP-4 is related to various diseases such as type 2 diabetes and cancers, DPP-4 is a potential therapeutic target and biomarker^{1,2}. Thus, the detection of DPP-4 activity *in vivo* will be a powerful technique for diagnosis.

Nuclear magnetic resonance imaging (NMR/MRI) is an imaging method that can observe and visualize the dynamics of molecular targets deep inside the body at high spatiotemporal resolution. In the medical field, however, the observation targets are limited to ¹H nuclei of water or lipids abundant in the body. This is due to the low sensitivity of NMR. Dynamic nuclear polarization (DNP) can solve this problem by enhancing NMR sensitivity as much as 10³–10⁵ times. DNP is achieved by irradiating microwave to probes in the presence of stable radicals at a cryogenic temperature under high magnetic field to transfer polarization of electron spins to nuclear spins³. DNP-NMR molecular probes are required to satisfy the following requirements: (1) sufficient length of spin-lattice relaxation time correlated with hyperpolarized lifetime, (2) sufficiently large chemical shift change to distinguish a molecular probe and a product, (3) fast reaction with targets, and (4) selective reaction with targets (Figure 2).

In this study, we attempted to develop a DNP-NMR molecular probe for the detection of DPP-4 activity *in vivo* by designing the molecular structure to satisfy these requirements. In the presentation, we will show the design strategy and the recent results.

Tables and Figures

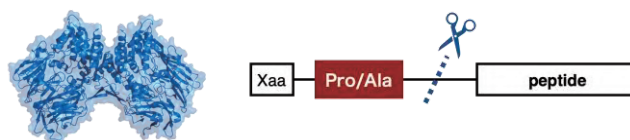


Figure 1. DPP-4 and preferential cleavage site.

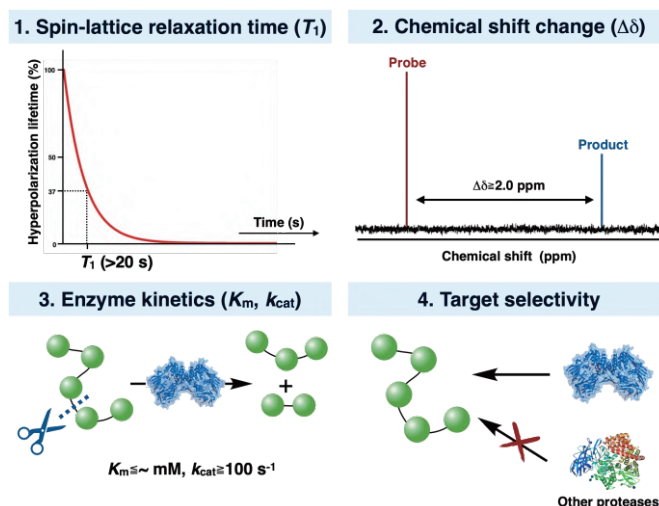


Figure 2. Requirements for DNP-NMR molecular probes.

References

- ¹C. F. Decon, *Front. Endocrinol.* 10, 80 (2019).
- ²K. Ohnuma *et al.*, *Front. Biosci.* 23, 1754–1779 (2018).
- ³J. H. Ardenkjaer-Larsen *et al.*, *Proc. Natl. Acad. Sci. U. S. A.* 100, 10158–10163 (2003).

This work was supported by MEXT Q-LEAP Grant Number JPMXS0120330644

Generation of polarized triplet electron spins at solid-liquid interfaces

Reiya Yabuki¹, Tomoyuki Hamachi¹, Koki Nishimura¹, Kenichiro Tateishi², Tomohiro Uesaka² and Nobuhiro Yanai^{1,3,4}

¹Department of Applied Chemistry, Graduate School of Engineering, Kyushu University

²RIKEN Nishina Center for Accelerator-Based Science

³Center for Molecular System, Kyushu University

⁴FOREST, Japan Science and Technology Agency

yanai@mail.cstm.kyushu-u.ac.jp

Introduction

Triplet-DNP can enhance NMR sensitivity at room temperature utilizing the electron polarization of the triplet state^{1,2}. However, it has been difficult to enhance the solution NMR signal by triplet-DNP due to the immediate relaxation of polarized triplet electron spins in solution. Towards the direct polarization of solution by triplet-DNP, we aim for the generation of polarized triplet electron spins at solid-liquid interfaces.

Method

In this study, we used tetrakis (4-carboxyphenyl) porphyrin (TCPP, FIG. 1a) as a polarization agent and aminopropyl silica gel (ASg, FIG. 1b) as a solid support. TCPP-modified ASg was dispersed in toluene. We evaluated whether polarized electron spins of triplet states are generated at the solid-liquid interface by time-resolved ESR measurements.

Under pulsed laser excitation at 527 nm, ESR spectrum and the peak decay of TCPP on ASg surface in toluene were measured. The ESR spectrum showed a characteristic line shape of the spin-polarized triplet state of TCPP³ (FIG. 2). Furthermore, the lifetime of the spin-polarized state was approximately 3.0 μ s, which was long enough to carry out the triplet-DNP measurement. This result indicates that the use of solid support suppressed the dynamics of the polarization agents and the relaxation of electron spin polarization at the solid-liquid interface.

Reference

- ¹W. T. Wenckebach et al., *Chem. Phys. Lett.*, **165**, 6-10 (1990)
- ²N. Yanai et al., *J. Phys. Chem. Lett.*, **10**, 2645-2650 (2021)
- ³L. Bolzonello et al., *Phys. Chem. Chem. Phys.*, **19**, 27173-27177 (2017)

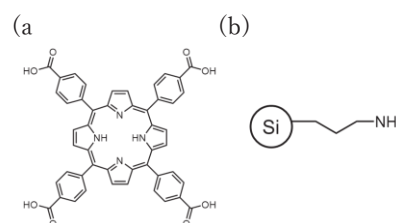


FIG. 1. Chemical structures of (a) TCPP and (b) ASg

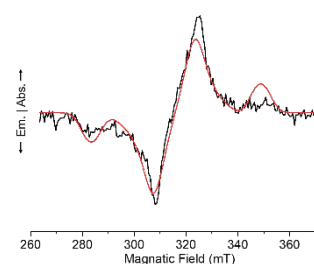


FIG. 2. ESR spectrum of TCPP-ASg in toluene

Photoreaction study of a primate blue-light sensitive photoreceptor using vibrational spectroscopy

Yosuke Mizuno¹, Kota Katayama¹, Hiroo Imai², and Hideki Kandori¹

¹ Graduate School of Engineering, Nagoya Institute of Technology

² Center for the Evolutionary Origins of Human Behavior, Kyoto University

y.mizuno.092@stn.nitech.ac.jp

Introduction

Photoreceptor proteins are expressed in eyes and function as vision systems. There are two types of photoreceptors. One is rhodopsin which responsible for twilight vision, another one is cone pigments which responsible for color vision. These proteins commonly bound 11-*cis*-retinal as a chromophore. Retinal absorb UV light (370 nm) in the solution and absorb about 440 nm by making Schiff base linkage. Further, protein moiety determines the absorption range from UV to red light¹.

The photoreaction mechanisms and structural information were well known in rhodopsin. However, Cone pigment have been less known than rhodopsin because of low expression level and handling difficulty. We previously observed the first structural data of the primary Batho intermediate state of primate red (MR), green (MG) and blue (MB) cone pigments by low-temperature FTIR spectroscopy². Recently, we also reported the structural study of BL intermediate in MB which is formed from initial photointermediate³. Here, we extended these vibrational structural studies by identifying subsequent photointermediate of cone pigments, especially MB.

Results

By using low-temperature UV-visible spectroscopy, we found that the Lumi intermediate (223K) of MB formed in transition from the BL intermediate (163K) shows an absorption maximum in the UV region (Fig.1), indicating the deprotonation of the retinal Schiff base. Comparison of the light-induced difference FTIR spectra of Batho (77K), BL, and Lumi showed significant α -helical backbone C=O stretching (1661 and 1652 cm^{-1}) and protonated carboxylate C=O stretching vibrations (1714 and 1712 cm^{-1}) only in the Lumi intermediate (Fig.2). Thus, the transition from BL to Lumi involves dramatic changes in protein environment with a proton transfer reaction between the Schiff base and the counterion resulting in an absorption maximum in the UV region⁴.

Tables and Figures

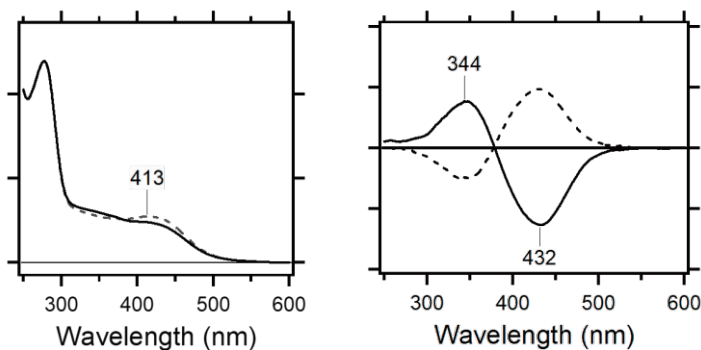
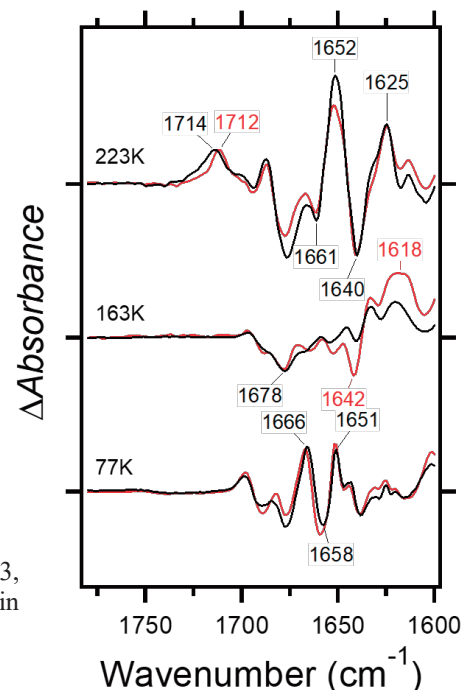


FIG.1. UV-visible absorption spectra of MB (left) and light-induced difference spectra (right) with >430 nm illumination (solid line) and 360 nm illumination (dash line) at 223K

FIG.2. Light-minus-dark difference FTIR spectra of MB at 223, 163, and 77 K in the 1780–1600 cm^{-1} region. Spectra were measured in H_2O (black) and D_2O (red).



Reference

¹O.P. Ernst et al., *Chem Rev*, **114**, 126-163 (2014).

²K. Katayama et al., *Sci Rep*, **7**, 4904 (2017).

³S. Hanai et al., *Biophys Physicobiol*, **18**, 40-49 (2021).

⁴Mizuno et al., *Biochemistry*, in press

SE-03B- α 2-09

Novel photoisomerization reaction in near-infrared light absorbing enzymerhodopsins

Masahiro Sugiura^{1*}, Kazuki Ishikawa¹, Kota Katayama^{1,2}, Yuji Sumii¹, Rei Abe-Yoshizumi¹, Satoshi P. Tsunoda^{1,2}, Yuji Furutani^{1,2}, Norio Shibata¹, Leonid S. Brown³, Hideki Kandori^{1,2**}

¹ Department of Life Science and Applied Chemistry, Nagoya Institute of Technology, Japan

² OptoBioTechnology Research Center, Nagoya Institute of Technology, Japan

³ Department of Physics and Biophysics Interdepartmental Group, University of Guelph, Canada

*: m.sugiura.734@stn.nitech.ac.jp, **: kandori@nitech.ac.jp

Introduction

Rhodopsins is a large family of retinal-binding photoreceptive membrane proteins found in microbes and animals¹. Microbial rhodopsins has different functional family, including light-driven ion pumps, light-gated ion channels, light sensors, and light-activated enzymes (FIG.1). Microbial rhodopsins possess retinal chromophores that capture light energy and isomerize from all-trans to 13-cis (FIG.1). Although this isomerization reaction was universally conserved in microbial rhodopsins, a recently discovered microbial rhodopsin, bestrhodopsin, offered surprising photochemical properties.

Bestrhodopsin is a far-red light absorbing novel microbial rhodopsin, in which one or two rhodopsin domains are fused to a bestrophin channel and function as light-gated ion channels². The surprises were that bestrhodopsin performs an all-trans to 11-cis photoisomerization and it show no photoreaction at low temperatures at <170K, despite any microbial rhodopsin can react².

Our target protein is enzymerhodopsin (NeoR) which was reported in 2020³. This NeoR is similar to bestrhodopsin in the following four points³. First, it absorbs far-red and near infra-red light. Second, the rhodopsin domain forms heterodimers. Third, it has eight transmembrane α -helices whereas normal rhodopsin is composed of seven transmembrane α -helices. Finally, three carboxylic acids are conserved around the retinal as a chromophore, different from normal microbial rhodopsins which have one or two carboxylic acids near the retinal. Despite these similar properties between bestrhodopsin and NeoR, the detailed photochemical properties of NeoR remained unknown.

Thus, we clarified the photochemical properties of NeoR using HPLC and spectroscopy.

Results

We studied a novel near-infrared light-absorbing enzymerhodopsin from *Obelidium mucronatum* (OmNeoR). OmNeoR show guanylyl cyclase activity upon light irradiation, when it form heterodimers. Using UV-vis spectroscopy, it is revealed that OmNeoR absorbs near infrared light, and its absorption wavelength converts the dark state into a stable UV-absorbing state.

Using HPLC analysis which can determine composition ratio of retinal isomers in rhodopsin, anti-oxime peak (X) is observed different from f 13-cis, 11-cis, 9-cis, or all-trans form. In previous research, peak (X) is probably 7-cis. However, 7-cis retinal is unstable, because of a steric hindrance between the 9-methyl group and methyls in the β -ionone ring. In addition, an HPLC peak of di-cis retinal oxime, such as the 9,11-di-cis form, can appear between those of 9-cis and all-trans retinal oxime. Thus we weren't sure if peak (X) was really 7-cis form. Here, we isolate same isomer as peak (X) and measure the ¹H NMR spectra which is consistent with 7-cis form. Therefore, we conclude that peak (X) is 7-cis retinal.

In addition, OmNeoR show no photoreaction at <270K. It indicate that there exist potential barrier for 7-cis isomerization in excited state of OmNeoR.

In this presentation, we would like to discuss the unique photoisomerization reaction of NeoR.

Reference

- O.P. Ernst et al., *Chem Rev*, **114**, 126-163 (2014).
- A. Rozenberg et al. *Nat. Struct. Mol. Biol.*, **29**, 592-603 (2022)
- M. Broser et al. *Nat. Commun.* **11**, 5682 (2020)

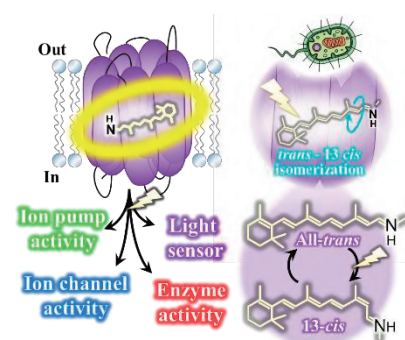


FIG.1 Functions and photoisomerization of microbial rhodopsin

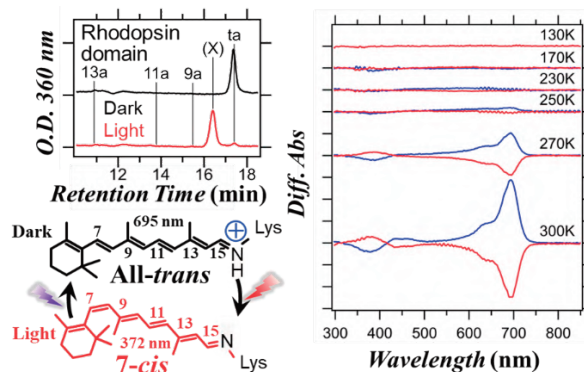


FIG.2 Retinal isomerization in NeoR and photoreaction at low temperature.

Development of a real-time 4D quantum temperature imaging system to measure intercellular thermal diffusivity

Haruka Maeoka¹, Ryuji Igarashi², Shin Usuki³, and Takuma Sugi¹

¹*Program of Biomedical Science, Graduate School of Integrated Sciences for Life, Hiroshima University*

²*Quantum Science and Technology Organization*

³*Research Institute of Electronics, Shizuoka University*

m211518@hiroshima-u.ac.jp

Cellular function is severely affected by temperature change. Heat produced within a cell controls its own cellular function cell-autonomously and neighboring cells' function non-cell-autonomously. While several studies have focused on intracellular thermal diffusion, few have reported on how intercellular thermal diffusion influences neighboring cells' function. This question could be addressed by estimation of the intercellular thermal diffusivity, which requires quantifications of temperatures at three-dimensionally distributed multiple cells during thermal diffusion. However, assuming that the thermal diffusivity in cells is the same as that in water, $1.5 \times 10^{-7} \text{ m}^2 / \text{sec}$, it takes 1 millisecond for heat to diffuse through multiple $10 \text{ }\mu\text{m}$ cells in all XYZ directions. In contrast, when we take images using a 100 fps camera with 100 scans along Z-axis and 30 times data accumulations, current 3D imaging technologies such as confocal microscopy take 50 milliseconds to measure temperature of multiple cells along Z-axis. This means that the measurement speed of the current technologies is insufficient to observe 3D intercellular heat diffusion which completes within 1 millisecond.

Recently, we developed the high-resolution light field microscopy (HR-LFM) capable of 'scan-less' 3D imaging by capturing 3D space as a 2D image using a micro-lens array. We also focused on the fluorescent nanodiamonds (FNDs) which allow for highly sensitive temperature measurement. Here, these two cutting-edge technologies inspired us to establish a system for measuring the temperatures of multiple cells with an acquisition rate faster than heat diffusion rate. First, (1) we constructed a 'selective imaging' system to selectively extract the fluorescence of only FNDs from among background fluorescence by irradiating microwave that induces electron spin resonance to modulate the fluorescence of FNDs. Then, we synchronized 'scan-less' 3D detection of multiple signals by HR-LFM with microwave irradiation. This enabled simultaneous selective extraction of multiple FNDs' fluorescence from among fluorescent beads in a 3D sample and from among an autofluorescence in *C. elegans*, thereby achieving 3D selective imaging 50-fold faster than confocal microscopy. Second, (2) we attempted to establish the system for measuring 3D heat diffusion. We successfully measured temperature changes at multiple 3D locations simultaneously in nematode *C. elegans*, thus achieving 3D temperature imaging 100-fold faster than confocal microscopy. Using this method, we will calculate the intercellular thermal diffusivity by measuring the intercellular heat diffusion from a heat source cell to neighboring cells *in vivo*.

Bidirectional neural network and its application to image denoising, super-resolution, and image completion

Kei Majima^{1,2}, Noriaki Yahata¹

¹*Institute for Quantum Life Science, National Institutes for Quantum Science and Technology (QST), Chiba, Japan*

²*PRESTO, Japan Science and Technology Agency (JST), Japan*

majima.kei@qst.go.jp

Introduction

Quantum sensing technology has enabled the development of new methods to visualize various physical parameters of interest in biological systems. For example, the concentration of specific molecules can be visualized by magnetic resonance imaging (MRI), and an electromagnetic field or distribution of temperature can be reconstructed by nitrogen-vacancy center sensing (NV-center sensing). Because observed image data are sometimes noisy/low-resolution/incomplete, image processing to recover clean/high-resolution/complete images from the observed ones is a critical step that must be developed. In this report, we present a unified framework for the above-mentioned image-processing tasks using neural networks.

Methods

We describe our proposed framework by taking the super-resolution task as an example. Note that the same framework can also be used for image denoising and image completion. In our framework, we assume that a set of low-resolution images and the corresponding high-resolution images are available as training data. Then a bidirectional neural network, which is a neural network whose each layer is bidirectional, is trained using the training data (Fig 1A). Following the neural network training, for new low-resolution images, the corresponding high-resolution images can be estimated using this neural network as a converter.

Results

Using two types of toy image data, we tested the proposed framework on three types of image-processing task: 1) image denoising, 2) super-resolution, and 3) image completion. Results of the super-resolution task are shown in Fig. 1B and C.

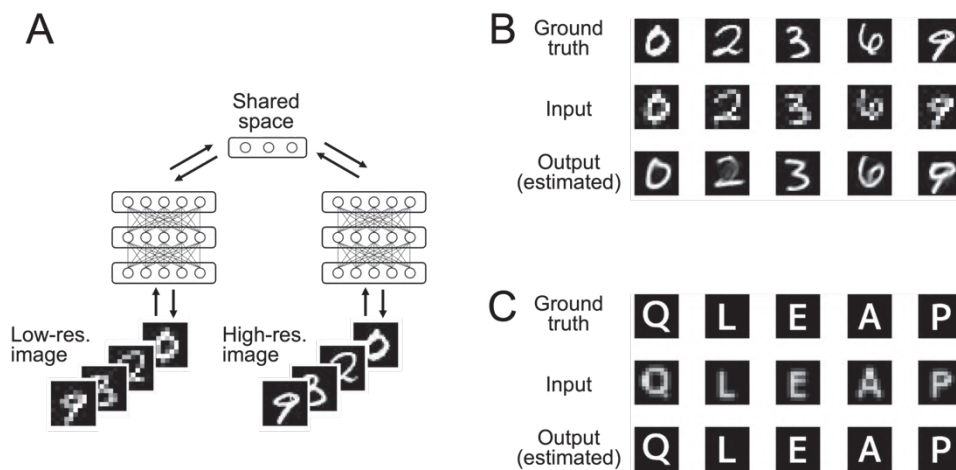


FIG 1. Neural network-based image-preprocessing framework. A schematic of neural network training (panel A) and results of the super-resolution task (panels B,C) are shown.

Discussion and Conclusions

In this report, we presented an image-processing framework using a bidirectional neural network, and our preliminary results showed that this framework can effectively perform several types of image-processing task. The application to real experimental data in the field of quantum sensing will be addressed in our future studies.

Acknowledgments

This research was supported by MEXT Q-LEAP (JPMXS0120330644), JSPS KAKENHI (20K16465), JST ERATO (JPMJER1801), and JST PRESTO (JPMJPR2128).

SE-03B- α 2-12

Molecular insight into photoactivation mechanism of BLUF protein by QM/MM free energy simulation

Masahiko Taguchi, Shun Sakuraba, Justin Chan, and Hidetoshi Kono

Institute for Quantum Life Science, National Institutes for Quantum Science and Technology

taguchi.masahiko@qst.go.jp

Introduction

OaPAC is a photoactivated enzyme that forms a homodimer [1,2]. It has two BLUF photoreceptor domains connected to the catalytic domains via long coiled-coil C-terminal helices. It is thought that during photoactivation, reorganization of hydrogen bonding network between Tyr6, Gln48, and chromophore and keto-enol tautomerization of Gln48 occur in the BLUF domain [3,4]. However, the free-energy profile of the photo-isomerization reaction and how the structural change in the BLUF domain propagates toward the catalytic domain have not been revealed yet.

Method

We first focused on the BLUF domain dimer with the C-terminal helices from the dark state X-ray crystallographic structure of OaPAC [1]. We free-energetically optimized the dark state structure using QM/MM RWFE-SCF method [5]. We considered two possible light state structures that were free-energetically optimized. The free-energy differences between the dark and two light state structures were evaluated by the free-energy perturbation calculation. To clarify differences in protein dynamics upon photo-isomerization, we performed long-time MD simulations for the dark and light state structures.

Results

The free-energy difference between the two light state structures was estimated ~ 4.7 kcal/mol. The light state model with a lower free energy is consistent with a FTIR experiment result [4], but is inconsistent with light state X-ray crystallographic structure [2] in the assignment of nitrogen and oxygen atoms of Gln48 sidechain. Our component analysis of free-energy difference between the dark and light state structures showed that the chemically unstable enol tautomer of Gln48 in the light state is stabilized by a strong hydrogen bonding network with chromophore and Tyr6. Moreover, in the light state, we observed a flip of Trp90 nearby the C-terminal helix, causing the subsequent structural changes in the BLUF core and the C-terminal helix.

This work was supported by MEXT Q-LEAP Grant Number JPMXS0120330644.

References

- [1] M. Ohki *et al.*, Proc. Natl. Acad. Sci. USA **113**, 6659 (2016).
- [2] M. Ohki *et al.*, Proc. Natl. Acad. Sci. USA **114**, 8562 (2017).
- [3] T. Domratcheva *et al.*, Sci. Rep. **6**, 22669 (2016).
- [4] T. Iwata *et al.*, J. Am. Chem. Soc. **140**, 11982 (2018).
- [5] S. Hayashi *et al.*, Annu. Rev. Phys. Chem. **68**, 135 (2017).